

**Foam Formation in Low Expansion Fire
Fighting Equipment**

**A thesis submitted for the degree of Doctor of Philosophy
Engineering Department, Lancaster University**

By

Lucy Elizabeth Rogers

B.Eng (Hons)

C.Eng MIMechE

Submitted: January, 2001

Abstract

Foam Formation in Low Expansion Fire Fighting Equipment

A thesis submitted for the degree of Doctor of Philosophy

Engineering Department, Lancaster University

By: Lucy Elizabeth Rogers B.Eng (Hons) C.Eng MIMechE

Submitted: January 2001

This thesis describes an investigation into the foam generation mechanisms involved in producing foam from a low expansion fire fighting branchpipe. The investigation was carried out using scale models of branchpipes, and a high-speed video camera was used to study the formation of the foam. The experiments provided evidence of three possible methods of bubble formation within this type of system:

- Stage 1 - Mixing within the branchpipe.
- Stage 2 - Air entrainment and bubble growth during the flight of the jet.
- Stage 3 - Aeration produced from the collision of the high speed jet onto a surface.

Each stage is described in detail and the mechanism which has the greatest effect on the expansion ratio of the foam produced has been determined. The relevance of these findings to the design of branchpipes is discussed.

Declaration

I hereby declare that this submission is my own work and that, to the best of my knowledge and belief, it contains no material previously published or written by another person nor material which to a substantial extent has been accepted for the award of any other degree or diploma of the university or other institute of higher learning, except where due acknowledgement has been made in the text.

Lucy Rogers

January, 2001

Acknowledgements

I would like to take this opportunity to express my gratitude to all those who have assisted in this project.

In particular to my supervisor, Martin Widden, for his encouragement, support and continual efforts to obfuscate me with philology.

Thanks are also due to Stephen, my parents and to Benjamin, for their continual support and numerous morale-boosting telephone conversations.

The high speed video equipment was kindly loaned by the EPSRC engineering instrument pool at Rutherford Appleton Laboratory.

This programme was funded by CounterFire Limited and thanks are due to the Managing Director, M.J.Osborne, for this opportunity.

Table of Contents

Table of Contents	1
1. Introduction	3
1.1 Background	3
1.2 Fire Fighting Foam Generation	4
1.3 CounterFire Limited	11
1.4 Aims of Project	12
1.5 Experimental Work	13
1.6 Findings	14
1.7 Discussions and Conclusions	16
2 Literature Review on Foam	17
2.1 Introduction	17
2.2 Formation and Structure	18
2.3 Surface Tension	21
2.4 Properties of foam	28
2.5 Fire Fighting Foams	36
3 Experimental Work	47
3.1 Introduction	47
3.2 Development of the Test Rigs	47
3.3 Atmospheric Conditions	59
3.4 Foam Property Measurement Techniques	59
3.5 High Speed Video	67
3.6 Factorial experiment design and statistical techniques	68
4 Foam Formation Process Stage One (Mixing)	74
4.1 Introduction	74
4.2 Literature Review	75
4.3 Experimental Findings and Results	78
4.4 Conclusions	99
5 Foam Formation Process Stage Two (Flight)	103
5.1 Introduction	103
5.2 Literature Review	105
5.3 Experimental Findings, Results and Theory	113
5.4 Conclusions	120

6	Foam Formation Process Stage Three (Collision)	122
6.1	Introduction	122
6.2	Literature Review	123
6.3	Experimental Findings and Results	131
6.4	Conclusions	140
7	Discussions and Conclusions	142
7.1	Introduction	142
7.2	Discussion	142
7.3	Conclusion	149
7.4	Further work	150
	References	151
	Glossary	159
	Appendices	161

1. Introduction

This chapter details the background to the thesis, including an introduction to fire fighting foam generation and CounterFire Limited. The initial and final aims of the project are then explained, followed by a synopsis of the chapters on the experimental work, the findings, discussions and conclusions.

1.1 Background

Foams were first used as a fire fighting agent in 1877 (Johnson 1877). They are now in general use throughout the world to control and extinguish fires of flammable liquids and for inhibiting re-ignition. The type of fire determines the properties of the extinguishing agent and how far it must be projected. Examples include an oil storage tank fire that requires a blanket of foam to be thrown over 20 metres upwards, or a warehouse fire that may require filling from floor to ceiling, through a doorway. Many fire fighters disagree over the optimal fire fighting foam for specific situations and so there is a strong incentive to stay with the tried and trusted. There has been relatively low investment in (published) scientific effort related to fire fighting equipment. The design of foam generating equipment appears to have progressed by empirical means.

One method of categorising equipment is by the expansion ratio of the foam it produces. This is defined as the ratio of the volume of foam to the volume of surfactant solution from which it was made. A ratio in the range of 1 to 20 is low expansion, between 21 and 200 is medium expansion and high expansion is over 200. Fire fighters often gauge the quality of a foam by its drainage rate (the time taken for 25% of the liquid to drain from the foam) as well as its expansion ratio.

The literature review (Chapter Two) provides a thorough introduction to all aspects of foams and bubbles. The chapter includes information on their formation, structure and properties. The history of foam as a fire fighting medium and the properties and definitions used within the fire fighting industry are also discussed.

1.2 Fire Fighting Foam Generation

Fire fighting foam is produced by mixing a surfactant concentrate with water in the correct proportions and then, if appropriate, aspirating the resulting solution into a mass of bubbles. It is then applied either to the fire or to the area it is protecting. Producing and applying fire fighting foam can therefore be summarised in three operations:

1. The proportioning process
2. The foam generation
3. The distribution method

1.2.1 The Proportioning Process

Proportioning devices ensure the correct amount of water is mixed with the surfactant concentrate. Two systems are used – jet pumps (or eductors) and proportioners. Jet pumps use the water flow to induce the surfactant concentrate by venturi action. Proportioners utilize external pump or pressure heads to inject concentrate into the water stream at a fixed ratio flow.

Jet Pump or Eductor: A jet pump is a device in which a jet of fluid (the motive or driving fluid) is used to entrain more fluid. It consists of a nozzle, an orifice, a mixing tube or “throat” and, generally, a diffuser on the downstream side (see Figure 1:1).

The high-pressure driving fluid is directed through a nozzle designed to produce the highest possible velocity. The resultant jet of high velocity fluid creates a low-pressure area in the throat causing the secondary fluid to flow in through the orifice.

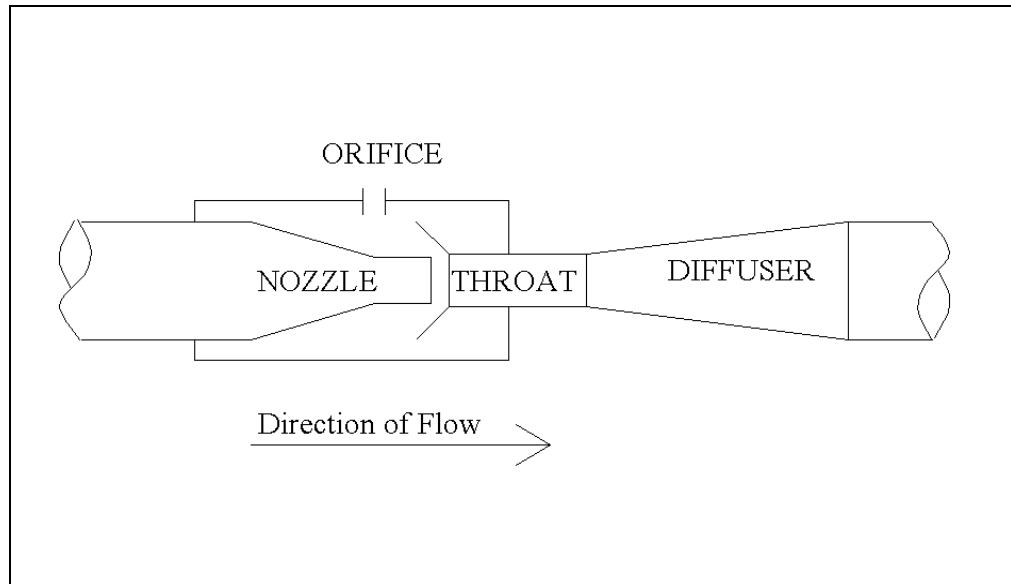


Figure 1:1 Jet pump

An orifice plate or other metering device can be used to regulate the surfactant concentrate (secondary fluid) intake. A non-return valve can also be placed in this intake to prevent the motive fluid flowing back into the surfactant concentrate container.

The jet pump has no moving parts but it has the disadvantage of a low efficiency. The principles of its operation, definition of terms, uses and the theory and design behind each type have been described in numerous publications (Jumpeter), (Wakefield 1989), (Hatton 1993), (BHRA 1968). Mathematical models of jet pumps have been suggested (Anderson 1980), (Cunningham 1956), (Cunningham 1975), (Cunningham 1995), (Neve 1993), (Mueller 1964) although there is some disagreement over the

values of the various loss coefficients. These values also vary with the scale of the jet pump.

Proportioner

There are numerous types of proportioner, including Around-the-Pump and Balanced Pressure. The Around-the-Pump proportioner also works on the venturi principle, however, it must be situated at the pump and connected to both suction and pressure sides. The Balanced Pressure proportioner uses a separate pump for pressurizing the surfactant concentrate. This thesis does not consider this type of proportioner, however Scheffey (Scheffey 1997) describes both of these in more detail.

1.2.2 The Foam Generation

After proportioning, the solution is sprayed into air. This is either directly (non-aspirating) or into an aerating tube or branchpipe (aspirating). The non-aspirating generators do not entrain air into the branchpipe. Non-aspirating nozzles have a longer reach than aspirating nozzles. However, DiMaio et al (DiMaio et al. 1984) and the Civil and Environmental Engineering Development Office of the U.S. Navy (CEEDO 1978) conclude that aspirating nozzles provide a better quality foam in terms of expansion and 25% drainage than conventional non-aspirating systems. An aerating branchpipe improves the air-solution mixing. The aspirating devices can be divided into two basic categories:

- Foam making branchpipes for low expansion or medium expansion foam
- Generators for high expansion foam

Most foam generating equipment will fit into one of the above categories. Exceptions include equipment designed by Hoover (Hoover 1989), by Fittes and Nash (Fittes and Nash 1965) and the “compressed air foam system” (CAFS). Hoover obtained a patent for a foam generator that is able to be adjusted to produce foam with different expansion ratios. This is achieved by projecting the surfactant solution onto variable areas of a screen. However, as fire water is often extracted from lakes and rivers it usually contains debris and this can easily clog the screen. This type of equipment is not in common use. Fittes and Nash produced an experimental gas turbine operated foam generator that produced large quantities of fire fighting foam at various pre-determined physical characteristics for use in experimental mock fires. This equipment was, however, far too large and cumbersome for regular use. The “compressed air foam system” (CAFS) is designed to produce finished foam without the use of a branchpipe, although it is also not yet in common use. Thomas (Thomas 1994) investigated the performance of a CAFS and compared this to a standard UK Fire Service low expansion aspirating branchpipe with a similar flow rate. He concluded that the CAFS throws low expansion foam further than conventional Fire Service branchpipes when used at the recommended flow rate, and also produces a good quality foam. However, the system is limited by the concentrate injection pump and by the maximum air supply from the compressor. Further work on CAFS has been published by Colletti and Davis (Colletti and Davis 1998) and Rochna (Rochna 1998).

1.2.2.1 Foam making branchpipes for low or medium expansion foam

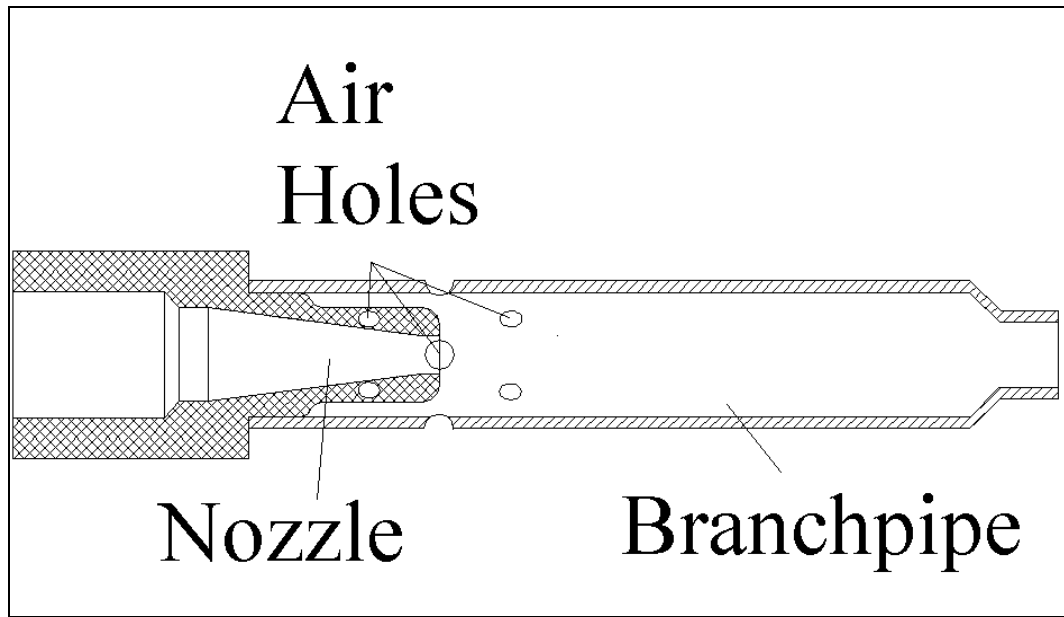


Figure 1:2 Low expansion foam making branchpipe

A typical low expansion branchpipe system is shown in Figure 1:2. The surfactant solution is pumped through a nozzle, jet or orifice plate into the branchpipe tube. Air is induced into the liquid stream and this is mixed by violent turbulence. The resulting mixture is projected from the branchpipe as a “rope” or free jet.

In 1951 a mechanical low to medium expansion foam generator was developed for use in laboratory experiments by Fry and French (Fry and French 1951b). This produced similar quality foam to that formed from practical fire fighting equipment. It was designed to determine the fire fighting capabilities of different surfactant compounds on different fire types without the cost and difficulties involved in full-scale experiments. However, the generation method of the foam produced in this way is not comparable with foam produced from branchpipes. In Fry and French’s set-up, the air

and liquid supplies were controlled independently and the foam was formed by passing the air and liquid through gauze discs.

In the 1970's the UK's Fire Research Station developed branchpipes for standard tests to determine properties of surfactant concentrates and to see how the properties of the foam affected its ability to extinguish fires (Benson et al. 1973b), (Benson and Corrie 1976), (Corrie 1976a). However, the actual process of foam generation has not been investigated with respect to fire fighting equipment, to the author's knowledge.

1.2.2.2 High Expansion Foam Generators

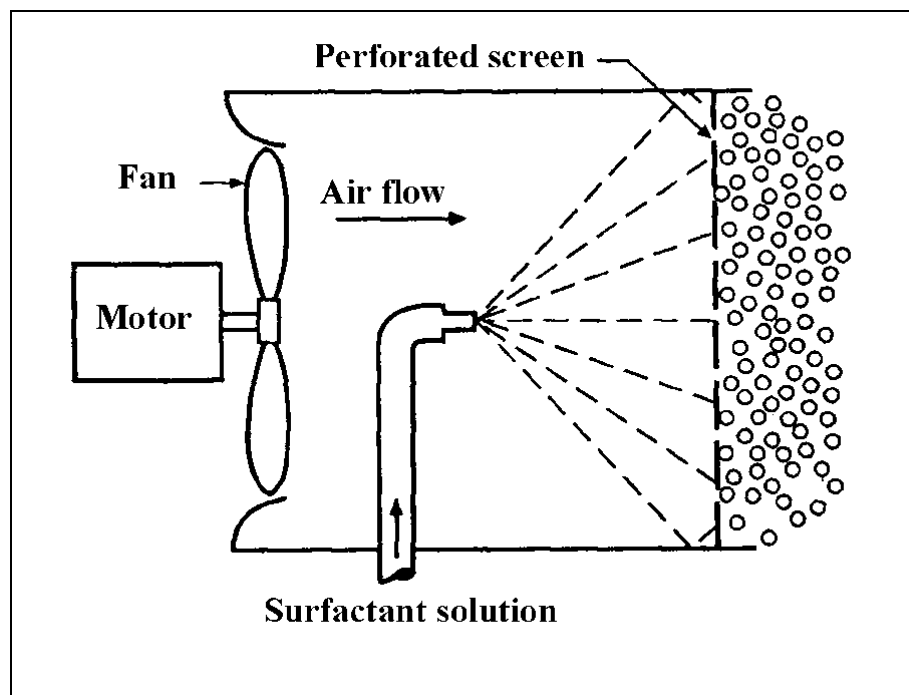


Figure 1:3 Basic high expansion foam generator

Most high expansion foam generators are based on the design in Figure 1:3. A fan is usually present, and is powered as described below. The expansion of the surfactant solution is achieved by spraying the solution onto a perforated screen. An air stream

created by the fan attached to the motor blows air through the screen to produce a mass of bubbles.

High expansion foam generators fall into one of four categories based on whether there is a motor and fan and, if so, how it is powered: Air aspirating, Water Powered, Nozzle Reaction or Electric Powered.

Air Aspirating: There is no motor or fan. The foam is produced just by the momentum of the surfactant solution through the screen. Some air aspirating foam generators can be starved of air even in a light crosswind and therefore the expansion of the foam generated is limited.

Water Powered: Part of the solution flow is directed onto a pelton wheel, which is directly connected to the fan.

Nozzle Reaction: This is similar in principle to a garden sprinkler system. It drives the fan less efficiently than a turbine. It has working parts and hence higher maintenance.

Electric Powered: An electric motor drives the fan. This leads to increased maintenance and less reliability. An electricity supply is also required.

Research conducted into high expansion foam generators has included work by Foster (Foster 1984), who reports the results of trials by an UK fire brigade, of a compact high expansion generator. The generator was designed to have a comparable

performance to existing generators in use by the UK's Fire Service. It was also designed to be small enough to be stowed in the locker of a fire engine and to be used as a smoke extractor. The quantity and quality of the foam generated and the ease of deployment received favourable comments. Butlin (Butlin 1967) discusses the different types and materials used for the screen in high expansion foam generators. He also discusses the fan usage, and the importance of air speed.

1.2.3 The Distribution Method

The type of fire will determine the distance the foam is to be projected. A medium expansion foam flows less readily than a low expansion foam, and it can only be projected small distances. High expansion foam is very slow flowing and is poured rather than projected. A 200 l/min low expansion branchpipe can produce a throw of approximately 15 m. This size of branchpipe can be held by one fireman. In larger sizes, the low expansion branchpipe is called a monitor. Large monitors, having a capacity of up to 20,000 l/min, can have a throw of over 100 m.

1.3 CounterFire Limited

CounterFire Limited design and build fire fighting equipment. They are the UK market leader in the large monitor (water cannon) area and in the top four in the world market. They are strong in the marine and petrochemical fields, with 80% of sales being made to overseas customers. CounterFire tends to sell direct to the ship builder by selling a whole package - from the engine to the jet. This makes the sale a project, which may include gearboxes, pumps, foam and water monitor systems etc. CounterFire are driven to develop new products by being unable to purchase

equipment to the right specification / quality / price. As they sell a package, they develop more equipment to improve their margin. This also makes them less dependent on others. CounterFire produces the design, but the majority of components are sub contracted. These are then assembled and tested in-house to ensure integrity.

CounterFire believe that it should be possible to control the properties of the foam produced with one type of surfactant concentrate, through design changes in the mechanical equipment. If the properties of the foam could be controlled by the fire-fighter within one standardised product, then different types of fire-hazard could be tackled with just one piece of equipment and one type of surfactant concentrate. Although Hoover (Hoover 1989) has obtained a patent for a foam generator adjustable to produce foam having various expansion ratios, CounterFire believe this equipment could be improved. It could then be marketed, as the fire fighting industry presently does not use this type of equipment. This research was therefore assisted by CounterFire and was intended to increase CounterFire's sales potential as well as portfolio. By increasing their knowledge of the foam generation process, CounterFire Limited should be able to improve aspects of their current foam generation equipment.

1.4 Aims of Project

The initial aim of the project was to determine which physical characteristics of fire fighting foam generating equipment have the most influence on the properties of expansion ratio and drainage rate. CounterFire suggested various parameters that were thought would be major contributors to these properties and helped develop Test Rig One. However, these experiments were very inconclusive, as the variables of fan

setting, pump setting, gauze, nozzle angle, cone type and surfactant concentration had little effect on the expansion ratio in this test rig. Even with a vastly suppressed surface tension, the foam expansion rose only slightly, and not to the accepted industry standard of between 10 and 20. It was assumed that Test Rig One was unable to expand the surfactant concentrate sufficiently and it was decided that the actual mechanism of foam formation should be investigated further. Distinguishing the properties that affect the expansion ratio and drainage rate could be completed after this had been determined.

After another literature search, it was discovered that very little work had been conducted on the manner of foam generation and the final aims of the project were therefore:

- To determine, using scale models, the foam generation mechanisms involved in producing foam from a low expansion fire fighting branchpipe.
- To distinguish which mechanism has the greatest effect on the expansion ratio.
- To discuss the relevance of these findings to the design of branchpipes.

1.5 *Experimental Work*

Chapter 3 describes the experimental work and techniques used in this research. It includes the refinements and development of Test Rig One to produce Test Rigs Two and Three and a review of the published foam measurement techniques, along with their drawbacks and the improvements that were incorporated. A description and overview of the equipment used is presented along with a full description of the statistical method of experiment design, which it is believed has not previously been

used in this context. The chapter also incorporates details of the high-speed video camera that was used to capture images of the jet from the nozzle to the final collision.

1.6 Findings

Three stages of bubble formation within the low expansion branchpipe system were identified:

- | | |
|--------------------------------|--|
| Stage One – Mixing | Mixing of the liquid and gas and the formation of bubbles occur within the branchpipe. |
| Stage Two – Flight | During the flight, bubbles grow, new bubbles are formed and the jet entrains air. |
| Stage Three – Collision | Foam forms when the jet collides with a solid or liquid. |

These findings were presented at the “Euro Foam 2000” Conference in Delft. They have been published in the Conference Proceedings (Rogers et al. 2000), a copy of the paper is included in Appendix A. This thesis elaborates on the paper and incorporates further work.

Chapter 4 describes the Stage One (Mixing) process, along with a literature review on mixing. The chapter investigates the relationships between the upstream liquid pressure, the liquid flow rate and the air entrainment rate. A comparison of the theoretical and actual expansion rates is included, along with a discussion of the differences. The shear force generated on the branchpipe by the jet was investigated and the results shown. The effects of incorporating obstructions into the branchpipe and changing the number and size of air holes were also investigated.

Chapter 5 describes Stage Two (Flight). The mixture of small bubbles, larger air slugs and liquid leave the branchpipe as a jet. As the jet travels it begins to break-up and entrain air. There are many factors involved in the break-up of the jet and therefore the literature review of this chapter has been subdivided into sections. The experimental findings section details the appearance of the jet at different stages in its flight. Evidence that bubbles are formed during the flight is also shown; this type of bubble formation within a jet does not appear to have been previously discussed in published work. Data on the difference in expansion ratio of foam produced after different lengths of flight is included.

Chapter 6 details Stage Three (Collision). When a liquid jet collides with a liquid, more bubbles are formed by the "plunging jet" method. In this method, air is taken under the surface by the jet entering the liquid. Although there have been comprehensive studies on air capture by the plunging jet method it has not been applied to the formation of foam. In addition, the majority of the work on plunging jets has been done with water and not with a surfactant solution. The Ross-Miles test is often used to determine the foaming properties of liquids, but again, to the author's knowledge, it has not been used to determine the actual properties of foam formation. The methodology of these techniques and the results of the Stage Three Collision process are included in this chapter. The factors that have the most effect on the formation of foam are highlighted with the use of a high-speed video camera. The development of a new method of measuring the amount of air entrained by a plunging jet, which is simpler than those in current use, is also described. The effects of a jet colliding with a solid are also included in this chapter. The effects of a two-phase jet

colliding with a solid or liquid surface have not been investigated, although hypotheses are suggested and included in this chapter.

1.7 Discussions and Conclusions

Chapter 7 discusses the results found and the conclusions drawn with respect to the aims of the project. It also highlights further work that would help the efficiency of the design process of fire fighting branchpipe systems. Further work in other areas resulting from the thesis is also discussed.

2 Literature Review on Foam

2.1 Introduction

This chapter provides a review on foams and bubbles, including their formation, structure and properties. The history of foam as a fire fighting medium and the properties and definitions used within the fire fighting industry are also discussed.

Foam is an aggregate of two-phases – a gas in a liquid or in a solid. This thesis focuses on the first group - gases in liquids. Foams having a high liquid content and wide distribution of bubble sizes are called fluid foams, gas emulsions or “Kugelschaum”. These bubbles are spherical. When the foam has a much lower liquid content, the foam bubbles deform into polyhedral shapes, and the liquid is present as thin films separating the bubbles. They are sometimes known as dry foams.

Bikerman (Bikerman 1953), (Bikerman 1973), Exerowa and Kruglyakov (Exerowa and Kruglyakov 1998) and Prud'homme and Khan (Prud'homme and Khan 1995) have published comprehensive books on foams and foam properties. This chapter draws on their works.

The main measures used to characterise a foam are expansion ratio and 25% drainage time. The foam expansion ratio is defined as the ratio of the volume of foam to the volume of the solution from which it was made (ISO-7203-1 1995), (ISO-7203-2 1995). Thus, a foam made from one volume of liquid and nine volumes of air has an expansion of 10. The 25% drainage time is defined as the time for 25% of the liquid content to drain from the foam (ISO-7203-1 1995), (ISO-7203-2 1995). The

International Standards Organisation (ISO) Standard also gives a method of determining the expansion and drainage times for fire fighting foams.

2.2 Formation and Structure

Foams are usually produced in one of two ways, condensation or dispersion.

Condensation: The gas is originally present but dissolved in the liquid. As the gas molecules or ions join, bubbles are formed. Condensation is responsible for the foam on beer.

Dispersion: The gas is generally present as a large separate phase at the start and is introduced into the bulk phase (the liquid) in order to form bubbles. Examples of foam formation by dispersion include blowing soap bubbles, injecting air into a surfactant solution and whipping eggs.

When dry foam is formed spherical bubbles meet and distort. The area where two identical bubbles touch will be a plane, and the thin film of continuous liquid sandwiched by these planes is known as a lamella. The point where three or four bubbles meet is called the Plateau border (Figure 2:1). The lamellae between these Plateau borders act as liquid drainage channels throughout the foam. If all three bubbles are of equal size the pressures at A, B and C (Figure 2:1) will be equal. If the bubbles are different sizes, the smaller bubble, which always has a higher internal pressure, will bulge into the larger bubble.

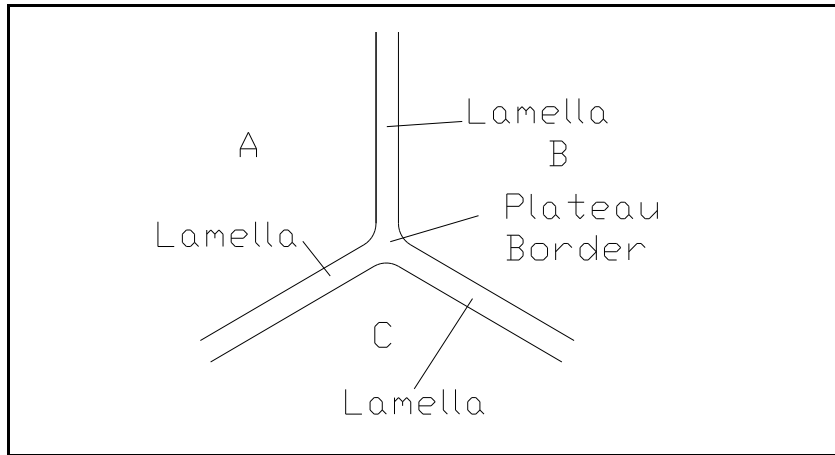


Figure 2:1 Interface between three bubbles

To be mechanically stable the angle between the Plateau borders where three bubbles meet will be 120° , regardless of their relative size (see Figure 2:2). Presupposing equilibrium, this can be shown as follows: six gas-liquid interfaces can be seen in Figure 2:1. Each tries to contract with a force γ (surface tension) per unit length; thus, each lamella pulls at the Plateau border with the force (per unit length) of 2γ . Three equal forces acting in one plane can balance each other only if the three angles between them are equal (120 degrees).

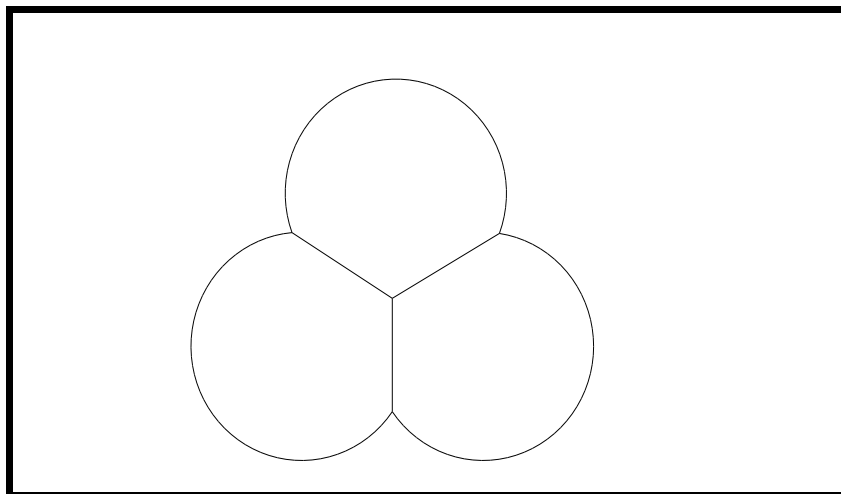


Figure 2:2 Mechanically stable foam

If a fourth bubble were added, as in Figure 2:3 A, the system would become unstable. The slightest movement would lead to an increase in pressure in one bubble compared to its neighbour. The bubbles would then move to an arrangement such as Figure 2:3 B, where again all the intersections meet at 120° (Bikerman 1973). The meeting of more than three films at a Plateau border is hardly ever observed in stable foams (Aubert et al. 1986).

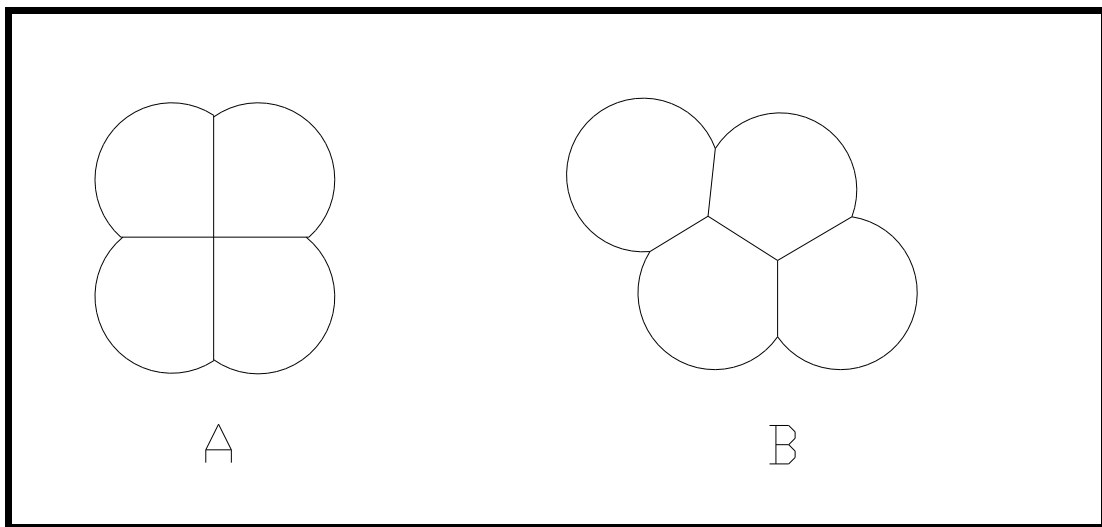


Figure 2:3 A: Unstable Four Bubble Arrangement, B: Stable Four Bubble Arrangement

A two dimensional foam consists of an approximately uniform hexagonal type of network. Three-dimensional foam however, is more complex. If all the bubbles had the same volumes, the equally sized bubbles would be regular pentagonal dodecahedra (a figure having twelve pentagonal sides). Unfortunately, foams never consist of exactly identical bubbles, and not all films between the bubbles are straight. On investigation, only 10% of the faces in an actual foam are pentagonal (Adamson 1982). Monnereau-Pittet and Vignes-Adler (Monnereau-Pittet and Vignes-Alder 1999) investigated foam topology using optical tomography and concluded that 99% of internal bubbles have a number of faces ranging from 12 to 15. Weaire's book

(Weaire 1996) collates many works on the problem of space filling. Rivier's article (Rivier 1996) reviews the investigations into space filling throughout history. He starts with Reverend S. Hales' work on the froth associated with peas. Hales stated that, after taking up water, the froth deformed into "pretty regular dodecahedra". This was challenged 150 years later by Kelvin's theoretical 14-hedra bubbles that were truncated cube or truncated octahedron, with six square faces and eight hexagonal faces. Much more recently (1994) Kelvin's model has been challenged by the Weaire-Phelan A15 structure. This is a space filling combination of one pentagonal dodecahedron to three "Goldberg" 14-hedra, with twelve pentagonal and two hexagonal faces. The difference in surface area between simple bubble shapes of volume 16.39 cm³ (1 inch³) is highlighted in Table 2:1. This shows that a sphere has the least energy in its surface, and therefore all single bubbles will try to form a sphere.

Shape	Number of sides	Surface Area (cm ²)
Tetrahedron	4	46.52
Cube	6	38.71
Octahedron	8	36.90
Dodecahedron	12	34.32
Icosahedron	20	33.23
Sphere	Infinite	31.23

Table 2:1 Properties of various structures (Exploratorium 1997)

2.3 Surface Tension

Surface tension (γ) can be defined as the force per unit length acting on either side of any line drawn in the surface of a liquid. It is therefore expressed in units of

force / unit length. Sometimes it is preferable to define the property in terms of surface energy / unit area, which is the work required to create one unit of new surface area. Both methods give the same numerical value.

The formation of bubbles in a liquid requires an increase in the free energy of the system, ΔF .

$$\Delta F = \gamma \cdot A \qquad \text{Equation 2:1}$$

Where:

A is the total interfacial area

γ is the surface tension

The Laplace Equation 2:2 relates the radius (r) and surface tension (γ) of a spherical bubble in a foam with the pressure difference between the outside and inside of the bubble. Therefore, lowering the surface tension at the site of bubble formation will make it easier for a bubble to form.

$$\text{Laplace Equation} \qquad = \text{---} \qquad \text{Equation 2:2}$$

Surface-active agents (surfactants) strongly depress the surface tension of a liquid - typically to about a third that of pure water. Solutes that do not affect the surface tension, in general, will not cause any foaming tendency.

Surfactant molecules are composed of long chains of carbon and hydrogen atoms. At one end of the chain is a configuration of atoms which is hydrophilic (likes water). The other end is hydrophobic (dislikes water). In a surfactant and water solution, the hydrophobic ends of the surfactant molecule do not want to be in the solution at all.

Those on the surface squeeze their way between the surface water molecules, and “push” their hydrophobic ends out of the water. This separates the water molecules from each other (see Figure 2:4). Since the surface tension forces become smaller as the distance between water molecules increases, the intervening surfactant molecules decrease the surface tension.

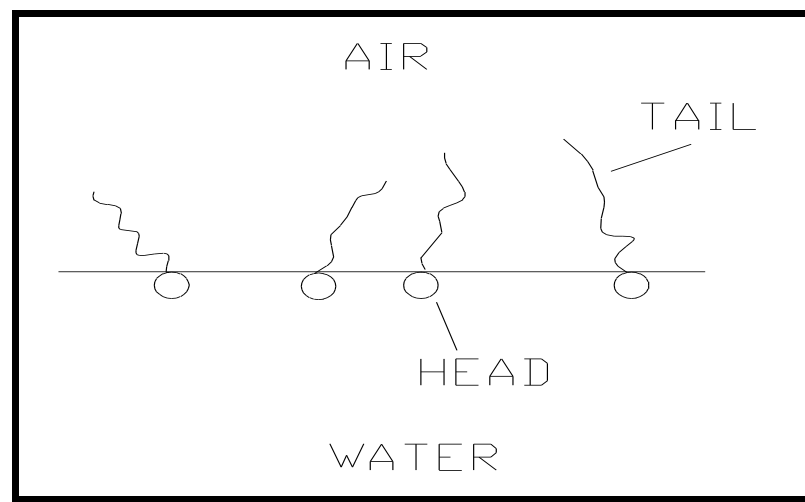


Figure 2:4 Surfactant in water

If a solution has at least one surface-active solute that can adsorb at the aqueous solution-air interface to form a coherent and elastic surface film, foaming can occur. The thin films of the solution show elasticity and mechanical strength (Rosen 1985).

Molecular Theory: Laplace introduced a working hypothesis for surface tension, based on the concept of a radius of molecular attraction, as quoted by Champion (Champion 1943). Each of the molecules in a liquid exerts an attraction on others within a certain radius, “C”. Beyond this distance the attraction is considered to be zero. If a molecule “A” is below the surface of the liquid by a distance greater than “C”, then the molecule will experience no resultant force as it is attracted equally in

all directions (see Figure 2:5a). However, if the molecule is less than distance “C” from the surface, it will experience a downward force, as there will be more molecules attracting it from below than above (Figure 2:5b). This downward force will be at a maximum for molecules at the liquid surface as there is a completely unbalanced hemisphere of forces acting from below on the molecule (Figure 2:5c). The molecule will therefore experience a force normal to the surface of the liquid. These normal forces acting over the whole of an isolated portion of a liquid, such as constitutes a drop, will cause that surface to take up a curved shape.

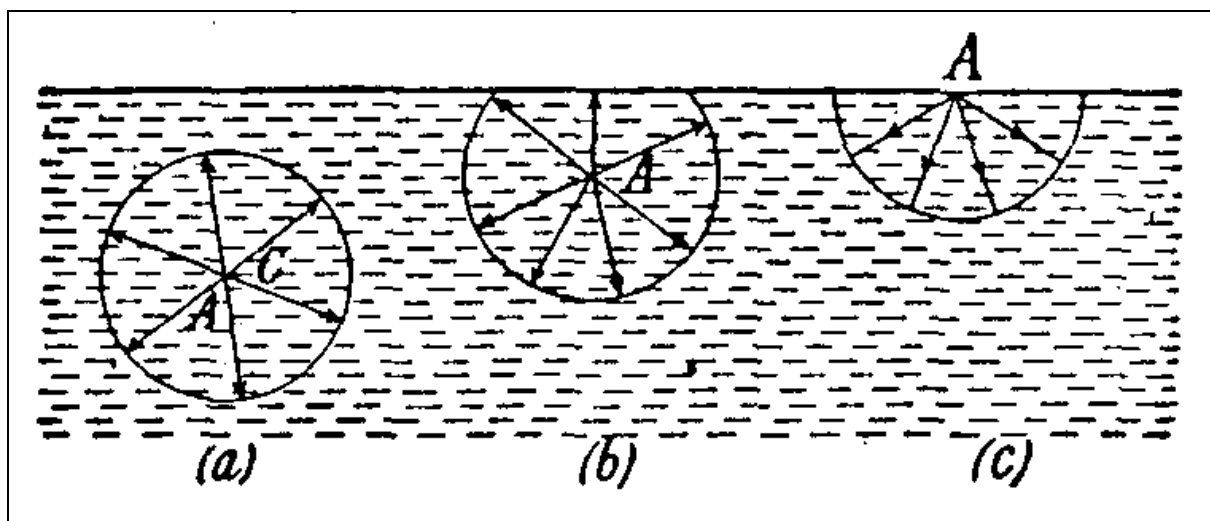


Figure 2:5 Molecular theory of surface tension

Solutions have a lower surface tension than the pure solvent but no simple law of variation with concentration is observed. However, a rise of temperature results in a fall in the surface tension and vice versa (Adamson 1982).

Dynamic Surface Tension: The dynamic surface tension of a solution is the surface tension as a function of the time after the creation of a new surface. The variation of surface tension with time is due to the migration of surfactant molecules to the surface

(Bikerman 1973), (SensaDyne 1995). The dynamic surface tension will vary from one non-equilibrium situation to another. It also depends on the time that has elapsed since the formation of the surface. Table 2:2, produced by Rayleigh and confirmed by Bikerman (Bikerman 1973), shows the difference between static and dynamic surface tension for fresh solutions and those that have reached their equilibrium state.

Liquid		Surface Tension (dynes/cm)	
		Fresh	Aged
Water		72	72
Sodium oleate	1:40	56	25
Sodium oleate	1:80	59	25
Sodium oleate	1:400	76	25
Sodium oleate	1:4000	76	53
Infusion of horse chestnut		73	49

Table 2:2 Surface tension of fresh and of aged surfaces

Micelles: Many solutions of surfactants exhibit unusual behaviour. At very low concentrations, the solutions behave like normal liquids, with predicted surface tension, osmotic pressure, ionic conductivity etc. Quite sharply, at a definite concentration, a new dispersed phase begins to form, osmotic pressure falls below that expected and the molar conductivity and the surface tension change abruptly. This is because the organic anions aggregate to form “micelles”. Micelles are considered to be roughly spherical with the hydrophobic ends of the ions pointing inwards and the hydrophilic ends forming the outer layer (Adamson 1982), (Lancaster_Univ_Chem._Dpt. 1998), (Aubert et al. 1986) (See Figure 2:6). The

number of ions in the micelles is of the order of tens. There are also similar cationic electrolytes.

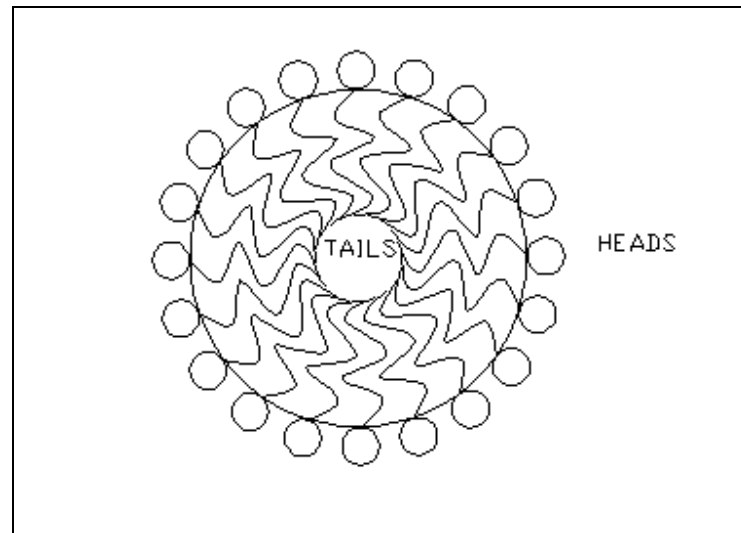


Figure 2:6 Micelle in aqueous surfactant solution

Rosen (Rosen 1985) describes the effect of chemical structures of different surfactants on the ease of adsorption, micellization and the orientation and packing of surfactant molecules. He concludes that, with reference to foaming, structural factors that decrease the surface area per molecule generally increase foaming power, whereas those that increase the surface area decrease it. For example, adding a substance that neutralizes or buffers the charge on an ionic surfactant causes a decrease in the surface area per molecule. This is due to mutual neutralization of the ionic head groups, which produces a surface film that is much more closely packed than that of either component, and will have a greater foaming tendency.

The critical micelle concentration (CMC) refers to the point at which the properties of the solution change abruptly due to the appearance of the new phase. When the micelle concentration increases beyond the critical value the excess is used in building

up more micelles, rather than contributing to the surface layer, and so the surface tension tends to remain steady beyond this point.

Measurement of Surface Tension: There are at least seven different methods for measuring the surface tension of a liquid (Champion 1943), (Adamson 1982). The classical method of measurement for static surface tension is the Du Nuoy torsion balance, which uses a platinum ring or a glass test plate in the “frame method”. This relies on the ring being gently pulled out of the liquid. When the upward force is greater than the pull downward, due to the surface tension, the ring parts from the liquid. The force required to do this is measured, and from this value, the surface tension is calculated. This method relies on a clean surface and difficulties are produced when there is foam or contamination on the surface.

The Fast Bubble Technique, as described in the American Society for Testing and Materials (ASTM_D3825-90 1990) and by Adamson (Adamson 1982), can be used to measure the dynamic surface tension. A capillary tube is immersed in the liquid and the pressure required for bubble formation at the capillary tip is measured at different gas flow rates. The pressure and a calibration constant are used to calculate the dynamic surface tension at various surface ages. The US Department of Commerce has produced a paper, (US_Dpt.Commerce Approx. 1950), which describes and uses the vibrating jet technique, which is more complex and time consuming than the Fast Bubble Technique.

If a fluid is used in a dynamic process it may be operating in the dynamic surface tension zone and have actual fluid surface tensions much higher than anticipated.

Using the classical du Nuoy ring techniques for testing the surface tension, in such cases, will not give accurate results. Hosseini (Hosseini 1991) and Christensen et al (Christensen et al. 1995) show that dynamic property measurements can reveal the most effective concentration of surfactant for purposes such as spray cleaning and oil recovery. However, this effective concentration is not necessarily related to the equilibrium CMC value, which most industries base their calculations on.

2.4 Properties of foam

2.4.1 Flow

A foam can flow like a liquid or remain motionless under stress like a solid. It may remain stationary under the force of gravity, but may easily flow when rubbed in the hand. The flow and deformation of foams are influenced by the manner in which the foam is generated, the properties of the liquid and gas, distribution of bubble size and the expansion ratio. There appear to be as many methods of measuring each of the properties, as there have been researchers. Previous work on foam rheology by one author using one technique is difficult to compare with the results from another author using another technique. The main reason for this is that any deformation, which is necessary in a rheological experiment, will alter the properties of the foam (Lucassen 1981). Heller and Kuntamukkula (Heller and Kuntamukkula 1987) have produced a literature review on foam rheology. They state that many of the reported rheological measurements do not truly or uniquely represent the rheological character of foams. Instead, the results appear to be strongly influenced by a factor that was not measured or reported - the thickness of a film liquid that formed along the pipe walls or against the rotating members of the viscometer used.

Foams are non-Newtonian, possessing a yield stress and a non-linear shear characteristic. This is probably due to the foam being two-phase, and may also be due to the concentrated surfactant itself being non-Newtonian. Typical foam bubble dimensions (10 μm – 1 cm) are much larger than the very fine scale dimensions of simple molecules that compose Newtonian fluids. Kraynik (Kraynik 1988) states that this promotes strong interactions between the foam structure and the flow and gives rise to non-Newtonian rheological effects. Viscosity is constant for Newtonian fluids, but for non-Newtonian two-phase fluids, like foam, viscosity decreases when shear rate increases (Bobert et al. 1997), (Corrie 1976c). The viscous nature of the foam depends on whether the yield stress is exceeded. Aubert (Aubert et al. 1986) defines the yield stress as the amount of force per unit area that triggers a deformation in which foam bubbles “jump” past one another to take up new positions. He states that for “dry” foams the yield stress is proportional to the surface tension in the films and inversely proportional to the size of the cells. Calvert and Nezhati (Calvert and Nezhati 1986) conclude that yield stress varies strongly with both flow rate and expansion ratio. Savage (Savage 1958) shows that the critical shear stress (yield stress) is related to the 25% drainage time. She states that the relation differs for different foam compounds and for different batches of the same compound, but for any one batch it is shown to be independent of expansion and compound concentration.

Gardiner et al (Gardiner et al. 1998) use a simple pendulum device to measure yield stress of aqueous foams approaching the dry limit. They conclude that the yield stress can be determined as a function of the expansion ratio and the bubble size. The

results using this method, when scaled by surface tension / average bubble radius, agree well with previous studies. This method appears repeatable and is the simplest and easiest method known to the author.

Various authors have proposed models for the rheology of foam. Kraynik and Hansen (Kraynik and Hansen 1987) have developed a two dimensional theoretical model of foam rheology by considering the deformation of spatially periodic cells in simple shearing and planar extensional flow. However, they ignore liquid drainage and so their model is only valid for very thin films, where the resistance to drainage is large. Calvert and Nezhati (Calvert and Nezhati 1986) have shown that the flow of a fire fighting foam can be modelled by a modified Bingham-Plastic system, with a liquid rich slip layer at solid surface. This model can also be used to describe the flow of fire fighting foams through a pipe. More recently, Neethling and Cilliers (Neethling and Cilliers 1999) have produced a model that simulates the liquid profiles of a flowing, coalescing foam. Their model has yielded physically realistic simulations when compared to actual flowing foam.

Persson and Dahlberg (Persson and Dahlberg 1994) have produced a theoretical model of foam spreading on liquids. The model is analogous to the spreading of oil slicks on water surfaces. Dahlberg (Dahlberg 1994) carried out foam spreading experiments in a water pool and water channel. The results from the experiments agree well with the theoretical predictions given by Persson and Dahlberg.

2.4.2 Foam Stability and Drainage

Foams are most commonly generated as spherical bubbles. As soon as they are formed, they begin to change and deteriorate. Murphy (Murphy 1996) and Jacobi et al (Jacobi et al. 1956) have produced good literature reviews that describe equations and models relating to drainage. The foam drainage is sensitive to the manner in which the foam is generated (Germick et al. 1994). As a foam drains the film lamellae become increasingly thin, and rupture begins to occur. In some cases, the uppermost films rupture first, so that the volume of foam decreases steadily with time. In other cases, it is mostly the interior laminae that rupture, so that the gas cells become increasingly large (Adamson 1982). Sarma and Khilar (Sarma and Khilar 1988) show that the higher stability of high expansion foams can be attributed to the presence of smaller lamellae thickness and a relatively more uniform bubble size distribution.

Germick et al (Germick et al. 1994) took experimental measurements of the foam-liquid interface for foams stabilised by different proteins, in a column. The foam was produced by bubbling air through the surfactant. The rate of foam drainage was found to be faster, and the extent of drainage larger, for smaller bubbles, larger initial foam heights and larger superficial gas velocities. Jacobi et al (Jacobi et al. 1956) completed similar experiments with standard fire fighting foams and also concluded that, in general, foams with the highest expansions exhibit the lowest drainage rates. Jacobi et al produced theoretically derived equations that fit the experimental data well.

There are two drainage laws that are particularly relevant to fire fighting foams, although several laws have been proposed. High expansion foams appear to conform

to the First Order Drainage Law - The instantaneous rate of drainage is proportional to the liquid remaining in the foam. This law implies a simple dependence on the “head” of foam, in which the mechanism of drainage is relatively unimportant. The Third Order Drainage Law - The instantaneous rate of drainage is proportional to the cube of the liquid remaining in the foam (Thorne 1970), is based on the model of drainage through Plateau borders. As low expansion foams generally have thicker Plateau borders than high expansion foams, they are more prone to drainage through these borders. Low expansion foams are therefore more likely to conform to the Third Order Drainage Law.

Benson et al (Benson et al. 1973d) investigated the method of determining the 25% drainage rate of fire fighting foams. They found that the sample size must be related to the flow rate of the foam stream being tested. They found that the 25% drainage time was independent of the drainage pan diameter but was related to the depth of the pan. They recommend standardising on a pan of depth 20 cm, but have also recommended pan diameters. For a foam stream of 5 l/min (of liquid) they suggest that a 6320 ml drainage pan should be used of 20 cm diameter by 20 cm deep. For a foam stream of $\frac{3}{4}$ l/min (liquid) they suggest that a 1630 ml drainage pan should be used of 10 cm diameter x 20 cm deep.

Foam made with a surfactant is relatively stable due to a pair of related phenomena - the Gibbs effect and the Marangoni effect (Klempner and Frisch 1991), (Ramesh and Malwitz 1994), (Baser and Khakhar 1994), (Aubert et al. 1986). A stretched film will “try” to contract, like an elastic skin. The stretching increases the film’s surface area,

and surfactant molecules from the interior of the liquid diffuse to the surface. This is the Gibbs effect. This process does not restore liquid to the film, although it does replenish the surfactant concentration at the surface. The Gibbs effect is often called Gibbs elasticity.

The Marangoni effect is temporary. If a bubble is indented, there is a time delay before the Gibbs effect takes place – whilst the surfactant molecules diffuse to the surface of the newly stretched film. Initially, therefore, the surface has a very low concentration of surfactants and the surface tension is greater than that of the surrounding surface. This greater surface tension tends to protect the bubble from bursting. The tension slowly decreases to the equilibrium value as surfactants diffuse to the surface.

The above is based on the concept that the Gibbs effect is so slow that the Marangoni effect has time to operate. The different surface tensions in the surface are maintained for long enough to cause some flow of liquid. This idea is confirmed by direct measurements of dynamic surface tension i.e. of the surface tension of solutions as a function of the time after the creation of a new surface.

2.4.3 Bubble Size

The average bubble size and the distribution of bubbles according to their dimensions are important properties of foams. They affect the rate and extent of bubble drainage and the flow of the foam. The diameter “ l ” of bubbles is often measured. However, as foam bubbles are not spheres they actually have no diameter. Usually the largest distance between two opposite walls of a bubble is identified with “ l ”. The frequency

distribution of bubble size has been proven to be independent of the position of the bubble in the foam (Bikerman 1973), (Chang et al. 1956). When bubble formation is slow, bubble volume increases with surface tension. This relationship diminishes with faster bubble formation (Bikerman 1953). Holder (Holder 1977) suggests that from bubble size and wall thickness measurements, it is possible to calculate all other existing properties of foam.

Measurement of Bubble Size: There are different methods of measuring bubble size. If an invasive method is used there is a problem in disturbing the local structure. Remote methods, such as optical or ultrasonic are possible. Ultrasonics, however, are unlikely to have the required resolution (Calvert and Nezhati 1987). Optical methods include a travelling microscope, a photograph of a sample of foam on a microscope slide and a narrow gap between two plates. The methods for obtaining average bubble numbers over a relatively large volume include electrical conductivity and the speed of sound in foam. Lewis et al (Lewis et al. 1984) describe a detection and analysis method for measuring bubble sizes and velocities in bubbly gas-liquid flows using a two electrode conductivity system. Their method requires discrete bubbles, rather than a foam. Calvert (Calvert 1987) states that electrical conductivity and speed of sound measurements are unlikely to be accurate enough to give variations across a flow field. An algorithm for froth surface bubble size distribution measurement has been put forward by Sadr-Kazemi and Cilliers (Sadr-Kazemi and Cilliers 1997). The model is based on the flow rate of bubble surfaces overflowing a weir in a free flowing froth. It requires an image processing system, which applies a segmentation algorithm to the original image of the froth. The algorithm is largely insensitive to

factors such as froth type, lighting conditions and bubble size and is only available for the surface of the foam.

Calvert and Nezhati (Calvert and Nezhati 1987) describe various methods of measuring bubble size and number. They used a travelling microscope but explained that it is extremely laborious and is subject to error arising from decay of the foam during the measuring period. They then photographed samples of slides on microscopes magnified between 40 and 80 times. The prints were of poor contrast and it was possible to see small bubbles through larger ones. These caused problems in the analysis using semi-automated image analysers. It also made the process laborious. The final analysis method used involved manual matching of the size of a light spot to each bubble image, followed by automatic logging of the counts in each size range and marking of the image to avoid duplication.

Amiri and Woodburn (Amiri and Woodburn 1990) use the Stokes's rise velocity in stagnant liquid to calculate the bubble size in a creamy foam. However, this appears only to be valid for spherical bubbles of diameter of around 35 μm . Chang et al (Chang et al. 1956) quick-froze foam and then microphotographed it to evaluate bubble sizes and bubble size distribution. They show that quick freezing does not significantly change the structure of the foam with respect to bubble size and distribution.

Thickness of a Bubble's Skin: Optical properties can be used to measure the thickness of the skin of a single bubble. Light reflects off both the surfaces of a lamella. The ray of light that reflects off the inside surface travels a longer distance

than the ray that reflects from the outside surface. When light reflects from the outside surface of the bubble (an air-to-water surface), the direction of vibration of the wave is reversed. When light reflects from the inside surface of the bubble (a water-to-air surface), the direction of the vibration is not changed. When the rays recombine they can get "out of step" with each other and interfere. Given a certain thickness of the bubble wall, a certain wavelength will be cancelled and its complementary colour will be seen (see Table 2:3). Long wavelengths (red) need a thicker bubble wall to get out of step than short wavelengths (violet). If the skin of the bubble is very thin, much shorter than the wavelength of visible light, then the two reflected rays of light will always meet crest-to-trough and destructively interfere. There will be no visible reflection, and the bubble looks black.

Thickness of Bubble's Skin	Colour Cancelled	Leaving
Thickest (approx. 500 nm)	Red	Blue/Green
	Yellow	Blue
(approx. 200 nm)	Green	Magenta
	Blue	Yellow
Thinnest (approx. 30 nm)	All	Black

Table 2:3 Complementary colours

2.5 Fire Fighting Foams

Water is unable to extinguish burning oils and many other flammable liquids, as it sinks below the surface. Foam however, due to its low density, floats on top of the burning liquid and suffocates the fire by acting as a blanket. As well as preventing the

oxygen from combining with the fuel, it also prevents the fuel from being evaporated (Jeulink 1983). By the 1950's the use of foam as a fire fighting medium was well developed and the basic types and definitions are still in common use today. Ratzer (Ratzer 1956) produced an in depth paper on the history and development of foam as a fire fighting medium. The rest of section 2.5 is largely based on his work and the work by Perri (Perri 1953).

The first British patent for the use of foam as a fire fighting agent was registered by J.H. Johnson in 1877 (Johnson 1877). In the early 1900's Laurent (Laurent 1904) extinguished a naphtha fire by application of foam, generated by the reaction of two aqueous solutions. By the 1920's, these 'chemical foams' were in common use in the English Fire Brigades. World War II saw the Armed Forces using various forms of soap solutions as foaming agents in their aircraft crash fire fighting vehicles. By the mid to late 1940's specifications for protein based foams were produced in both Britain and America for military applications and these helped to raise performance standards. By 1947, complete fire protection systems became a standard by petroleum processors for refineries (Angus 1985). Fire fighting foams are now in general use throughout the world to control and extinguish fires of flammable liquids and for inhibiting re-ignition. They are also used to prevent ignition of flammable liquids and, in certain conditions, extinguish fires of solid combustibles.

The properties of most concern to fire fighters include expansion ratio, drainage, flow, burn-back resistance, fuel pick-up, knockdown and contamination resistance. These are all defined in the glossary.

2.5.1 Fire Fighting Foam Types

Different risks in fire fighting and protection gave rise to differences in perceived needs of foam characteristics and therefore different foams have been developed. Some foams are thick and viscous and form tough, heat resistant blankets over burning liquid surfaces and vertical areas. Other foams are thinner and spread more rapidly. Chemical foam extinguishers are becoming obsolete, as liquid foam-forming concentrates are easier to handle and are more cost effective.

The types of fire fighting foams can be divided into three categories based on their expansion ratio - High, Medium and Low Expansion foams. The type of foaming agent (surfactant concentrate) is also used to group the foams. Scheffey (Scheffey 1997), Martin (Martin Approx. 1970) and NFPA (NFPA 1992) describe the types of foams in detail, and sections 2.5.1 and 2.5.2 largely draw from these works.

2.5.1.1 Expansion Ratio

Low Expansion Foam: Foam with an expansion ratio of below 20 (20 parts foam from every 1 part liquid) is described as low expansion. It is used principally to extinguish burning flammable or combustible liquid spill or tank fires by developing a cooling, coherent blanket. Low expansion foams can be made from all but the detergent concentrates.

Medium Expansion: This is foam with an expansion ratio in the range 21 to 200. It is used in minor incidents such as fires involving small hydrocarbon-liquid spills and in cellars and basements. Medium and high expansion foams are most effective when dealing with outbreaks of fire in inaccessible locations. Examples include fires where

direct application of conventional agents, such as water, is difficult or impossible due to smoke or restricted access. Medium expansion foams can also be made from all but the detergent concentrates.

High Expansion: A high expansion foam is defined as a foam with an expansion above 200. They are generally made from detergent concentrates. Jamison (Jamison 1967), (Jamison 1969) and Butlin (Butlin 1967) discuss high expansion foam and its use within the UK's fire departments, and include a survey of high expansion air foam, its properties and uses. Langford and Stark (Langford and Stark 1964b) and Langford et al (Langford et al. 1962) investigated the control of fires in large spaces using air and inert gas filled high expansion foams, from a novel turbo-jet engine powered generator. They conclude that high expansion foams are a practical and useful agent in fighting many types of fires. Inert gas filled foam can extinguish both wood and liquid fuel fires efficiently. Air foam is less efficient for liquid fuel fires, but has a similar efficiency for extinguishing wood fires. As high expansion foam can be generated in large volumes quickly, it has proved particularly useful in fighting unventilated and inaccessible fires such as in mines, basements, cellars, service tunnels and railway tunnels. High expansion foams are also commonly used in areas such as ships' holds, tyre deposits, high stock storage rooms, warehouses, cable ducts, aircraft hangars, paper/cardboard packaging plants, flammable liquid stores, incineration plants, chemical stores and transformer rooms. New or growing applications include: ships' engine rooms, ships' machinery spaces, ships' pump rooms, libraries, document stores/archives, historic buildings, agricultural pesticide storage, liquefied natural gas, liquefied petroleum gas, computer rooms and data

processing areas. High expansion foam is also being developed for use in fighting forest fires (Hendrickson 1990).

High expansion foams cannot be projected and generally roll along as a layer. They minimise the amount of wetting to equipment and contents. If the foam is filled with air, a person caught inside the deluge will still be able to breathe and move slowly around. High expansion foams may also be used in combination with other extinguishing media, particularly halons, carbon dioxide and powders.

Langford and Stark (Langford and Stark 1964a) conducted experiments to select satisfactory foaming agents for producing high expansion fire fighting foams. They concluded that the half-life (collapse to half the original volume) and half drainage times may be used for selection between concentrates.

2.5.2 Surfactant concentrate

There are a number of types of foaming agents available, known as surfactant concentrates, some of which are designed for specific applications. The surfactant concentrate percentage refers to the amount of concentrate that is proportioned or pre-mixed with water to give the resulting surfactant solutions. In addition to the surfactant, proprietary foam liquids contain other ingredients to make them more suitable for their intended use. Examples include antifreeze, viscosity reducers and antibacterial agents (Corrie 1976b), (Martin Approx. 1970).

Benson et al (Benson et al. 1973c) have reported on the long-term storage of four surfactant concentrates. They conclude that most showed a fall in 25% drainage rate

over time. If used at the correct concentration however, the time to control the test fire did not increase in most cases.

Surfactant concentrates, for use in fire fighting equipment are certified for use on a particular type of fire. This is completed by a demonstration of its ability to extinguish the fire and the properties of the foam it produces, as defined in the relevant ISO or NFPA standard or UL listings. Generally, one type of foam is only applicable to one type of fire. Angus' FP70, which is an industry standard low expansion surfactant concentrate, is billed as "a FluoroProtein fire fighting surfactant concentrate for extinguishing and securing flammable hydrocarbon liquid fires" (Angus-Fire 2000). The concentrate manufacturer will describe the type of equipment that should be used with the concentrate. Angus state that "FP70 should be used with air aspirating discharge devices such as low expansion branchpipes, monitors, top pourer sets, rimseal foam pourers, and foam / water sprinklers. It also produces top quality medium expansion foam when applied through medium expansion branchpipes and bund pourers." The foam generation equipment is also mainly specific to one type of fire, and does not usually require special certification. It must be able to produce foam with the properties specified by the surfactant concentrate manufacturer. Descriptions of the common types of surfactant concentrate are given below.

Protein Based Foams: The first protein based foams were produced by cooking, extracting and mixing protein by-products, such as hoof and horn meal, and hydrolysing with lime. Hoof and horn meal is still the most convenient source of protein, but other sources such as soya beans, fishmeal and feather meal are also

employed. Other alkalis or mixtures of alkalis are now used in place of lime. Protein foam has 30-35% solids content. The resulting product is very thick and does not roll easily, therefore it is difficult to apply. This product has a good burnback and is a highly stabilised mechanical foam with good expansion properties. Typically, these agents are used to protect flammable and combustible liquids where they are stored, transported and processed.

Fluoroprotein Foams: The concentrates used for the production of fluoroprotein foams utilise protein foam. They have fluorinated surfactants added to improve the fluidity and reduce fuel pick up by reducing surface tension. The total solids content is approximately 35-45%.

Film Forming Fluoroprotein (FFFP) foams are enhanced protein foams but with more stabilisers and stronger fluorosurfactants. These reduce surface tension to the point where weak film forming occurs, at the expense of burnback resistance performance. The film forming ensures the FFFP foams provide better control and extinguishing ability, greater fluidity and superior resistance to fuel contamination than protein foams. They are therefore often involved in applications involving hydrocarbon bulk storage and handling - such as refineries and petrochemical operations. Fluoroprotein foams are also useful for hydrocarbon vapour suppression. They are a very effective fire suppression agent for sub-surface application to hydrocarbon fuel storage tanks.

Fluorochemical Foams (Aqueous Film Forming Foams (AFFF)): The surfactant concentrate is based on a mixture of hydrocarbon, synthetic fluorinated surfactants and stabilisers. A very low energy is required to produce a high quality foam. They

can therefore be applied through a variety of foam delivery systems. The foam has the ability to form an aqueous film on the surface of some hydrocarbons. This type of foam has a better knockdown than protein but the burnback is not as good. Its versatility makes AFFF agents an obvious choice for municipal fire departments, airports, refineries, manufacturing plants and any other operation involving the transportation, processing and handling of flammable liquids and materials.

Detergent Foams: Detergent foams are a completely synthetic product. They are usually developed for high expansion foam, but are generally less stable than other fire fighting foams.

Alcohol Resistant Foams: Alcohol resistant foams can be made from both chemical and protein foams. They have polymers added as a barrier to protect the water in the foam from the water miscible fuels. They are therefore more resistant to breakdown when applied to the surface of alcohol or other polar solvents than other foams.

2.5.3 Fire Tests

There is a complex relationship between the properties of foam, its performance under different fire conditions and the best method of applying it to a fire. In 1961 Hird et al (Hird et al. 1961) developed a fire test to form part of the acceptance procedures for foam liquids for use by British Government Departments. Before this, a 'Figure of Merit Test' was used (Fry and French 1951a), but this did not distinguish between individual properties of the foam. By 1974, with the introduction of foam liquids other than protein, another test method was required and was devised by Benson et al (Benson et al. 1974). All these tests were conducted within a laboratory, which

enabled weather conditions to be eliminated from the results. In 1992 the scale of the fire test (4.5 m²) in the ISO Standard For Foams (ISO-7203-1 1995), was deemed to be too large. A smaller scale fire test was developed by Persson (Persson 1997). This had the following advantages:

- Reduced heat and smoke emission.
- Reduced testing cost.
- Avoidance of the disposal of large quantities of contaminated fuel.
- Suitable for routine quality control tests.
- Allowing testing of a number of flammable chemicals and hydrocarbons.
- Permitted the possibility to study the effects of various parameters such as water quality, temperature, foam ageing etc.
- Allowed cheaper and more environmentally friendly testing activity in the development of new foams.

However, ISO 7203 Parts 1 and 2 (ISO-7203-1 1995), (ISO-7203-2 1995) are currently still in use in the UK. They specify the essential properties and performance of liquid surfactant concentrates used to make low, medium and high expansion foams. These foams are used for the control, extinction and inhibition of re-ignition of fires of water immiscible liquids. These standards specify the minimum performances on certain test fires are specified.

French (French 1952) shows that the maximum resistance to radiant heat is obtained from a foam of low expansion and high shear strength. He also shows that heat-resistance depends on the water content of the foam over the range of expansion

factors. Persson (Persson 1992) shows that the rate of evaporation from the foam layer is almost the same for all types of foams and proportional to the radiation level. Persson also states that 65-75% of the incoming radiation is used in the evaporation of the foam. Isaksson and Persson (Isaksson and Persson 1997) state a further 5-8% is absorbed by drainage. Isaksson and Persson have also produced a test rig and method for measuring the heat exposure characterisation of fire fighting foam. They focus on the drainage and foam destruction rates and on the foam layer thickness. They conclude that the drainage characteristic is dependent on both the foam thickness and heat radiation.

The use of the different surfactant concentrates on petroleum and other industrial fires has been extensively studied (Rivkind and Myerson 1956), (Tuve and Peterson 1956), (French and Hird 1961), (Nash and Fittes 1968), (Tucker et al. 1972), (Nash 1975), (Corrie 1975), (Ayers 1989), (Johnson 1988), (Foster), (Johnson 1992), (Johnson 1993), (Johnson 1994), (Cash 1995a) and (Cash 1995b). They conclude that the effectiveness of any foam system depends on the correct choice of surfactant concentrate, equipment and application method for the particular hazard that requires protection.

Using two or more different foam liquids on a fire can have a detrimental effect. When fluorochemical and protein foams are used together there is no reduction in control and extinction performance, however, the protection from re-ignition is reduced (Chitty et al. 1972). Work by Benson et al (Benson et al. 1973a) describes a measurement of the compatibility between fluorochemical and fluoroprotein foams, by means of burnback resistance. They state that there is a definite decrease in

burnback time obtained when the two foams are used together, but it is not sufficient to warrant a strict avoidance of using the two foams together.

3 Experimental Work

3.1 Introduction

This chapter provides a description of the experimental work and techniques used in this research. It includes the development of the test rigs and a review of the published foam measurement techniques, along with their drawbacks and the improvements the author incorporated. It also includes a description and overview of the equipment used. A full description of the statistical method of experiment design, which the author believes has not previously been used in this context, is also incorporated.

3.2 Development of the Test Rigs

The following parameters were suggested as those most likely to affect the expansion ratio and drainage rate of the foam:

- Concentration of surfactant
- Solution flow rate and pressure
- Nozzle angle
- Cone type
- Gauze presence and type
- Airflow rate

3.2.1 Pipework and Pump

The pipework and pump were developed to enable the first four of these parameters to be changed easily (see Figure 3:1).

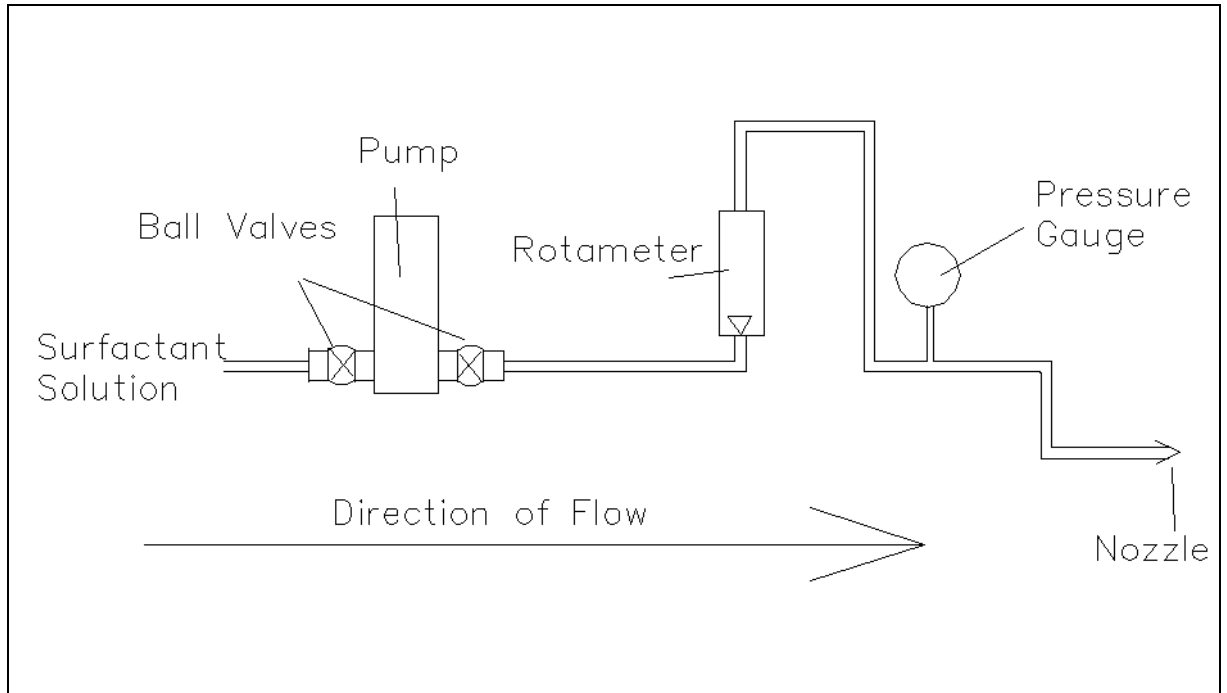


Figure 3:1 Pipework used in all tests

By using separate tanks prepared with the different concentrations of surfactant, the surface tension of the solution could be changed. The diluted surfactant solution was pumped to the nozzle, via a rotameter. The liquid flow rate was variable between 10 and 25 l/min and was controlled by a ball valve positioned downstream of the pump. Nozzles with different nozzle angles and cone types could be attached to the end of the pipework. The different nozzle types incorporated hollow and full cone nozzles (see Figure 3:2) with 60° or 120° spray angles. They were chosen to ensure that each produced a similar flow rate at specified pressures.

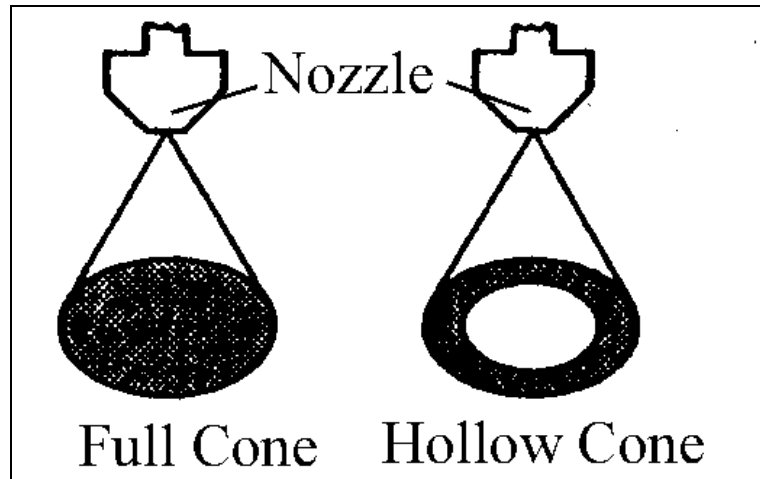


Figure 3:2 Pattern of spray from full and hollow cone nozzles

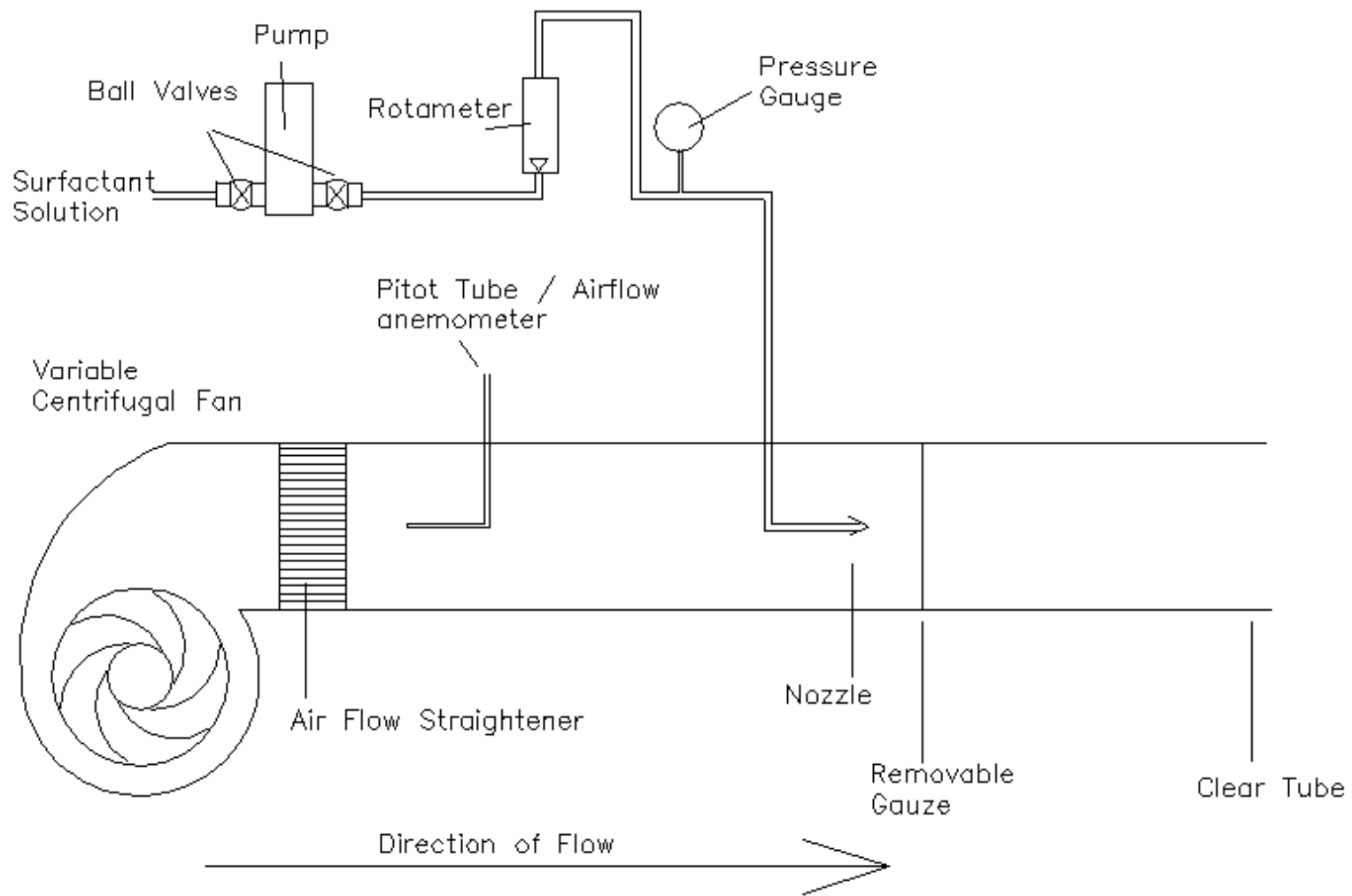


Figure 3:3 Test Rig One - Schematic with 200 mm diameter tube

3.2.2 Test Rig One

Test Rig One (Figure 3:3) was designed to enable the remaining two parameters to be changed:

- Gauze presence and type
- Airflow rate

The gauze was connected using a gauze adapter that could incorporate any design and thickness of gauze. A single layer of “Knitmesh” was used in the experiments requiring a gauze. The “Knitmesh” used was nylon with square holes of approximately 5 mm length sides. The gauze was completely removed when not required.

A centrifugal fan with a variable control was used to control the airflow rate. To reduce the turbulence generated by the fan, an airflow straightener was positioned downstream. A pitot tube was placed three diameters downstream of the straightener, to determine the air speed. However, in some experiments the air flow was very small, and so a higher sensitivity thermal anemometer was fitted.

To allow production of foam with an expansion ratio of 1000, the area of the tube was 1000 times larger than the area of the nozzle bore, to ensure a minimal change in velocity from surfactant solution to foam. To determine the effect of tube diameter on the expansion ratio of the foam produced, an adapter was used to enable the tube diameter to be reduced from 200 mm to 100 mm. The tube was clear acrylic, to enable the foam production to be seen.

Uncontrollable variables included the temperature of the liquid, atmospheric pressure (which were not recorded) and the air temperature (which was recorded).

The liquid flow rate through the pump on Test Rig One, at full pressure, was 25 l/min. Production of foam with an expansion ratio of 1000 would have generated approximately 25,000 l/min (25 m³/min). This would have caused a very large disposal problem. The ISO standard (ISO-7203-2 1995) for measuring the expansion ratio and drainage rate for high expansion foams calls for a collecting vessel of a nominal volume of 500 litres. Not only was this very difficult to procure, but it would also have been too heavy and cumbersome to lift and move between the test-rig and the scales. In personal communications with two surfactant solution manufacturers, it appears that high expansion foam is very rarely tested for expansion ratio using the ISO standard method, due to these difficulties. The manufacturers often scale up the medium and low expansion foam results. As they assert that low expansion foam can be used to calculate the properties of medium and high expansion foams, it was decided to use the low expansion surfactant solution, Angus' FP70.

The majority of the foams generated using the FP70 surfactant solution and Test Rig One had an expansion ratio of between 1 and 5, whereas it was expected to be nearer 20 - the boundary of medium and low expansion foams. On a few of the set-ups the ratio increased, but it was never larger than 11. Changing the diameter of the tube from 200 mm to 100 mm had no appreciable influence on the expansion, nor did including obstructions. Some of the experiments were repeated using a high expansion surfactant solution, Rockwood's Macrofoam. This again had little effect on

the expansion ratio of the foam produced. Appendix B includes the results and conclusions from the experiments using this test rig.

It was assumed that Test Rig One was unable to expand the surfactant solution sufficiently. It was therefore decided that the actual mechanism of foam formation should be investigated further, before continuing with work on developing an improved product.

3.2.3 Test Rig Two

As the first test rig had not been very successful, a scale model of an actual CounterFire Limited branchpipe was produced. This was a one tenth scale model (see Figure 3:4). This test rig was attached to the same pump and pipework described above, although the fan and airflow straightener were removed. Rockwood's Macrofoam is a detergent based concentrate, whereas the FP70 is produced from horn and hoof. The Macrofoam is therefore more user friendly (it does not smell like an abattoir), and it was decided to continue the experiments using this concentrate.

The nozzle was machined from nylon and had a smooth profile. The branchpipe was made from clear acrylic to enable the mixing within the tube to be viewed. The reducer at the end of the branchpipe was also machined from nylon.

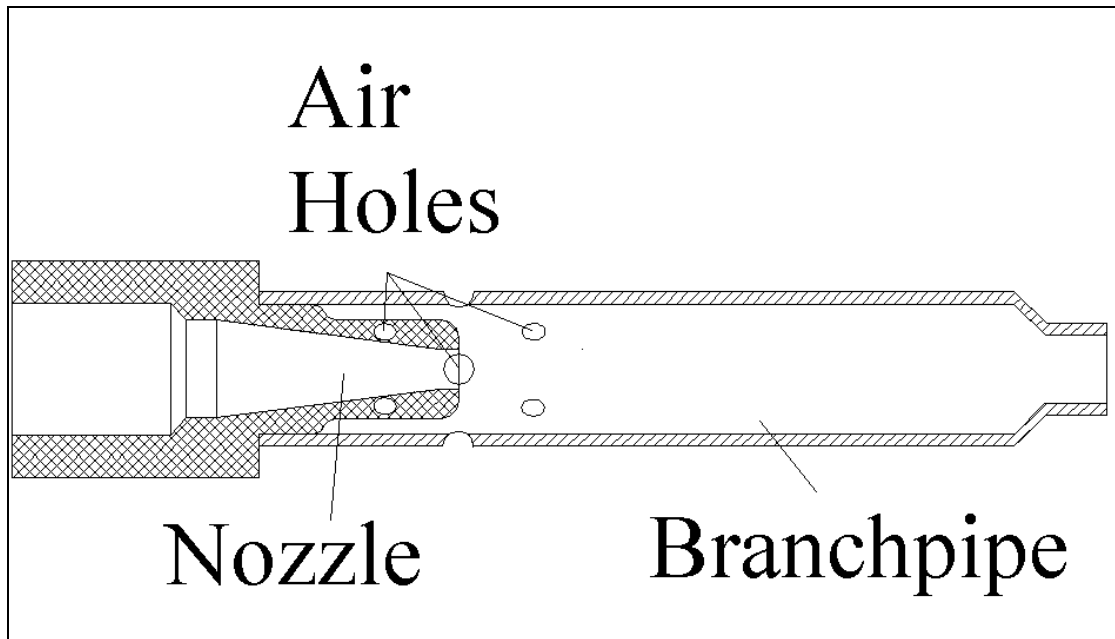


Figure 3:4 Test Rig Two: Schematic

In a full scale branchpipe, the jet appears to leave the reducer as a rope of foam, the diameter of which is the same as that of the reducer. However, in the scale model the jet of surfactant solution did not expand to the sides of the branchpipe, but just passed straight through. Hatton and Osborne (Hatton and Osborne 1979) state that in a large jet the turbulent eddy sizes are much greater and disrupt the jet surface smoothness more easily than for a small jet. This may explain the difference between the scale model and the full scale branchpipe.

The straight nozzle was then replaced by a 60 degree full cone nozzle. This caused the surfactant solution to spray out through the air holes, but a foamy jet was projected from the reducer.

3.2.4 Test Rig Three

Test Rig Three (Figure 3:5) was developed to overcome the problem of the surfactant solution spraying through the air holes. It was also simplified by removing the reducer, which is mainly used to increase the velocity and hence throw of the final jet. All the results using Test Rig Three are shown in Appendix F.

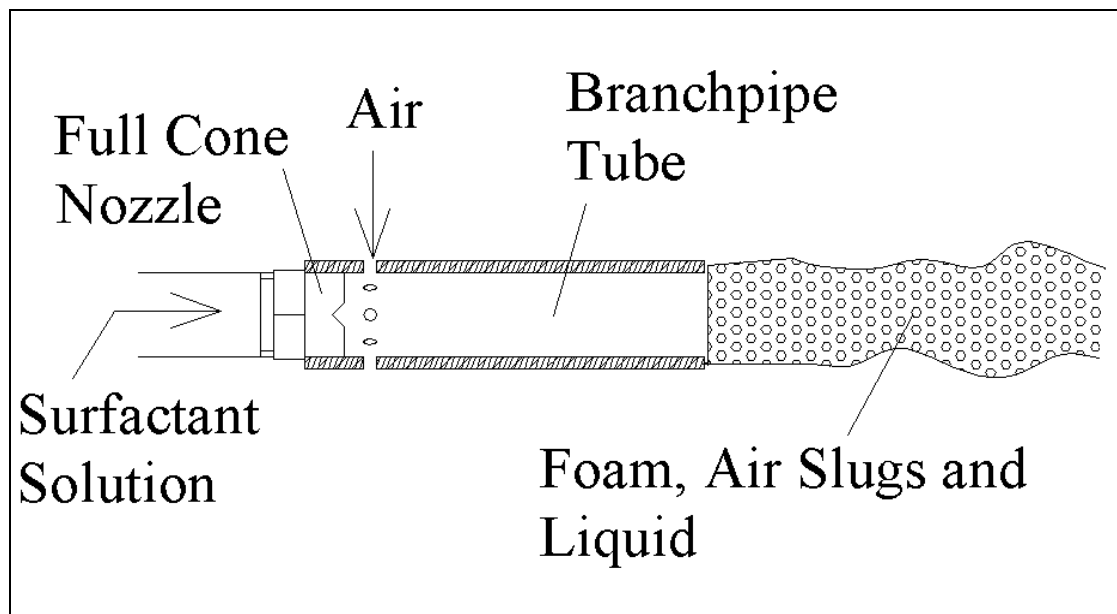


Figure 3:5 Test Rig Three: Simplified branchpipe

The pipework was the same as in the previous Test Rigs, with the fan and air flow straightener removed. The branchpipe was acrylic and had a 22 mm inside diameter. The 60 degree full cone nozzle was used, along with Rockwood Macrofoam, diluted at a nominal 3 %. The air holes in the branchpipe were drilled circumferential in one row, equally spaced. Different lengths of branchpipes were constructed with different numbers and sizes of air holes as seen in Table 3:1. Obstructions were placed within some of the tubes to see the effect of increased turbulence.

Tube length	No. Holes	Hole diameter
mm		mm
100	8	3.2
100	4	3.2
100	8	2.1
100	4	2.1
100	6	3.2
500	8	3.2
500	4	3.2

Table 3:1 Branchpipe Design

To calculate the flow rate of the air entrained, a tube - shaped shroud was made. This enabled a thermal anemometer to be inserted to measure the speed of the air entering the shroud (see Figure 3:6). The amount of air entrained was then calculated from the air speed and the diameter of the shroud.

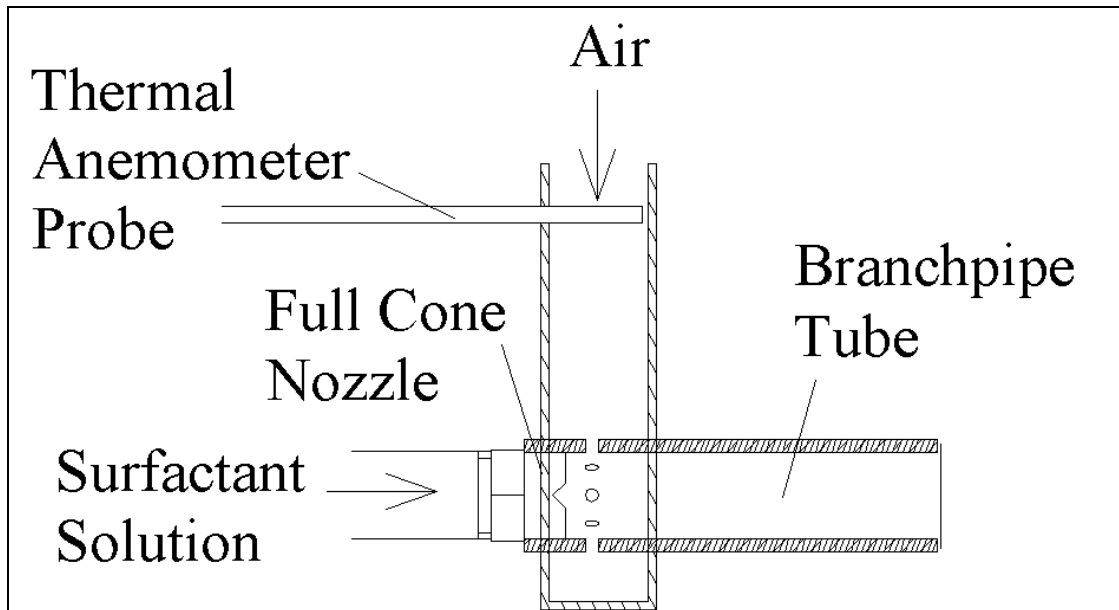


Figure 3:6 Air shroud with thermal anemometer probe

Shear force caused by the jet on the walls of the branchpipe was measured using the test rig in Figure 3:7. The branchpipe tube was restrained by two steel leaf springs so that it could move only in the “x” direction. With no flow, and so no force on the tube, the position of the pointer (A) on the rule was noted. When the liquid was pumped through the nozzle the shearing force on the branchpipe tube caused the leaf springs to flex and the tube to move to the right. Weights were then added at (B) until the pointer was at its original position. The force in newtons was then calculated.

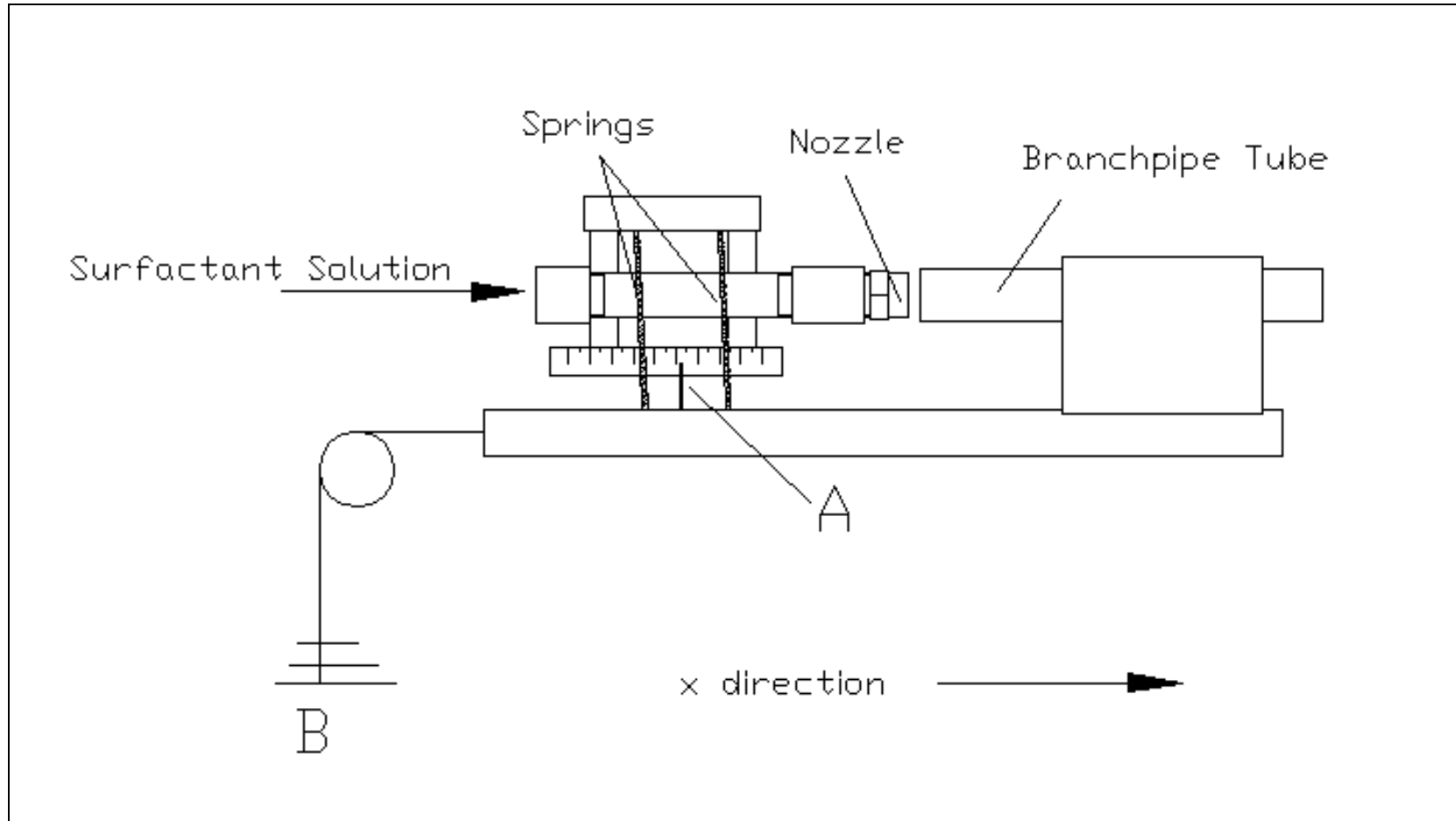


Figure 3:7 Test rig for force measurements

3.3 Atmospheric Conditions

As the experiments were conducted at different times of the year, the atmospheric pressure therefore varied and the air and liquid temperatures were not kept constant. Also, the surfactant solution was recycled after each experiment and it is therefore possible that each refilled tank had a slightly different surface tension. The air temperature was measured and appears to have had no effect on the expansion ratio of the foam produced. Experiments repeated using different tanks and on different days are in good agreement with each other. This implies that the uncontrollable variables had little effect on the foam generation process.

3.4 Foam Property Measurement Techniques

Fire fighters have different perceptions of the desirable properties of the foams they use, but the expansion ratio and drainage rate are commonly used criteria. The International Standards Organisation (ISO) produced standards ISO 7203 Parts 1 and 2 (ISO-7203-1 1995), (ISO-7203-2 1995). These standards specify the essential properties and performance of liquid surfactant solutions used to make low, medium and high expansion foams for the control, extinction and inhibition of re-ignition of fires of water immiscible liquids. The American National Fire Protection Association (NFPA) have also produced a standard for low expansion and combined agent systems (NFPA 1988). This standard has been approved by the American National Standards Institute. The NFPA standard is almost identical to the ISO standard for low expansion foams, with the procedure being the same, but with a slight difference in the wording.

3.4.1 ISO STANDARD 7203 Part 1 Annex F

The ISO standard for measuring the expansion ratio of low expansion foam (ISO 7203 Part 1 Annex F) is designed so foam impinges on a sloping board (see Figure 3:8) and drains into the measuring vessel (see Figure 3:9).

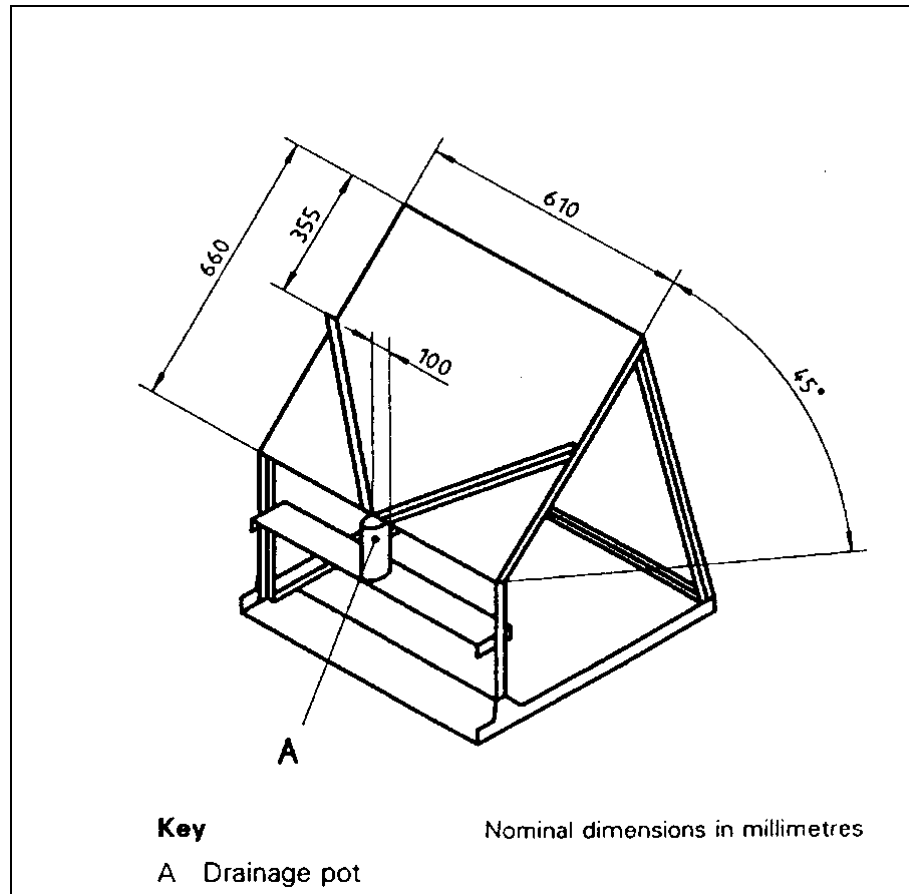


Figure 3:8 Foam collector for expansion and drainage measurement (ISO-7203-1 1995)

The procedure to measure the expansion and drainage rate used for the experiments with Test Rig One were based on the procedure in ISO 7203 Part 1, Annex F. The collecting vessel and the foam collector were manufactured to the ISO specification. However, as the test rig was measuring the effects of different branchpipe set-ups, the foam making nozzle was not standard. The distance from the nozzle to the foam collector also did not meet the standard. The temperature conditions were unable to

be kept within the specified limits, as the test area did not have heating. The surfactant solution temperature was not measured.

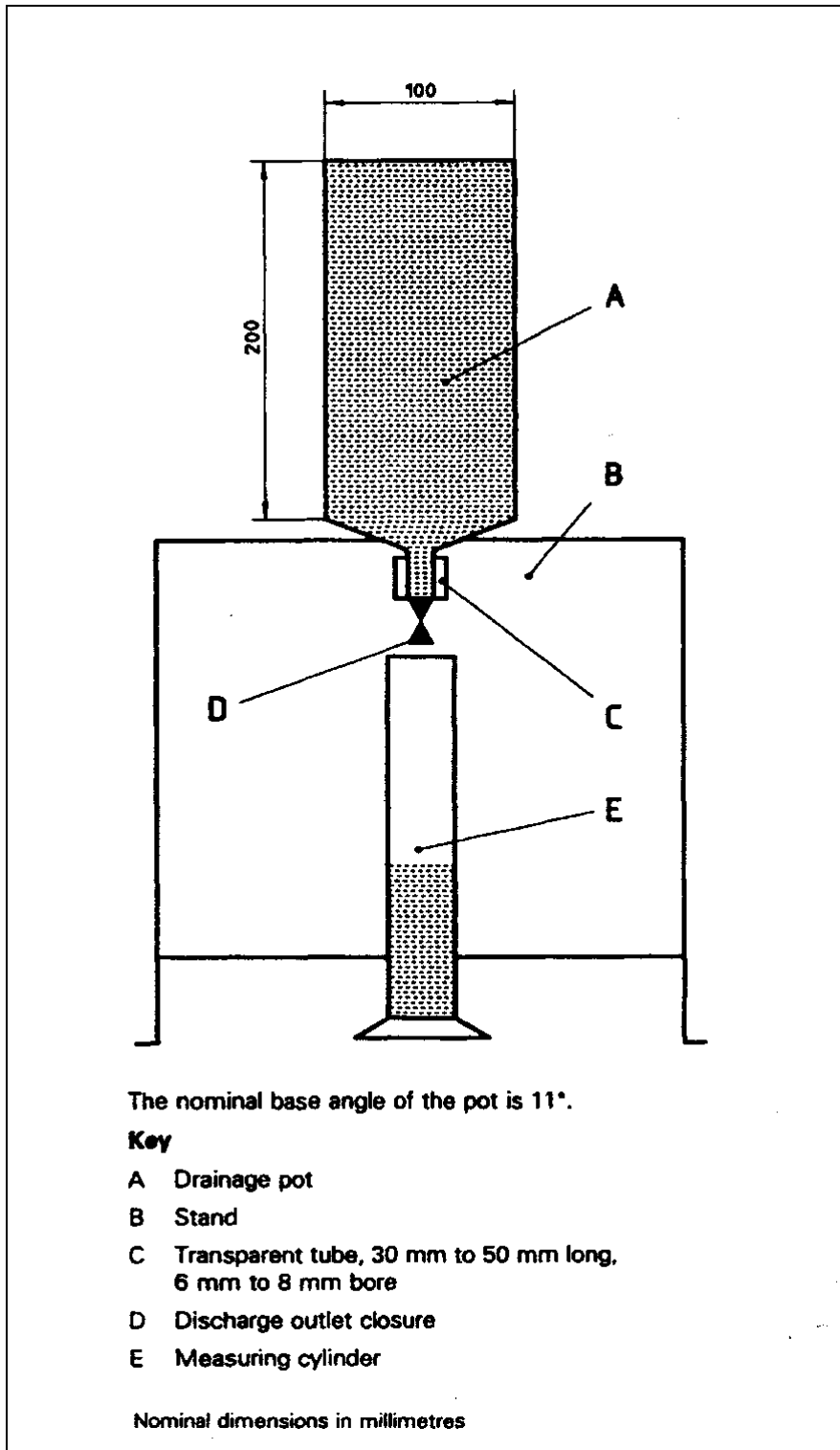


Figure 3:9 Collecting vessel for determination of expansion and drainage time
(ISO-7203-1 1995)

The procedure used was as follows:

1. Wet the collecting vessel internally and weigh it (m_1)
2. Start the pump
3. After 30 seconds, put the collecting vessel into the collector
4. As soon as the vessel is full, remove it from the collector, strike the foam surface level with the rim and start the clock
5. Weigh the full vessel (m_2)
6. Open the drainage facility and collect the surfactant solution in the measuring cylinder
7. Adjust the drainage facility such that the drained surfactant solution may flow out whilst preventing the passage of foam
8. Record level of foam drained and time approx. every 60 seconds for ten minutes

The 25% drainage rate was calculated from the time required for 25% of the liquid content to drain out of the foam. The expansion ratio was calculated using Equation 3:1, given in the ISO standard, with the assumption that the density of the surfactant solution is 1000 kg/m³:

$$E = \frac{V}{m_2 - m_1} \quad \text{Equation 3:1}$$

Where:

E is the Expansion Ratio

V is the volume in litres of the collecting vessel

m_1 is the mass, in kilograms, of the empty vessel

m_2 is the mass, in kilograms, of the full vessel

This method was not particularly successful when using the scale models, as any under expanded surfactant solution drained more quickly down the slope and into the vessel than the expanded foam, thus giving a false overall expansion calculation.

The ISO standard may be satisfactory for collecting foam generated through the standard foam making nozzle (branchpipe) at a distance of 3 ± 0.3 m. However, different branchpipe designs may produce a non-homogeneous foam and as mentioned above, the wetter foam will drain more quickly into the collecting vessel and provide a false expansion ratio. Also, low expansion foam is often projected distances further than 3 m in a real fire fighting situation. A surfactant solution may produce foam of the required expansion and drainage when generated through a standard foam nozzle and collected at 3 m. However, if it cannot be projected much further, it may not be suitable for certain fire fighting situations.

An improved method of determining the expansion ratio of a foam generated from a branchpipe is to collect all of the foam produced in a larger vessel, which also acts as the foam collector. The vessel should be put into the flow of the foam and the sides and back of the vessel used to ensure that all of the foam is collected. This would enable the average expansion ratio of all of the foam produced to be calculated. Such a vessel was manufactured (see Figure 3:10) and used in the experiments with Test Rigs Two and Three.



Figure 3:10 Photo of larger foam collecting vessel

3.4.2 Amiri Expansion and Drainage Method

The bubble size was to be calculated from Amiri and Woodburn's work (Amiri and Woodburn 1990). They proposed a method of determining the bubble size using Stokes's theory. As a result of "creaming" the foam separates into a clear water region and a froth (see Figure 3:11), in which the bubbles are inevitably crowded together more than in the original dispersion. The movement of the clear water interface reflects the rise velocity of the bubbles. The initial rise velocity of the bubbles is assumed to be the Stokes's velocity in stagnant liquid. By calculating the water content of the bubble, the density of the bubble can be inferred. From this and

the rise velocity the bubble size can be determined. However, this method is for bubble sizes in the order of 35 μm . The bubbles produced in Test Rig One were much larger than this and therefore this method of determining bubble size did not work for these experiments.

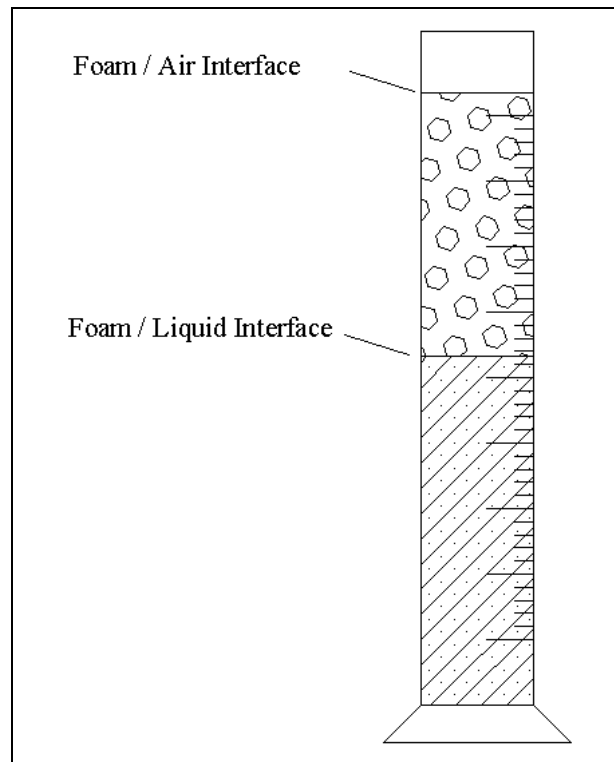


Figure 3:11 “Creaming” seen in a measuring cylinder

However, the drainage rate and expansion ratios were also determined from the “Amiri” set-up, as described below:

1. Wet the measuring cylinder internally and weigh it (m_1)
2. Start the pump
3. After 30 seconds, put the measuring cylinder into the flow of foam
4. As soon as the cylinder is full remove it and start the clock

5. Record the height of the foam
6. Record liquid level/foam level interface height and time at 60 second intervals for 10 minutes (or until 25% drainage has been reached)
7. Weigh the full vessel (m_2)

The expansion was again calculated from the ISO standard equation (Equation 3:1). The 25% drainage rate was calculated as the time required for 25% of the liquid content to drain out of the foam. A comparison of the results from the two methods is shown in Appendix C.

As the results from both methods were very similar, and the Amiri method was much simpler than the initial “ISO” method, the Amiri method was used in most of the Test Rig One experiments. The large purpose built measuring vessel had a volume of 14 litres and the “Amiri” method collected the foam in a measuring cylinder with a volume of only 500 ml. As the measuring vessel method used a larger foam sample than the “Amiri” method, the measuring vessel method was used in Test Rigs Two and Three.

3.5 High Speed Video

A Kodak HS 4540 high-speed video camera was used to capture moving images of the jet from the nozzle to the final collision. This video system could record at up to 4,500 frames per second (fps) with a full size picture and up to 40,500 fps with a reduced picture size. The system records 3072 full frames, so at 4500 fps a recording time of 0.66 of a second is available, however, at higher fps, the recording time is reduced. Illumination was provided by two halogen spot lights. The branchpipe

reflected the light straight back into the camera, but by careful positioning of the lights the worst of this was eliminated.

The images of the jet were taken at between 4500 and 18000 fps. These were downloaded onto a standard VHS video tape, and some were transferred to *.avi files to enable them to be viewed on a computer.



Figure 3:12 The Kodak HS4540 system

3.6 Factorial experiment design and statistical techniques

Many variables were considered important. An efficient method, which would obtain the required information with the required degree of precision and with the minimum expenditure of effort, was required.

Davies (Davies 1963) shows that if the result of changing two or more factors is to be studied, then, in general, the most efficient method is to use a factorial design. He illustrates this with the following example:

"A simple experiment has two factors, each at two levels. Let the factors be temperature and pressure and denote the levels T_0 , T_1 and P_0 , P_1 . The minimum amount of experimentation necessary to give information on both factors is three trials, say one at T_0P_0 , a second at T_1P_0 , involving a change of temperature only, and a third at T_0P_1 , involving a change of pressure only.

These trials occupy the cells (1), (2) and (3) of the following table:

Pressure	Temperature T_0	Temperature T_1
P_0	(1)	(2)
P_1	(3)	

The effect of changing the temperature is given by (2) – (1) and that of changing pressure by (3) – (1). Because of experimental errors some confirmation is desirable, and one way of obtaining this is to duplicate each of the trials, the effects being deduced from the averages of the duplicate responses. This method of approach is known as the One-Factor-at-a-Time Method, since each factor is investigated separately.

Suppose now the table is completed by carrying out a trial with the treatment T_1P_1 ; denote the response by (4). This completes the factorial design. The effect of temperature is estimated by $(2) - (1)$ at pressure P_0 and by $(4) - (3)$ at pressure P_1 . If there is no interaction between temperature and pressure these estimates will differ only because of experimental error, and the average of the two estimates gives the effect of temperature just as precisely as the duplicated observations of (1) and (2).

Similarly, the effect of pressure is estimated by $(3) - (1)$ and $(4) - (2)$; if there is no interaction this estimate is as precise as one based on duplicate trials of (3) and (1). Thus, if there is no interaction the four trials of the factorial design estimate the effects of the two factors with the same precision as the six trials of the duplicated one-factor-at-a-time design. All four observations are used in estimating each effect and the estimate is as precise as though only one factor were involved, whereas in the one-factor-at-a-time design only two-thirds of the observations are used in estimating each effect.

Let us now compare the two designs when the factors interact. If from the design shown in the table it were found that both T_1P_0 and T_0P_1 gave a better result than T_0P_0 , a natural conclusion would be that T_1P_1 would be even better. This involves the assumption that T and P do not interact, but such an inference may be seriously in error. Again, it might be found that T_1P_0 and T_0P_1 are little, if any, better than T_0P_0 , but it is quite possible that T_1P_1 may be much better - such a state of affairs is quite common. The one-factor-at-a-time design would miss the most favourable treatment. If the factors interact, therefore, the one-factor-at-a-time design may lead to the wrong conclusions.

To sum up:

- When there are no interactions the factorial design gives the maximum efficiency in the estimation of effects
- When interactions exist, their nature being unknown, a factorial design is necessary to avoid misleading conclusions.
- In the factorial design the effect of a factor is estimated at several levels of the other factors, and the conclusions hold over a wide range of conditions."

These conclusions have been arrived at for two factors only; they hold with even greater emphasis when more than two factors are involved. A two factor factorial design can be called a 2^2 factorial design, a three factor factorial design can be called a 2^3 factorial design, a k factor factorial design can be called a 2^k factorial design. However, interpretation of results with more than two factors is more complex. Box (Box et al. 1978) explains how Yates' analysis can be applied to a factorial design experiment:

"Yates' Algorithm is applied to the observations after they have been rearranged in what is called standard order. A 2^k factorial design is in standard order when the first column of the design matrix consists of successive minus and plus signs, the second column of successive pairs of minus and plus signs, the third column by four minus signs followed by four plus signs, and so forth. In general, the kth column consists of 2^{k-1} minus signs followed by 2^{k-1} plus signs. (See table below, which is for illustration purposes only. The values are invented and are of no physical significance to this thesis).

Run	T	P	V	Result	(1)	(2)	(3)	Divisor	Estimate	ID
1	-	-	-	60	132	254	514	8	64.25	Average
2	+	-	-	72	122	260	92	4	23.00	T
3	-	+	-	54	135	26	-20	4	-5.00	P
4	+	+	-	68	125	66	6	4	1.50	TP
5	-	-	+	52	12	-10	6	4	1.50	V
6	+	-	+	83	14	-10	40	4	10.00	TV
7	-	+	+	45	31	2	0	4	0.00	PV
8	+	+	+	80	35	4	2	4	0.50	TPV

Column “result” refers to the average response for each test run. These averages are now considered in successive pairs. The first four entries in column (1) are obtained by adding the pairs together. Thus $60 + 72 = 132$, $54 + 68 = 122$ and so on. The second four entries in column (1) are obtained by subtracting the top number from the bottom number of each pair. Thus $72 - 60 = 12$, $68 - 54 = 14$ and so on.

In just the same way as column (1) is obtained from column “Results”, column (2) is obtained from column(1). Finally column (3) is obtained from column (2) in the same manner.

To obtain the effects one only has to divide by the appropriate divisor, which is 8 for the first entry and 4 for the others. The first estimate is the grand average of all the observations. The remaining effects are identified by locating the plus signs in the design matrix. Thus in the second row a plus sign occurs only in the T column, so that

the effect in that row is the T effect. In the seventh row plus signs occur in both the P and V columns, so that the effect in that row is the P x V interaction."

Factorial design and Yates' analysis were therefore used to design the experiments for Test Rigs One and Three.

4 Foam Formation Process Stage One (Mixing)

4.1 Introduction

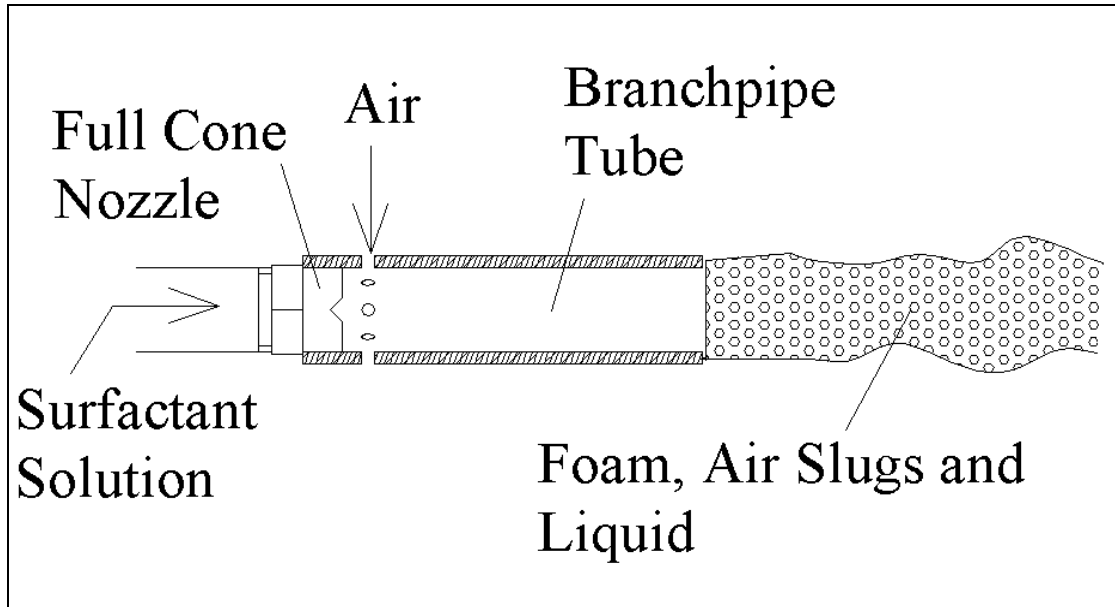


Figure 4:1 Schematic of Test Rig Three

Surfactant solution is pumped through the nozzle into the branchpipe tube (see Figure 4:1). This induces air through the air holes. The turbulent action produced by the nozzle and by the shear force exerted by the walls of the branchpipe tube partially mixes the air and liquid. This has been termed Stage One (Mixing), by the author.

In this chapter the relationships between the upstream liquid pressure, the liquid flow rate and the air entrainment rate are investigated. The theoretical and actual expansion ratios are examined and an explanation for the discrepancies is offered. The shear force generated on the branchpipe by the jet is also investigated. All the results using Test Rig Three are given in Appendix F. The video findings are discussed and the effects of incorporating obstructions into the branchpipe and changing the number and size of air holes are investigated.

4.2 Literature Review

In 1869, Plateau, as reported by Bikerman (Bikerman 1973), showed that a static cylindrical column of fluid was unstable if its length exceeded its perimeter. If the length did exceed the perimeter, two drops could be formed whose total surface area would be less than that of the cylinder. Therefore, if a bubble, which has become elongated, happens to drift into a more quiescent zone, it will separate into two or more nearly spherical bubbles. Plateau's work can be used to describe one of the processes involved in the formation of bubbles by mixing, but other processes have received little published attention. In 1953 Bikerman (Bikerman 1953) summed up the current level of knowledge about mixing behaviour. He stated that "the process of introducing air bubbles into a liquid by whipping, beating, etc., undoubtedly is very complicated and, apparently, has not yet tempted any physicist". Only limited work has been published on the subject since then.

There has been a great deal of work published on foam rheology and foam generation methods other than mixing (as described in Chapter Two) and the current theories provide a basis for further work. They also reinforce the need for careful characterisation of foam structure and systematic rheological measurements. However, as there are many methods of producing foams, only a few works can be related directly to foam generation within a fire fighting branchpipe. Calvert's work (Calvert 1990) is relevant and includes investigations into the flow of foam through constrictions. The work is of a qualitative nature and highlights that the behaviour of foam is very different from that of Newtonian fluids. Calvert states that low shear rates (low velocities and smooth passages) tend to produce a slight reduction in bubble

size. He also states that high shear rates (high velocities and complicated passages) lead to large-scale foam breakdown with the formation of very large bubbles interspersed with very wet, low expansion foam. These observations are reiterated by Briggs (Briggs 1995). Briggs states that moderate impact and turbulence of a solution / air mix within a branchpipe can be expected to increase the number of bubbles, but more severe stress tends to rupture them. The branchpipes manufactured by CounterFire incorporate this moderate impact idea having smooth profiles, although some competitors' branchpipes incorporate disturbances within the tube.

In the 1960's Witte (Witte 1969), (Witte 1962) described a “mixing shock” where a transition from jet flow to froth flow occurs in gas and liquid flows (see Figure 4:2). His apparatus was very similar to a fire fighting branchpipe. He characterised the jet flow as a core of fast-moving liquid droplets surrounded by a gas. The froth flow consists of liquid in which the gas is dispersed in the form of bubbles. He postulated that the shock could only exist when the jet flow impinges on a free surface that prevents the jet flow from penetrating further. He also assumed that the gas entrainment mechanism is similar to air enclosure during the impact of a water droplet on a free surface. This process is also known as the plunging jet mechanism, and is described in detail in Chapter Six (Foam Formation Process Stage Three (Collision)).

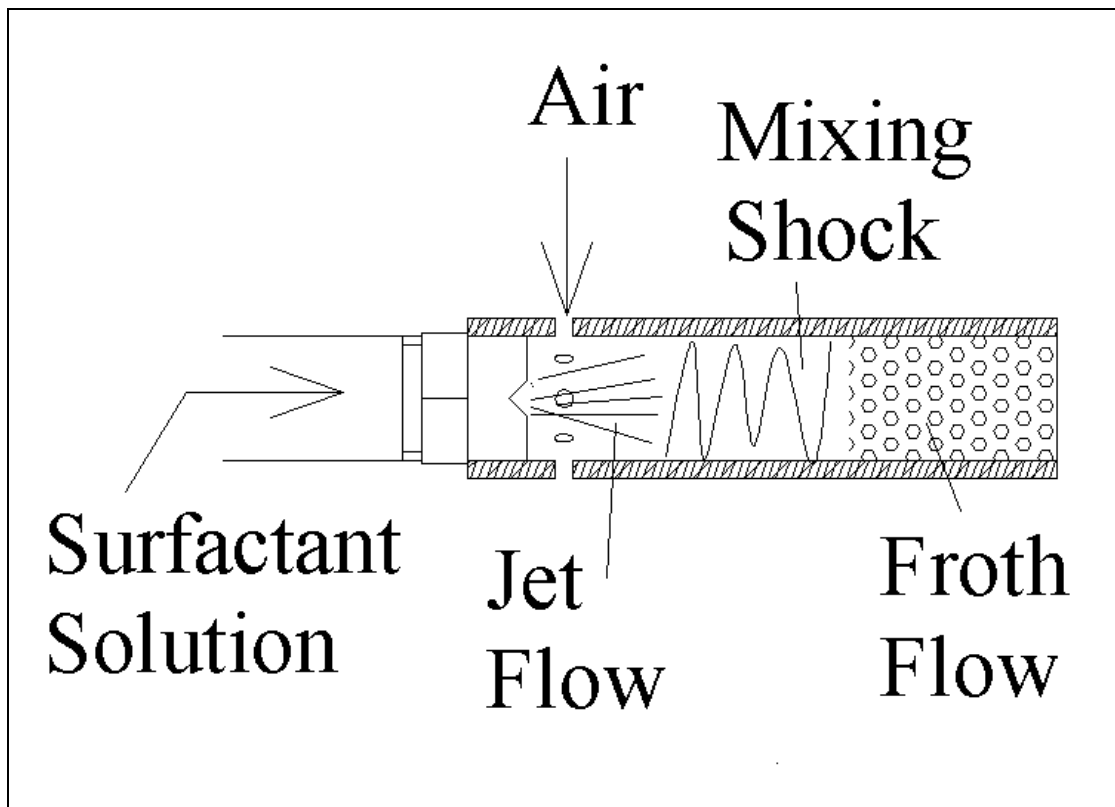


Figure 4:2 Mixing shock

A fire fighting branchpipe can be described as a jet pump without a diffuser section (see Figure 4:3). The amount of air entrained in both a jet pump and branchpipe is governed by the pressure difference generated between the jet of surfactant solution and atmosphere. Studies of the mixing process within the throat of a jet pump have mainly focussed on increasing the pump efficiency. The details of the mixing process have been avoided by using impulse-momentum equations, and these have often included the assumption that the primary and pumped fluids are incompressible and of equal density.

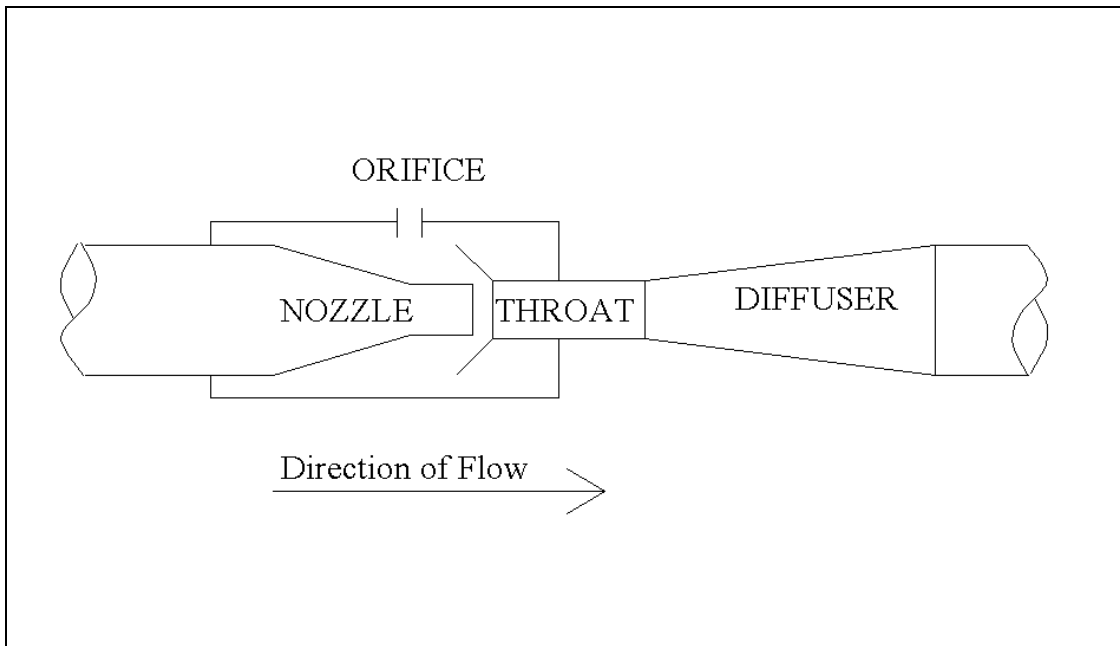


Figure 4:3 Jet pump

The work on two-phase jet pumps by Cunningham (Cunningham 1995), (Cunningham and Dopkin 1974) and the work by Noronha et al (Noronha et al. 1997) do, however, include density differences. Cunningham produces models for two-phase jet pumps, one of which has a two-phase secondary flow. Noronha et al also produce a two-phase model and they adopt Witte's mixing shock within the throat. Both Cunningham and Noronha et al assume that the flow is steady and one dimensional. They therefore use Bernoulli's equation with a friction loss coefficient to calculate the pressure difference across the nozzle.

4.3 Experimental Findings and Results

Test Rig Three, with a 100 mm long branchpipe and 8 air holes of 3.2 mm diameter, was used in all the tests unless stated otherwise. The expansion ratio of the foam was

measured by collecting the foam in a measuring vessel, as described in Chapter Three (Experimental Work).

The high pressure driving jet entered the branchpipe through the 60° full cone nozzle, at a flow rate of between 10 and 25 l/min. As the jet of fluid penetrated the stagnant air within the branchpipe, a dragging action occurred on the boundary of the jet between the high and low velocity particles. Mixing occurred between the liquid jet and the low velocity air surrounding the nozzle and the transfer of momentum accelerated the air in the direction of the liquid flow. As the jet of high velocity fluid left the nozzle, entrainment caused air from outside the branchpipe to flow through the air holes and into the branchpipe.

It was not possible to separate the effect of the mixing stage from the effect of the collision stage when measuring the expansion ratio of the foam. As far as possible the mechanism of collision was kept constant whilst different branchpipe tube types were tested.

4.3.1 Air Entrainment

Investigating a water spray into the axis of a short tube, McQuaid (McQuaid 1975) established a complex relationship between the rate of entrainment of air by the water spray and the spray-nozzle type, tube diameter and water flow rate.

The results from the branchpipe system, when plotted on McQuaid's graph lie off the scale (see Figure 4:4), but if the scale is increased, the majority of the points lie close to the continuation of his curve. The points to the left of the cluster in the branchpipe

results have a pressure upstream of the nozzle of less than 0.5 bar gauge and liquid flow rates less than 10 l/min. At these low values, experimental errors in measuring represent a larger proportion of the values measured, so that the position on the horizontal axis becomes more uncertain.

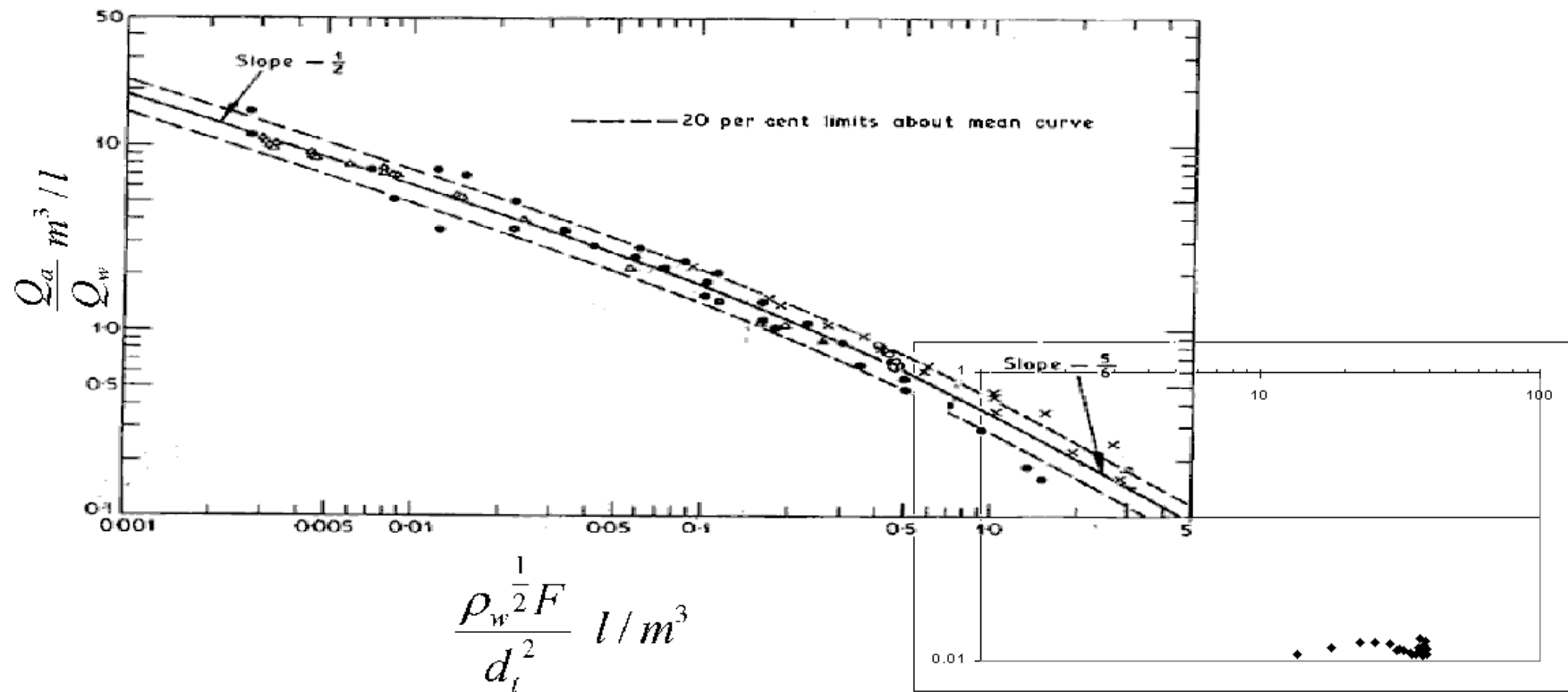


Figure 4:4 McQuaid's entrainment graph (left) with the author's results plotted to same scale (right)

Where: Q_a = Volume flow rate (air) Q_w = Volume flow rate (water) F = Flow number of nozzle $(= \frac{Q_w}{P_w^{1/2}})$

ρ_w = Density (water), d_t = Diameter of bounding tube, P_w = Pressure (water)

The branchpipe system results probably lie off McQuaid's scale because he used and correlated hollow cone spray nozzles and the jet end of the tube was open and not restricted by air holes. Test Rig Three's branchpipe system uses a different set-up, as it has a full cone nozzle with the upstream end of the tube sealed and with air holes around the circumference to allow the inflow of air.

As the author's results lie in such a small cluster and are off McQuaid's scale, it was decided not to use McQuaid's work as the basis of any theoretical model of the air entrainment rate in a branchpipe system.

The flow rates of both the liquid and the air entrained into the branchpipe were measured. These values were then used to calculate an expansion ratio, assuming that all of the liquid and entrained air were converted to foam (hereafter called the "air and liquid method"). A comparison of the expansion ratios measured by this and the measuring vessel method is shown in

Figure 4:5.

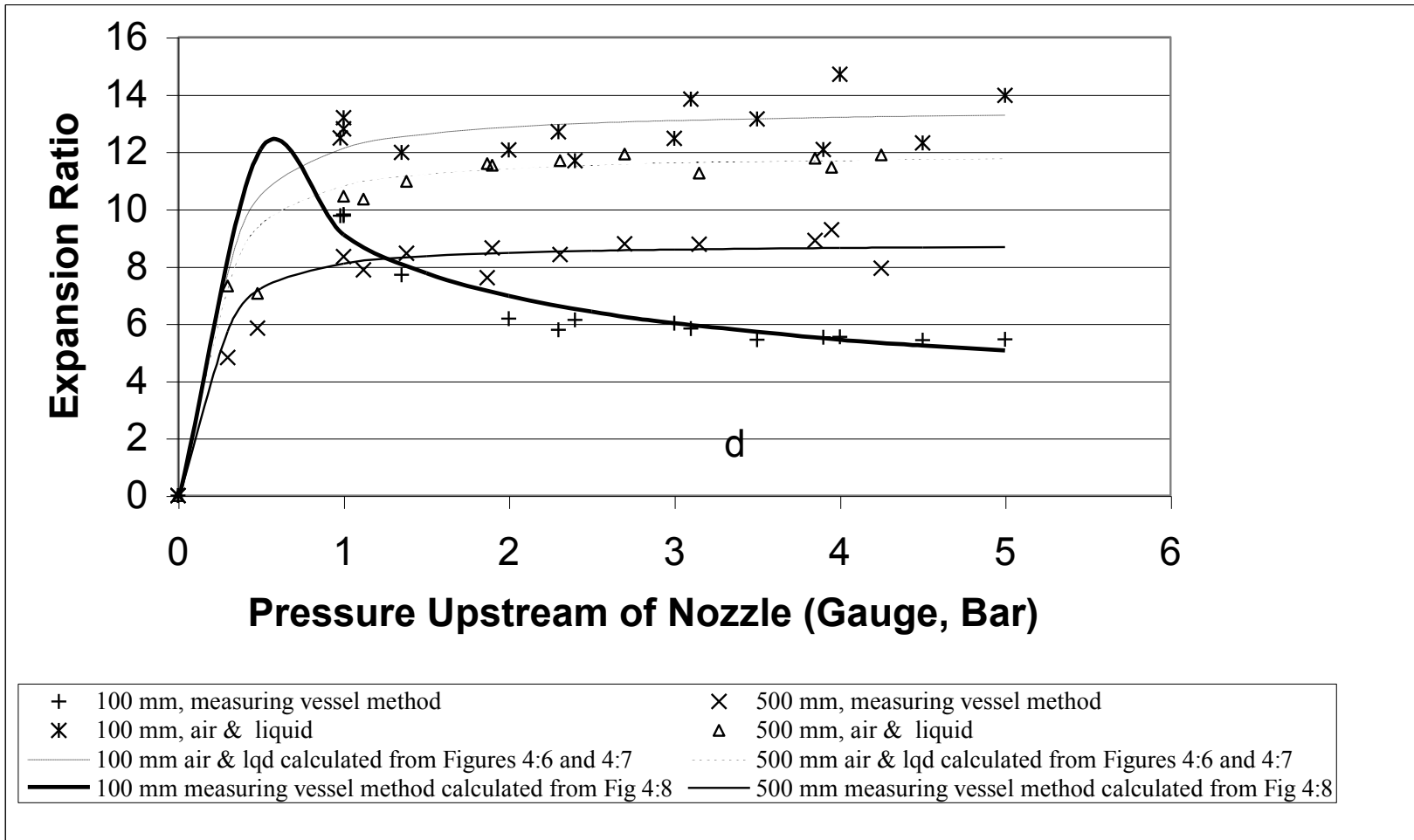


Figure 4:5 Pressure upstream of nozzle versus expansion ratio

It can be seen that the measuring vessel method returns a lower expansion ratio than the air and liquid method. This confirms that not all of the entrained air is incorporated into the final foam. For the 100 mm long branchpipe tube this can be explained, at least in part, by air slugs escaping to atmosphere from the end of the branchpipe. This can be seen on the video (CD Slug Escape.avi). However, the escaping slugs are not visible at the end of the 500 mm long branchpipe. This is because the slugs are broken down into smaller bubbles within the longer branchpipe. The remainder of the air not incorporated into the final foam, may be lost during the flight or at collision. The 500 mm branchpipe tube produces a slightly higher expansion ratio foam than the 100 mm long branchpipe, due to the transformation of slugs into small bubbles, but the flight distance is much shorter.

The 500 mm branchpipe jet did not reach the back of the collection tank (approximately 1.8 m) whereas the 100 mm jet did in all of the unobstructed experiments with a pressure upstream of the nozzle greater than 1 bar. The shorter flight distance from the long branchpipe can probably be attributed to the reduction in energy of the jet, both from the shear force and by the production of small bubbles from the larger slugs.

The air and liquid method results both start to level off at about 1 bar. From the graphs in Figure 4:6 and Figure 4:7, it can be seen that, for the experiments conducted, the square of the entrained air flow rate was proportional to the pressure, as was the square of the liquid flow rate. By using the equations of these two graphs, the dotted and dashed lines on Figure 4:5 were produced. The correlation of the calculated points and the experimental results is good and shows that the air and liquid method

expansion ratio can be calculated directly from the pressure upstream of the nozzle. However, the gradient of the lines in Figure 4:6 and 4.7 cannot be determined without experimental evidence, as each branchpipe type and length entrains air at a different rate.

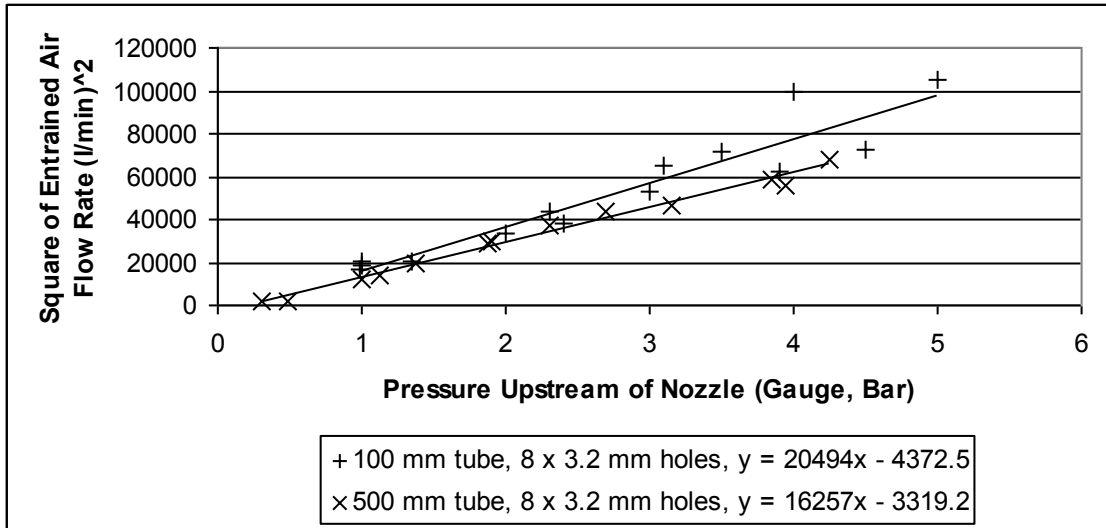


Figure 4:6 Pressure upstream of nozzle versus (entrained air flow rate)²

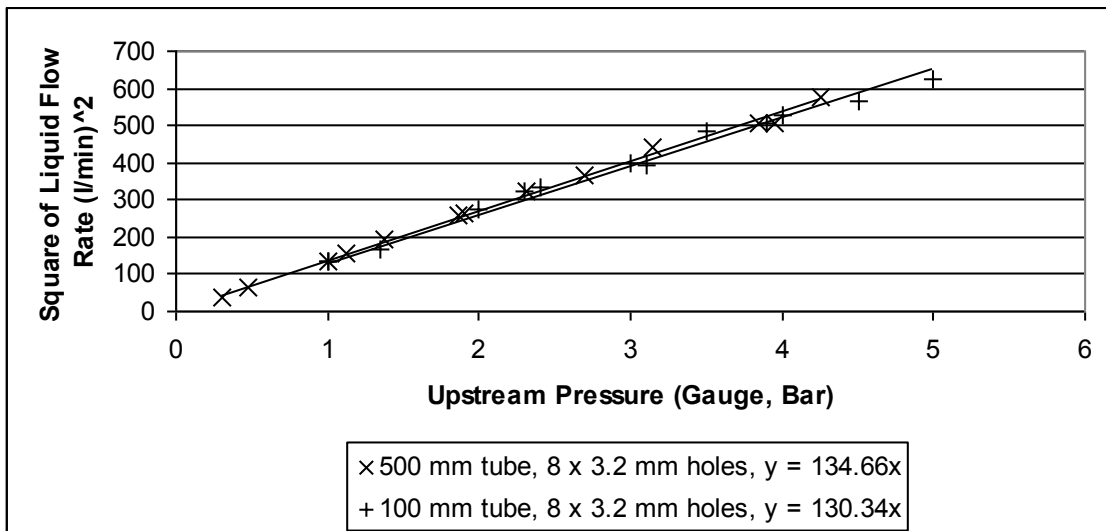


Figure 4:7 Pressure upstream of nozzle versus (liquid flow rate)²

The expansion ratio peaks at or below 1 bar for both of the results using the measuring vessel method. The expansion from the 500 mm branchpipe then levels out, but from the 100 mm branchpipe it drops off rapidly until it starts to level at about 2 bar.

By comparing the air flow rate found by the measuring vessel method with the flow rate of entrained air into the branchpipe, the amount of air lost (or not used in the final foam) can be calculated. As it was not possible to separate the mixing stage from the collision stage, it is possible that more air is lost after leaving the branchpipe, but incorporated during the collision stage. The final amount of air within the foam collected, however, was found to be directly related to the amount of air entrained (see Figure 4:8). The equations of these graphs have been used to calculate the expansion ratios of the measuring vessel method in

Figure 4:5 (solid lines). As these are a good correlation, it shows that the measuring vessel method expansion ratio can also be calculated directly from the pressure upstream of the nozzle. However, as for the air and liquid method, the gradient of the line in Figures 4:6, 4.7 and 4:8 cannot be determined without experimental evidence, as each branchpipe type and length entrains air, and loses it, at a different rate.

The peak in the 100 mm branchpipe results can be attributed to no air being lost below an entrained air flow rate of approximately 100 l/min (equivalent to an upstream pressure of 0.7 bar). Therefore, below 0.7 bar, all of the air entrained is used and the expansion ratio is higher than when air is lost. There is no equivalent “no air lost” stage with the 500 mm branchpipe, and therefore there is no corresponding peak.

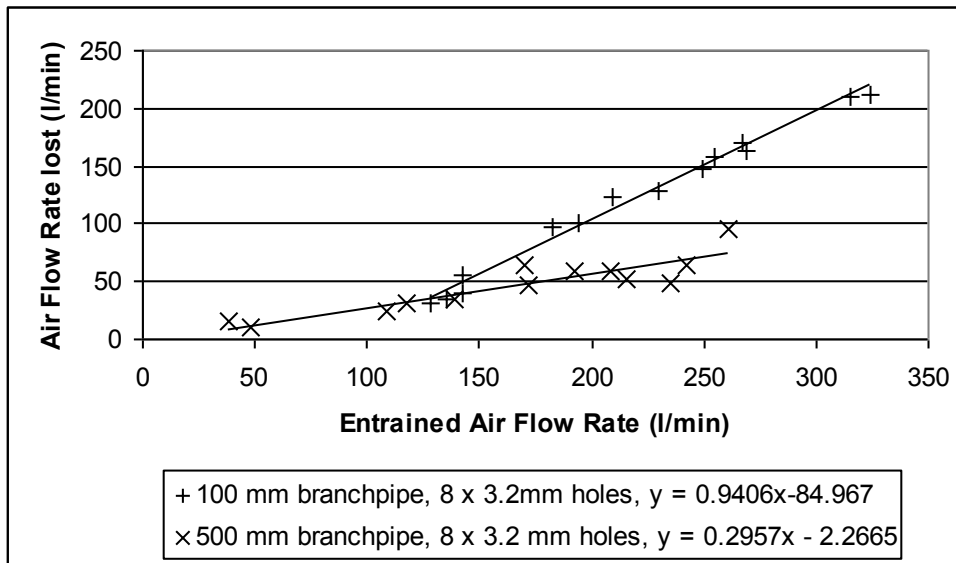


Figure 4:8 Entrained air flow rate versus air flow lost

Changing the number or size of the air holes appeared to have an effect on the amount of air entrained, although the $(\text{amount of air entrained})^2$ was still proportional to the pressure (see Figure 4:9). However, a much smaller effect on the expansion ratio of the foam produced was noted (see Figure 4:10 and Figure 4:11). This implies that a minimum amount of air is required, and if more than this is entrained, it is lost and not incorporated into the final foam. The author did not conduct experiments with less than the minimum hole area, but it is expected that a foam with a reduced expansion ratio would be formed in this case. At low air flows the measurement of the air flow was less accurate than at higher air flows, due to the experimental errors involved. It is expected that this is the reason that an expansion ratio higher than the air and liquid method was sometimes noted from the measuring vessel method, when the 2.1 mm diameter holes were used.

When more air is entrained than required for the foam expansion, an increase in the exit velocity of the jet from the branchpipe is seen. This is due to the increase in fluid (liquid plus air) flow rate.

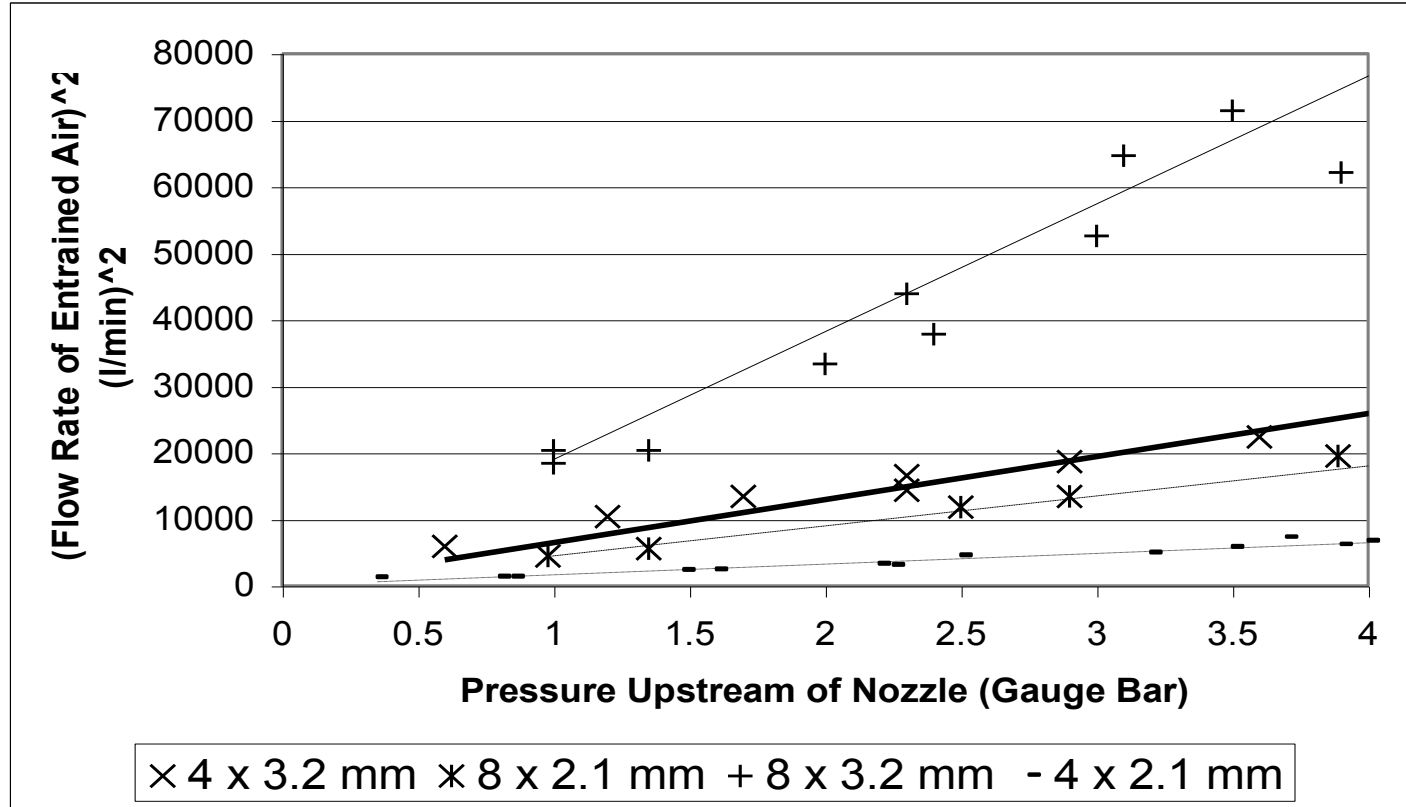


Figure 4:9 Pressure upstream of nozzle versus (entrained air flow rate)² for different number and size of air holes

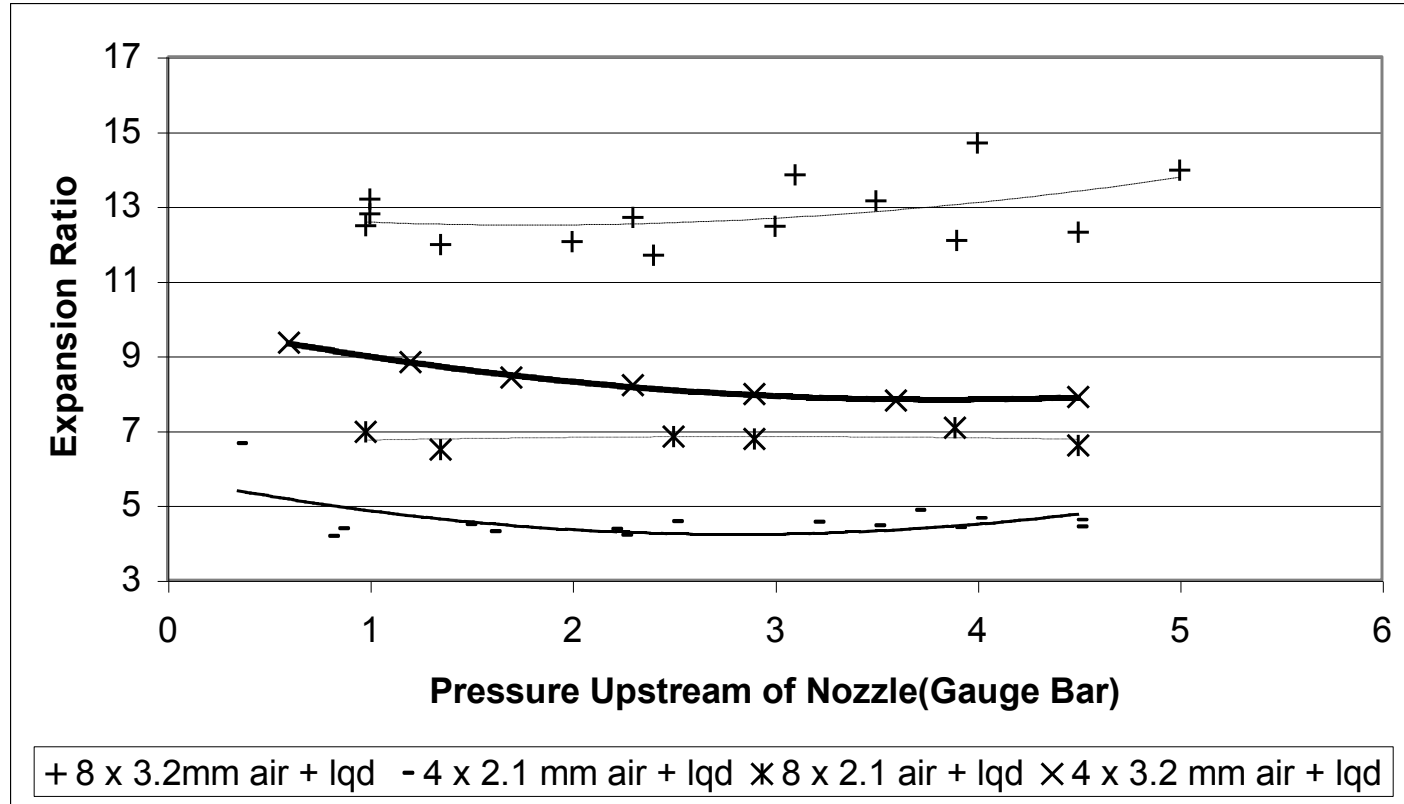


Figure 4:10 Expansion ratio based on “air and liquid” method, with different number and sizes of air holes

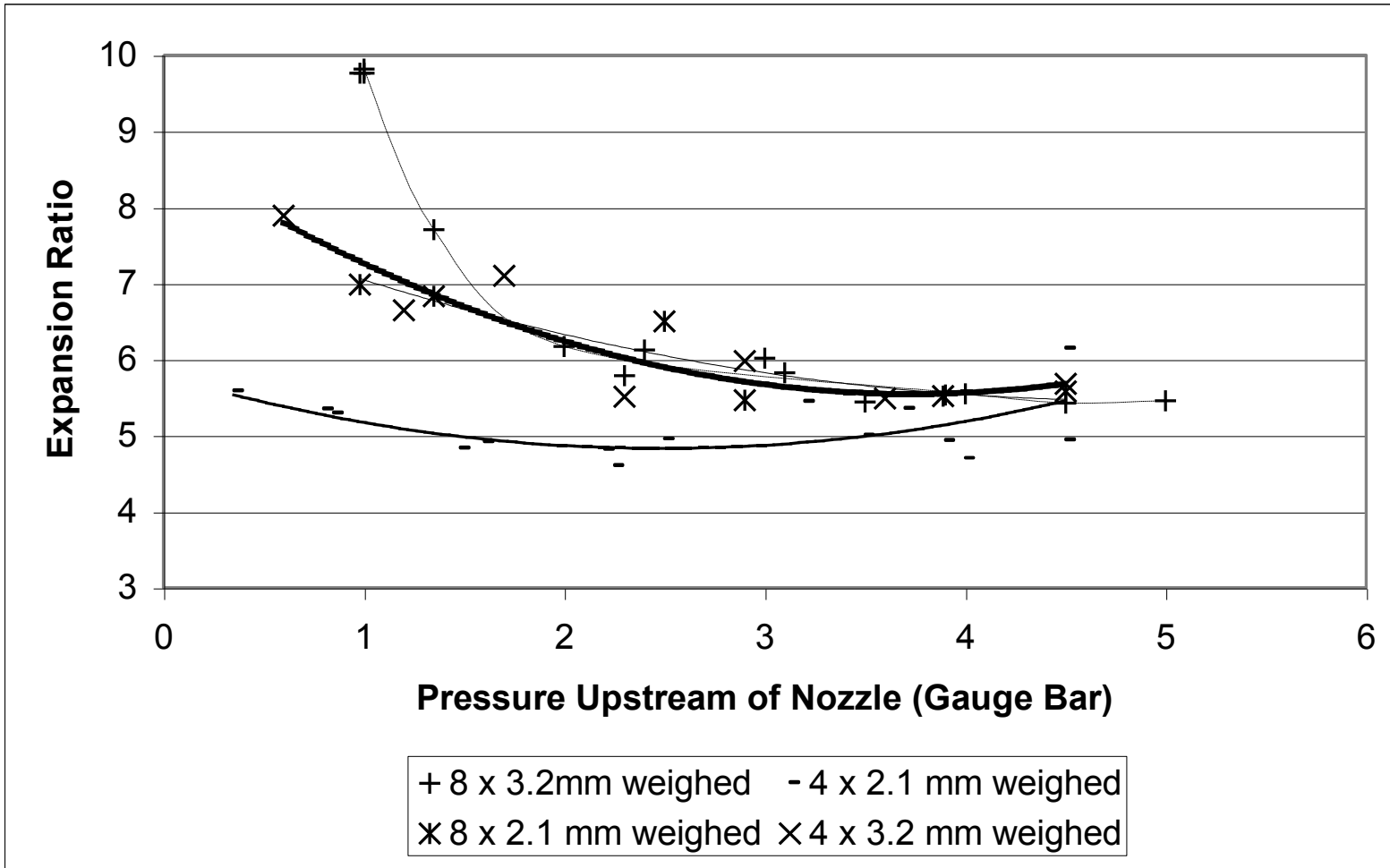


Figure 4:11 Measuring vessel method expansion ratio with different air holes

If the air holes of the 500 mm tube were almost completely restricted, Witte's mixing shock was seen. A definite line between the jet flow and froth flow could be seen, and this could be moved by changing the restrictions in the air holes. Mixing shock does not appear to occur under normal operating conditions, within either length of branchpipe system for the hole areas used. Witte described the froth flow as a liquid in which the gas is dispersed in the form of bubbles, whereas he described the jet flow as a core of fast-moving liquid droplets surrounded by a gas. The mixture exiting the branchpipes under normal conditions appears to be partially froth flow and partially jet flow. From the experiments conducted, it can be seen that froth flow has a very restricted flight distance compared to the jet flow. Therefore, there must be an optimum proportion of froth and jet flow to enable the jet to be projected and to keep the expansion ratio high.

Using a branchpipe tube with no air holes at all produced two distinct flow patterns. If liquid completely filled the branchpipe, air was drawn into the centre of the branchpipe tube through the open end (Figure 4:12), whilst some of the higher velocity liquid poured out with a very limited throw (around 50 mm). If air was trapped in the area of lower pressure surrounding the nozzle, however, the throw of the jet was steadier and travelled a similar distance to the jet from a branchpipe with air holes (see CD No Hole1.avi and No Hole2.avi). This is probably because the trapped air circulated freely around the nozzle and formed a barrier to the liquid circulating back.

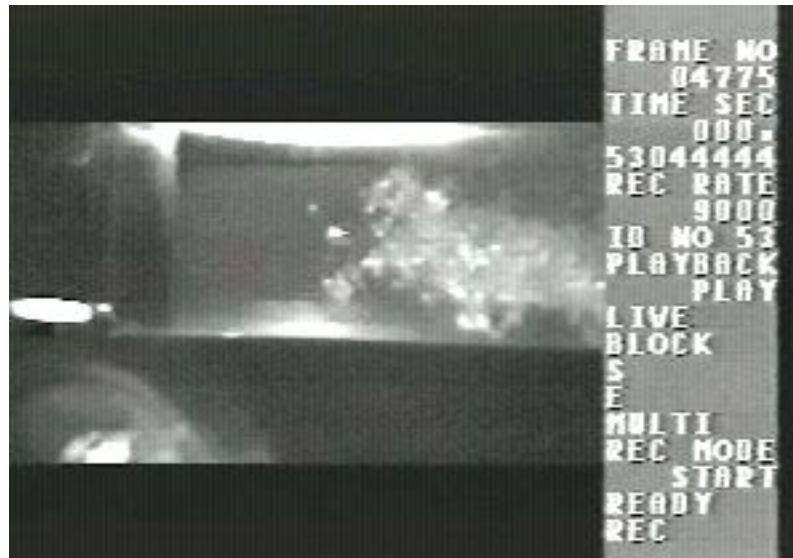


Figure 4:12 Air being drawn into branchpipe

4.3.2 Shear Force

In order to determine the shear force exerted on the liquid jet from the branchpipe, the test rig shown in Figure 4:13 was used. The method is described in Chapter 4 and the results are given in Appendix F.

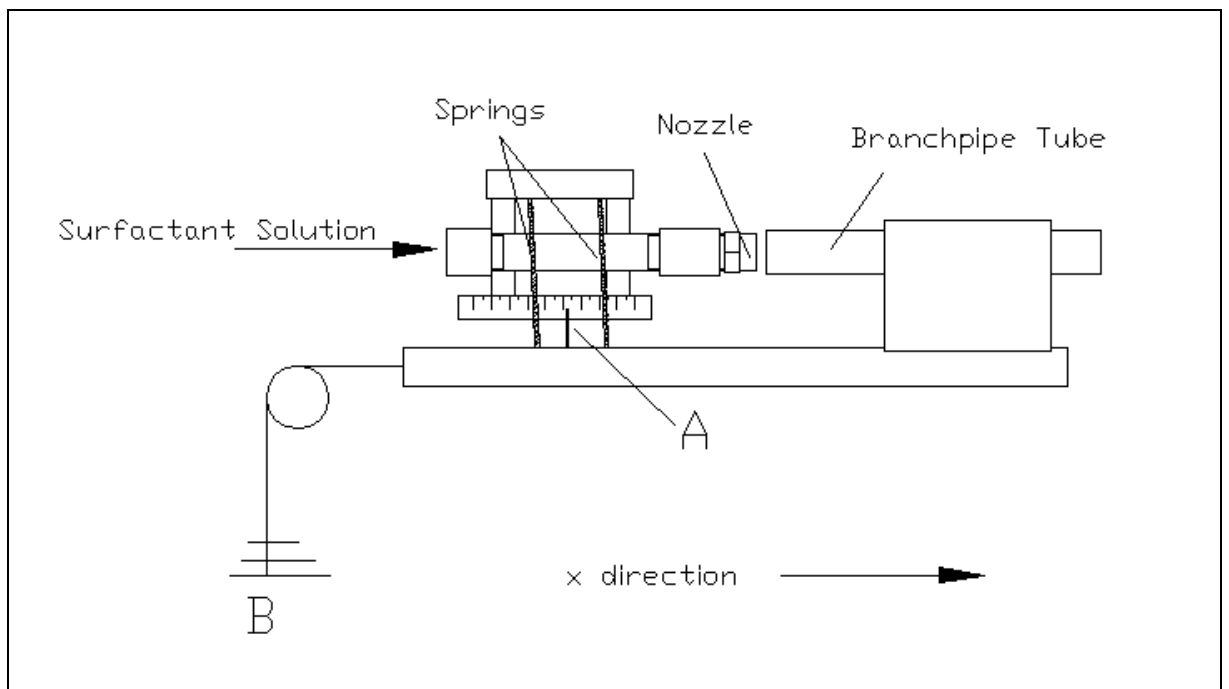


Figure 4:13 Force measuring test rig

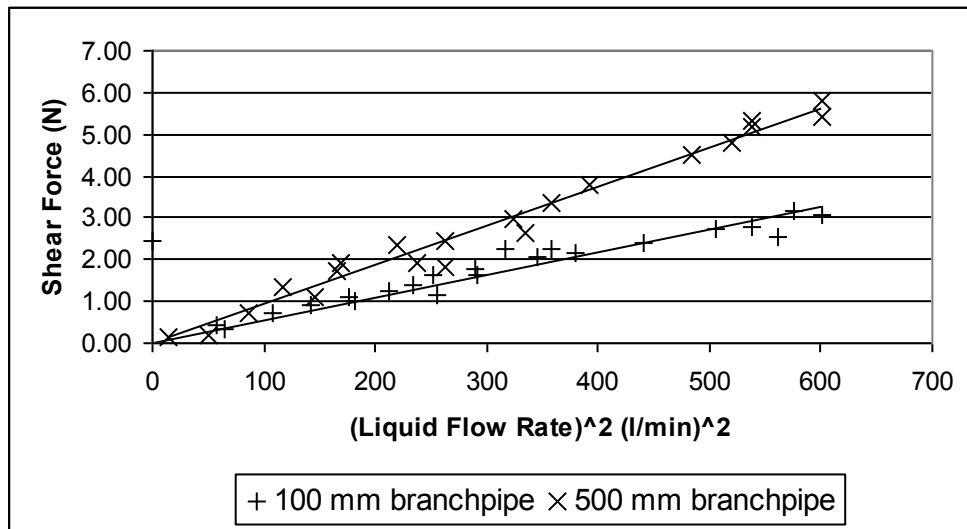


Figure 4:14 (Liquid flow rate)² versus shear force generated

The shear force is proportional to the liquid flow rate squared (see Figure 4:14). It also appears that a branchpipe tube of 500 mm only produces a shear force of nearly twice that of the 100 mm branchpipe tube. This is surprising as it was expected that the shear force would be proportional to the length of branchpipe, as it would be if pure water were passed through the tube. This may be explained by the surfactant solution being non-Newtonian, and the fluid passing through the branchpipe being two-phase, and therefore being liable to “slip”. It would also appear that the slip occurs at a very low, or no, shear stress, as the intercept on the graph appears to be zero.

Calvert (Calvert and Nezhati 1986), (Calvert 1990) states that near a solid surface, bubble migration leads to a liquid-rich layer, which gives the effect of slip between the foam and the wall. This layer may be responsible for the anomaly in the shear force noted above. Calvert idealises this liquid-rich layer as a lubricating layer of pure liquid separating the foam from the surface. The effective viscosity of a foam, once

slip effects have been removed, is usually several hundred times the viscosity of the base liquid.

4.3.3 Video and Visual Evidence

It can be seen in the video of the experiments that there is vigorous turbulent mixing within the branchpipe tube. Slugs of air are visible within the branchpipe as dark pockets. Lighter areas of liquid and / or small bubbles, both of which appear to reflect light in a similar manner, are also seen (see Figure 4:15 and CD Mix.avi). Distinguishing between the liquid and small bubbles is not possible in the branchpipe, but outside the confines of the tube individual bubbles of approximately 2 mm diameter can be identified. Unfortunately, it is only possible to see the fluid touching the sides of the branchpipe, and as mentioned above, this is likely to be a boundary slip layer, and may not represent what is happening within the tube.

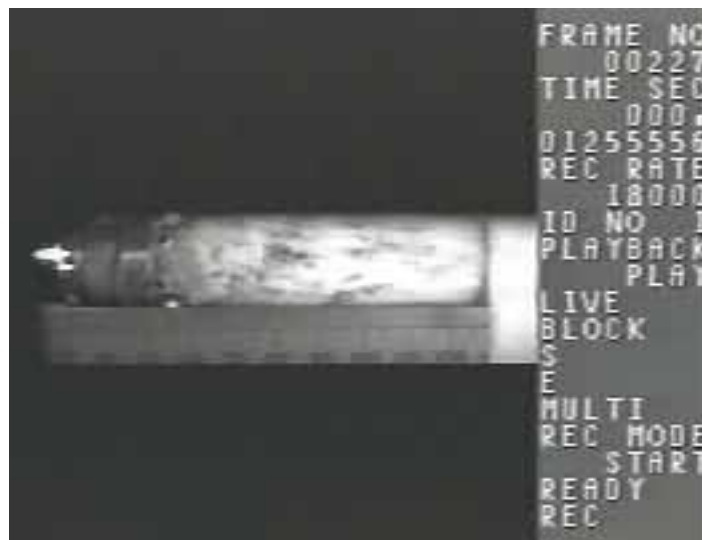


Figure 4:15 Air slugs seen as dark areas within branchpipe

The turbulence does not cease as the jet emerges from the tube, but the mixture is no longer confined by the walls. A slight swirl is noticed, and the jet is seen to rotate downwards, with the jet travelling to the right. Any liquid that is urged outwards by the turbulent motion and reaches the outer edge of the jet will be expelled as a droplet (unless retained by surface tension), and the jet will begin to break up. This is dealt with in Chapter Five (Foam Formation Process Stage Two (Flight)).

The bubble sizes on the surface of the final foam collected in the measuring vessel were visually compared. The lower the liquid flow rate, the larger the bubbles appeared, ranging from approximately 25 mm diameter at 0.5 bar to approximately 1 mm diameter at 4 bar. When the foam was collected in a transparent container, it was noted that the foam was not homogeneous. Immediately after collection, there was no foam / liquid interface, but one did appear after approximately 1 minute. This implies that any liquid slugs are transformed into a wet foam, which quickly drains. The bubbles at the bottom of the container were less than 1 mm diameter. The bubble diameters increased gradually the nearer to the surface they were.

4.3.4 Obstructions

As some of CounterFire's competitors' branchpipe tubes include baffles and obstructions, experiments were conducted on Test Rigs One and Three with a variety of obstructions, as seen in Figure 4:16. The experiments were not particularly accurate but do provide a general indication of the influence of baffles.

4.3.4.1 Test Rig One

The 100 mm diameter branchpipe was used in all of the experiments on Test Rig One. The results are tabulated in Appendix B. The expansion ratio of the foam produced, (estimated using the “Amiri” method) when no obstructions were present, was 2.8. Figure 4:16 (A) shows the rig with no obstructions. The simplest obstructions were bolts fitted through the sides of the branchpipe (B and C in Figure 4:16). The flow appeared to separate around the bolts, and left a wedge-shaped gap of length approximately 3 bolt diameters. The expansion ratio with the bolts was also 2.8. The bolts were removed and a funnel was then attached to the centre of the branchpipe tube (D). This made the jet diameter decrease, but the expansion ratio was still only approximately 3. Cutting castellations in the funnel (E) increased the expansion ratio to about 3.5.

Forcing the jet from the 100 mm tube through an adapter into a 50 mm tube (F) raised the expansion to about 4, as did putting angled blades in the branchpipe (G). Forcing the spray through a commercially produced jet pump (H) did produce some very large bubbles but also a lot of foam solution sprayed out, lowering the expansion ratio to about 2.5. The best increase in expansion ratio was through large holes in a polyurethane foam sheet (J) and also through an air flow straightener (K). The foam sheet produced a foam of about 5.4 but it had no throw at all, whereas the air flow straightener produced a foam with an expansion of 6.6. This was lowered to 5.0 if the fan was turned on full. The throw from the jet with the straightener was less than 0.3 m.

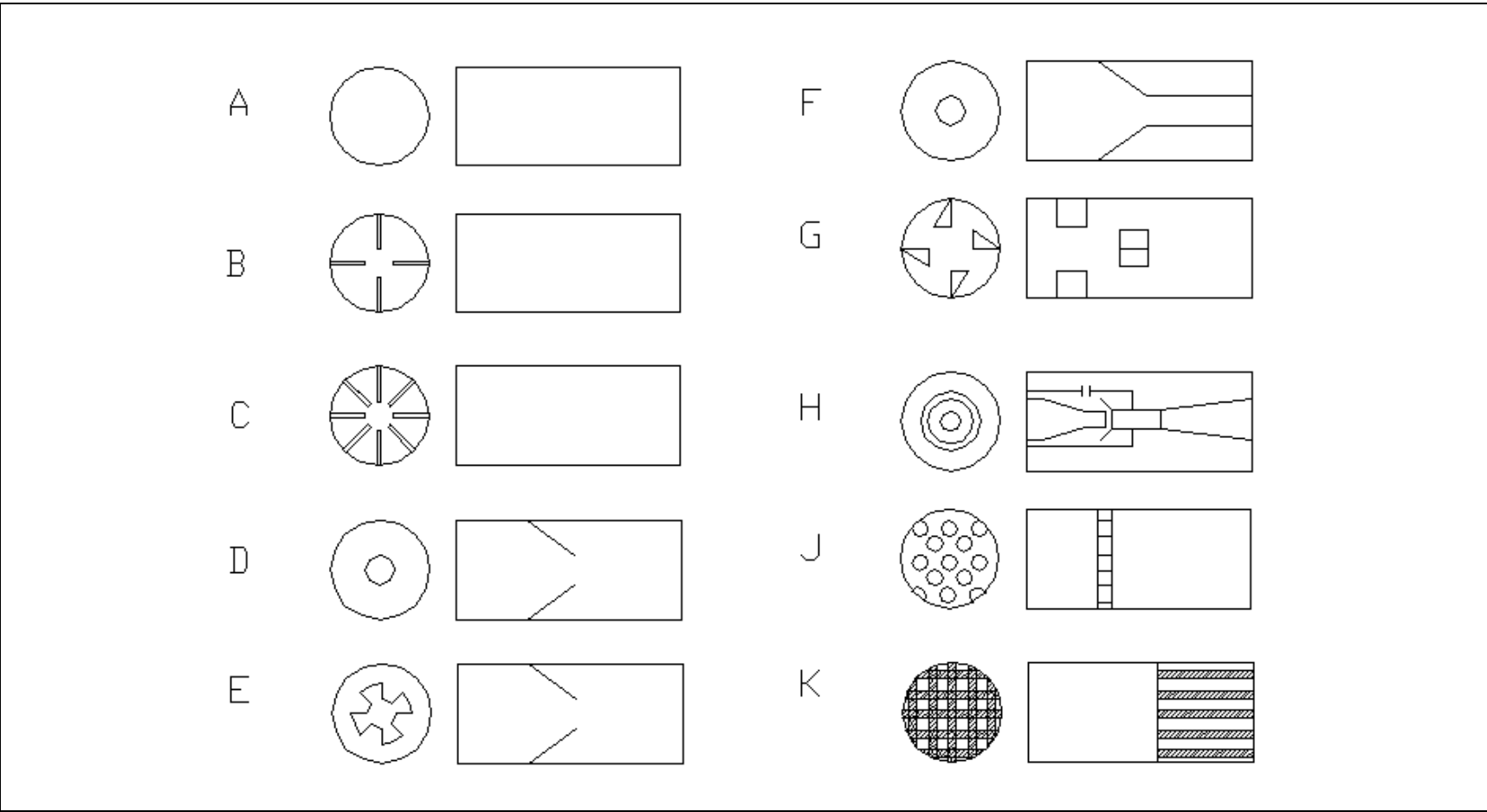


Figure 4:16 Obstructions

4.3.4.2 Test Rig Three

The inclusion of cross bars or coarse gauze over the end of the branchpipe tube in Test Rig Three did not significantly affect the expansion. The flow appeared to separate around the cross bars, and again left a wedge-shaped gap of length approximately 3 bar diameters. The wire mesh of the gauze separated the flow in a similar manner to the cross bar. It also caused a lot of spray normal to the branchpipe.

4.4 Conclusions

The first stage of foam generation in fire fighting equipment is in the branchpipe. The surfactant solution is pumped through a nozzle into a tube. This produces a turbulent jet of fluid. Pressure is reduced around the nozzle by the momentum exchange taking place in the branchpipe. Air is drawn into the tube, by the reduction in pressure, and the square of this flow rate is directly proportional to the pressure upstream of the nozzle. The constant of proportionality, however, depends on the size and / or area of the air holes.

Only the fluid against the branchpipe walls can be seen on the video. However, vigorous turbulent mixing appears to take place. Slugs of air are visible and liquid and / or small bubbles are also visible. After the jet leaves the branchpipe individual bubbles of approximately 2 mm diameter can be identified. The turbulence does not cease as the jet emerges from the tube, and a slight swirl is noticed. The resulting foam is non-homogeneous, with smaller bubbles of less than 1 mm diameter collecting at the bottom of the collecting vessel. The sizes of the bubbles on the

surface of the foam decrease with an increase in liquid pressure upstream of the nozzle.

Not all of the entrained air is incorporated into the final foam. For the 100 mm long branchpipe tube this can be explained, at least in part, by air slugs escaping to atmosphere from the end of the branchpipe. However, the escaping slugs are not visible at the end of the 500 mm long branchpipe. The remainder of the air not incorporated into the final foam, may be lost during the flight or at collision. The flight distance in all the experiments was 0.75 m from the end of the branchpipe, unless stated otherwise.

As is expected from Bernoulli's equation, the (liquid flow rate)² is also proportional to the upstream pressure. As it was not possible to separate the mixing stage from the collision stage, it is possible that air is lost after leaving the branchpipe, but incorporated again during the collision stage. However, the final amount of air within the foam collected was found to be directly related to the amount of air entrained. Therefore, from the pressure upstream of the nozzle, the flow rate of the liquid and the air entrained can be calculated. If the constant of proportionality between the flow rate of the air entrained and the amount of air lost is known for the design of branchpipe used, then the expansion ratio can be calculated. The value of the proportion of air entrained and lost cannot be determined without experimental evidence, as each branchpipe type and length entrains air, and loses it, at a different rate.

Changing the number or size of the air holes appeared to have only a minor effect on the expansion ratio of the foam produced. If the air holes of the 500 mm tube were almost completely restricted, Witte's mixing shock was seen. However, mixing shock does not appear to occur under normal operating conditions, within either length of branchpipe. The mixture exiting the branchpipes under normal conditions appears to be partially froth flow and partially jet flow. From the experiments conducted, it can be seen that froth flow has a very restricted flight distance compared to the jet flow. Therefore, there must be an optimum proportion of froth and jet flow to enable the jet to be projected and to keep the expansion ratio high.

Using a branchpipe with no air holes produced two distinct flow patterns:

1. The throw of the jet was steady and travelled a similar distance to the jet from a branchpipe with air holes.
2. Air was drawn into the centre of the branchpipe tube through the open end whilst some of the liquid poured out with a very limited throw (around 50 mm).

Pattern 1 was due to air being trapped around the nozzle, and thus not allowing the liquid to circulate back towards the nozzle. Pattern 2 did not have the trapped air.

Putting obstructions in the tube does not appear to increase the expansion significantly however, severe restrictions limit the throw of the jet dramatically.

It appears that the shear force generated on the branchpipe by the jet is proportional to the (liquid flow rate)². However, the shear is not proportional to the branchpipe length. This may be explained by a liquid-rich layer that gives the effect of slip

between the foam and the wall. There is no apparent yield stress before this slip occurs.

5 Foam Formation Process Stage Two (Flight)

5.1 Introduction

After the mixing stage within the branchpipe, the air slugs, liquid slugs and bubbles leave as a free jet. As the jet travels it begins to break-up and entrain air. There are many factors involved in the break-up of the jet and therefore the literature review of this chapter has been subdivided into sections covering nozzle design, polymer additives and entrainment, all with a special view towards fire fighting, where possible.

The experimental findings section details the appearance of the jet at different stages in its flight. Also included is evidence that bubbles are blown during the flight. To the author's knowledge, this type of bubble formation within a jet has not been described before in published work. This section also includes details of the different expansion ratios of foam produced after different lengths of flight. These sections have been grouped into Stage Two (Flight). The results are given in Appendix F.

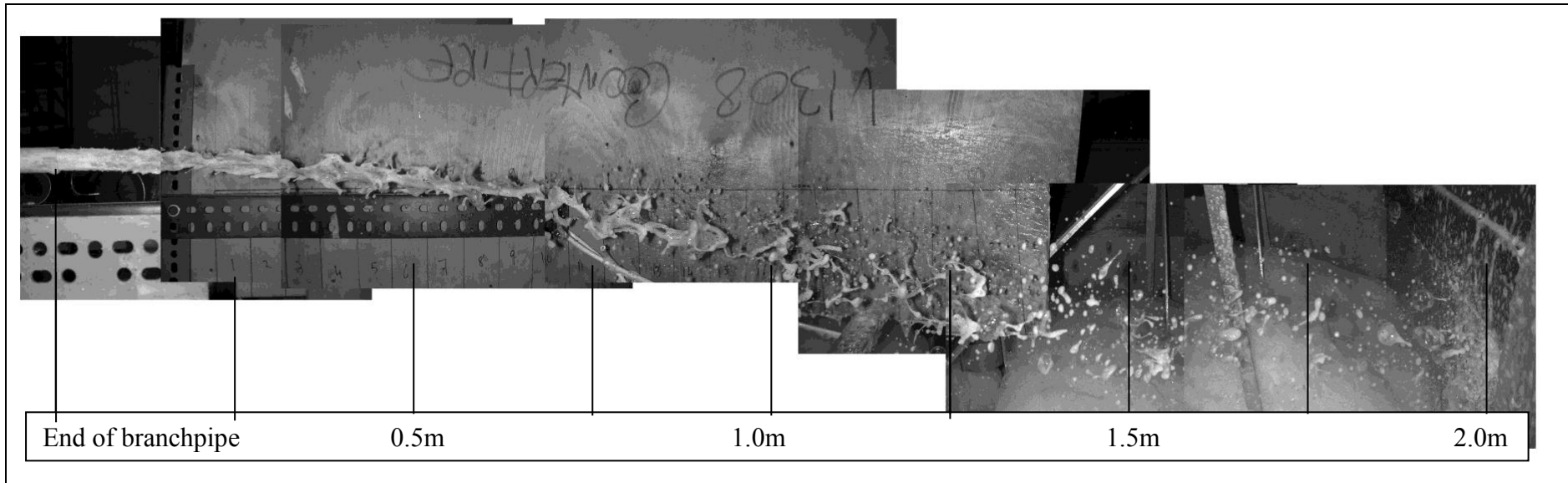


Figure 5:1 Picture of the jet from end of nozzle to break-up

5.2 Literature Review

The earliest investigations into jet flow phenomena appear to have been carried out in the 1830's by Bidone and Savart as cited by McCarthy and Molloy (McCarthy and Molloy 1974). Bidone studied the geometrical form of jets produced by nozzles of regular cross section other than circular. Savart provided quantitative data for jets with a circular cross section, from which he proposed two "laws" for jet disintegration. Plateau's work on stability of a liquid column, as described in Chapter Four (Foam Formation Process Stage One (Mixing)), in part explains Savart's results. Savart's "laws" are:

- 1) For constant diameter, the length of the continuous part of a jet is directly proportional to the jet velocity.
- 2) For constant velocity, the length of the jet is directly proportional to its diameter.

Although a jet of water from a circular cross-section nozzle retains its cross section, its diameter varies along its length as disturbances within the jet grow. There is an increase of pressure at the points of reduced diameter to balance the action of surface tension. Theoretically, the jet will break up to form a series of uniformly spaced drops, as shown in Figure 5:2 a. Perry and Green (Perry and Green 1984) records that Rayleigh, in 1879, calculated that this would yield a drop spacing of 4.5 times the column diameter. This would mean that the diameter of the droplets would be 1.89 times the initial diameter of the jet (D_j). As shown in Figure 5:2 b and c, the break-up of low-viscosity liquid is quite close to Rayleigh's prediction, although smaller satellite drops are also formed.

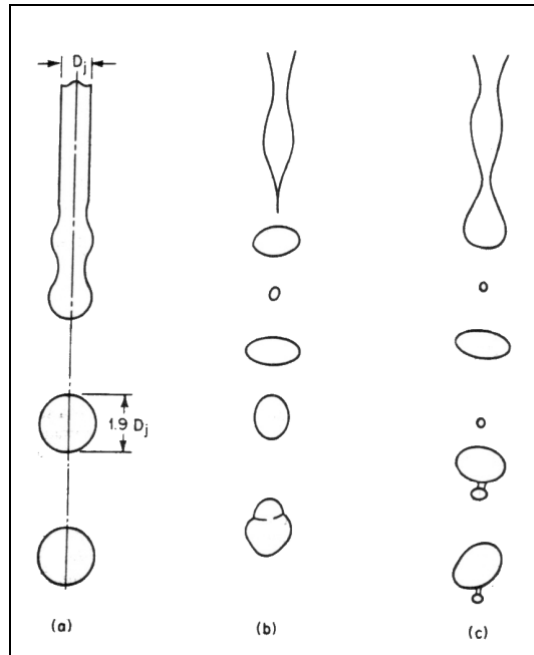


Figure 5:2 cited by Perry (Perry and Green 1984)

- a) Idealised jet break-up suggesting uniform drop diameter and no satellites**
b) and c) Actual break-up of a water jet as shown by high speed photographs

Weber modified Rayleigh's theory in 1931, as cited by Phinney (Phinney 1973). He proposed a theory that related the diameter, surface tension, jet viscosity and density of low-speed laminar jets issuing into stagnant air. He further modified his relationship to enable the break-up length of a laminar jet to be determined (cited in (Phinney 1973), (Chen and Davis 1964) and (Miesse 1955)):

$$\frac{L}{D} = \left(Ln \frac{a}{\delta^*} \right) \cdot \left(W + 3 \frac{W^2}{R} \right) \quad \text{Equation 5:2}$$

where

- L = Initial break-up distance of laminar jet
 D = Inside diameter of pipe and orifice
 a = Radius of jet
 $\overline{\delta^*}$ = The amplitude of the equivalent initial disturbance on the jet surface

$$W = \text{Weber Number} = \frac{V}{\sqrt{\frac{\sigma}{\rho D}}}$$

$$R = \frac{V\rho D}{\mu}$$

V = Mean velocity at exit

σ = Surface tension of liquid

ρ = Density of liquid

μ = Dynamic viscosity of liquid

By plotting the break-up length of a jet against the mean exit velocity, three distinct phases are seen – a laminar linear portion, a transition region and a turbulent region (see Figure 5:3). Using photographic evidence, Grant and Middleman (Grant and Middleman 1966) describe the break-up of jets using this graph:

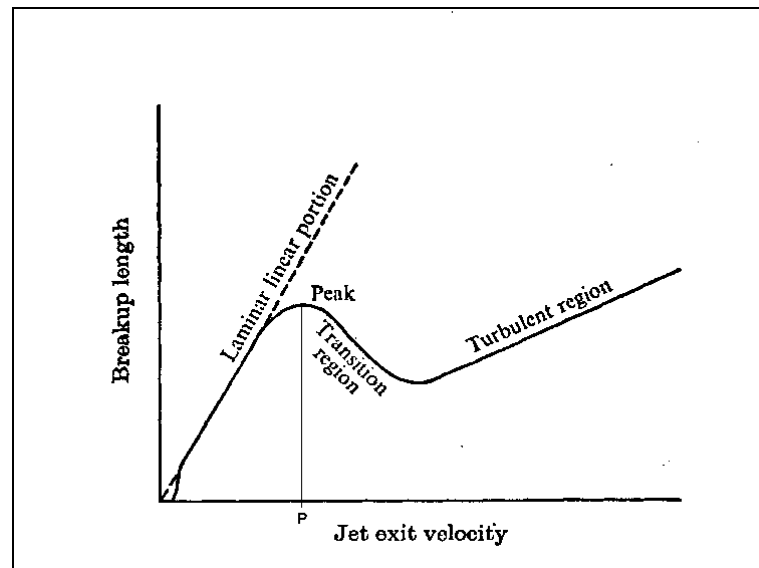


Figure 5:3 Typical curve of break-up length versus velocity (Phinney 1973)

"Over the linear regime, the jets are destroyed by a regular symmetrical disturbance. In the region of the velocity below "P" the break-up remains symmetrical, but the

tendency of the jet to segment is observed. All systems are characterised by the appearance of low amplitude transverse waves at velocities slightly in excess of "P". Initially, these waves appear to damp, and the jet continues to be destroyed by a symmetrical disturbance. To this point, all systems behave in the same manner. As the velocity is further increased, two paths may be followed, depending upon whether the flow in the nozzle remains laminar or becomes turbulent.

If the flow in the nozzle becomes turbulent, the low amplitude waves either disappear or are masked by the ruffled character of the surface. Whatever the case, the turbulent jet initially is destroyed by a symmetrical disturbance. As the velocity of the turbulent jet is further increased, the symmetrical break-up gives way to transverse wave break-up. If the flow in the nozzle remains laminar, the low amplitude waves continue to appear. As the velocity is increased, transverse waves destroy the jet and the break-up length decreases until it nearly coincides with the point at which low amplitude waves first appear on the jet. When this occurs the jet is destroyed by a violent bursting disintegration mechanism."

The laminar linear portion is defined by Weber's theory (Equation 5:1). The regimes beyond this case are not nearly so well understood. Due to the lack of theoretical background into which to fit experimental observations, progress of the understanding of the break-up of turbulent jets has been limited and no simple criterion for ultimate drop size and break-up length exists. Researchers who have attempted work in this area include Theobald (Theobald 1975), Hoyt et al (Hoyt et al. 1974), Hoyt and Taylor (Hoyt and Taylor 1977a), (Hoyt and Taylor 1977b), Merrington and Richardson (Merrington and Richardson 1947), Phinney (Phinney 1973), (Phinney

1975) and Miesse (Miesse 1955). However, comparisons of experimental work are difficult since the nature of any disturbances is often not in complete experimental control.

At low pressures (up to 4 bar), Chen and Davis (Chen and Davis 1964) found that the predominant factors affecting the disintegration of a turbulent water jet were the initial disturbances of the jet due to turbulence in the fluid, and the surface tension forces. However, Schweitzer (Schweitzer 1937) states that viscosity has a decisive influence on jet disintegration and that the effect of surface tension is minor in higher pressure sprays (between 33 and 333 bar). Hatton and Osborne (Hatton and Osborne 1979) found that the surface tension force becomes of decreasing importance as the jet diameter increases. They state that in a large jet the turbulent eddy sizes are much greater and disrupt the jet surface smoothness more easily than for a small jet. Therefore, attempting to correlate data from a small jet moving at low speeds with data for a large jet does not succeed.

5.2.1 Nozzle Design

To reduce the disturbances within the jet, investigations into nozzle designs have been carried out. The aim of many of these investigations has been to produce a jet having the maximum throw and coherence and the least spray formation. Most authors agree that it is of the highest importance to eliminate swirl, to obtain a uniform velocity profile and to reduce turbulence at the nozzle entry in order to achieve maximum jet throw distance. In 1889 Freeman (Freeman 1889) proposed the classical fire nozzle profile (Figure 5:4). His work is still the most widely accepted treatise on the subject of fire streams, although the projection of fire fighting foam is not considered. Further

work on fire fighting nozzles has included research by Murakami and Katayama (Murakami and Katayama 1966), Rouse, Howe and Metzger (Rouse et al. 1951) and Theobald (Theobald 1981).

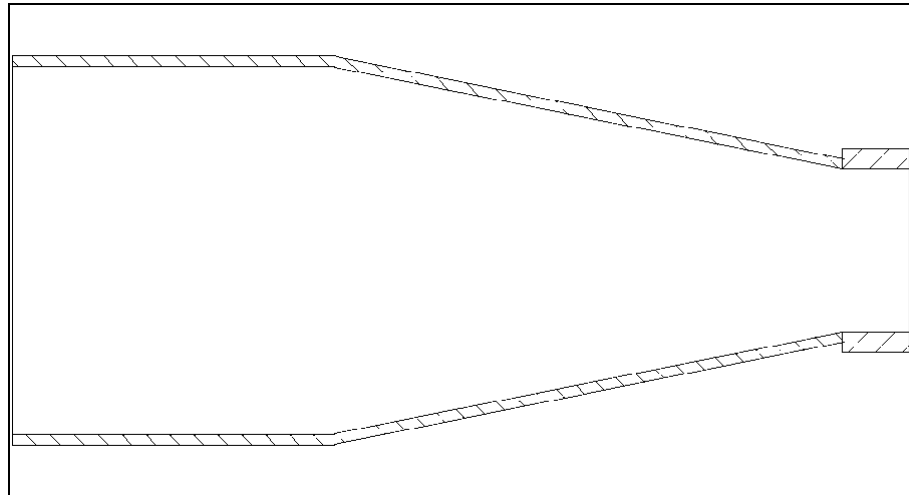


Figure 5:4 Classical fire nozzle

5.2.2 Polymer Additives

Ting and Hunston (Ting and Hunston 1977) have produced a literature review of the available data on polymeric additives in flow systems. This section is based on their work and work by Hoyt and Taylor (Hoyt and Taylor 1977a) and Hoyt et al (Hoyt et al. 1974).

When a polymer is introduced into a jet the initial laminar region becomes smaller or disappears completely. This suggests that the addition of a polymer has a destabilising effect on laminar flow. As the jet proceeds, it soon becomes fully turbulent but, unlike the jet of water without additives, the spray droplets are completely absent. The reduction of spray formation results in an increased transparency and smoothness of the external jet surface. When a water jet eventually

breaks up, it is characterised by a chaotic array of various size droplets. With polymer additives present, however, the break-up involves the formation of filaments linking the droplets. These filaments persist for a significant period, gradually thinning until finally they break. Hoyt et al (Hoyt et al. 1974) conducted experiments on water jets with a reduced surface tension but with no polymer added. They concluded that the changed surface tension plays only a small role in the major effects noted when polymers are present in the flow, although they do not state the nature of the role they do play. This implies that the reduction in surface tension is not responsible for the stringy effect seen.

Theobald (Theobald 1975) records that minute quantities of soluble drag-reducing additives in fire fighting equipment produce a marked change in the appearance of the jet leaving the nozzle. The presence of the additive reduced the pressure loss along the supply hose resulting in a higher operating pressure at the nozzle. It also resulted in a smoother, quieter more coherent jet.

5.2.3 Entrainment

When two fluid streams flow past each other with different velocities, particles from the boundaries of each fluid interact. Turbulent mixing then takes place between the streams to equalise their velocities. When a jet encounters stationary fluid it sets some of this in motion - a process known as entrainment. The amount of air entrained by water sprays and jets has been studied by various authors (McQuaid 1975), (McQuaid 1976), (Hill 1972), (Benatt and Eisenklam 1969), (Heskestad et al. 1976) and (Rasbash and Stark 1962).

McQuaid's work on air entrainment by a water spray on the axis of a short tube was discussed in Chapter Four. Benatt and Eisenklam (Benatt and Eisenklam 1969) also produced a model for gaseous entrainment into axisymmetric liquid sprays. Their set-up was different from Test Rig Three, as they did not have a bounded spray, they used hollow cone nozzles and they assumed that the air was incompressible. They also calculated the air entrained throughout the fall of the spray, rather than just that entrained near the nozzle. Figure 5:5 shows the liquid leaving the nozzle as a liquid sheet, which then separates into individual drops, which form a sheath. The gas is entrained into the drop sheath perpendicularly and leaves axially, the change in direction takes place abruptly at the surface of the sheath. They state that the entrained gas, which can be treated as an incompressible fluid, travels at velocities much smaller than that of the drop and the momentum of the induced gas on approach is negligible.

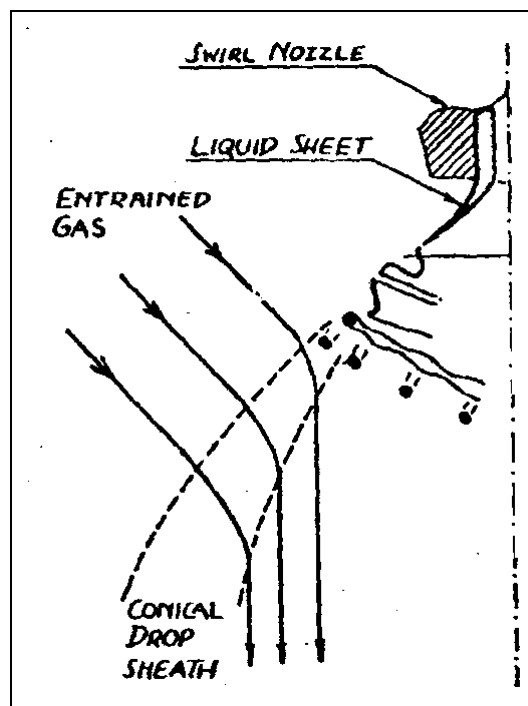


Figure 5:5 Schematic flow diagram (Benatt and Eisenklam 1969)

Heskestad, Kung and Todtenkopf (Heskestad et al. 1976) considered the entrainment of air into water solid cone sprays discharging into quiescent surroundings, both theoretically and experimentally. They conclude that the entrainment flow is sensitive to the water discharge rate when the nozzle pressure is varied at constant nozzle diameter. However, it is rather insensitive to the discharge rate when the nozzle diameter is varied at constant nozzle pressure. They assume that the air is incompressible. Ahmed (Ahmed 1993) continued this work and applied it to hot gases rather than the atmosphere. He records that visualisation studies have revealed that the entrained air approaches the spray sheath roughly perpendicular and quickly changes direction once in the sheath to become almost parallel to the spray axis. Ahmed also states that greater turbulence is observed in the liquid at increasing axial distances from the nozzle and that the air velocity increases with increasing injection pressure, indicating an increase in rate of air entrainment.

5.3 *Experimental Findings, Results and Theory*

The high speed video provided an invaluable insight into the break-up mechanisms of the jet. As the jet leaves the branchpipe, the flow appears relatively smooth, although not laminar. Within two diameters, the jet becomes lumpy and the air slugs start to become visible. This is seen clearly in Figures 5:6 and 5:7 and in CD Slug Escape.avi. At the end of the branchpipe, some of the air slugs are seen to escape into atmosphere. After about half a diameter, small bubbles, approximately 2 mm in diameter, become apparent throughout the mixture (see Figure 5:8). During flight, many of the remaining slugs grow in size as the enclosed gas, which was compressed as it was entrained into the branchpipe, expands. Other slugs are pulled

apart and then squashed by the turbulence introduced by the nozzle. This may cause some of them to split into two bubbles, as described in Stage One (Mixing), or they may burst. The jet is seen to twist gently downwards when viewed with the travel from left to right.

It is difficult to compare the foam jet break-up with published work, as it is a turbulent two-phase jet and little has been published on this topic. Also, the full cone nozzle sprays into, effectively, a second nozzle (the branchpipe) which is more like a cut pipe than a well defined nozzle.

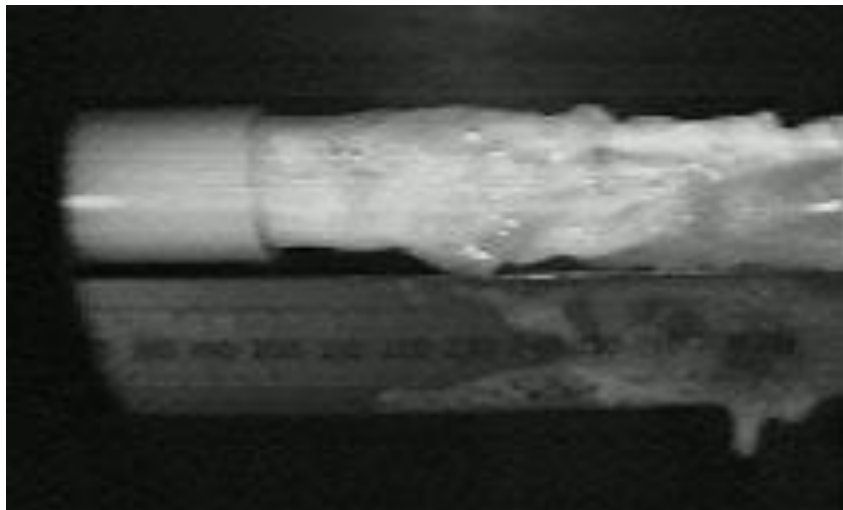


Figure 5:6 Transition from relatively smooth to lumpy flow

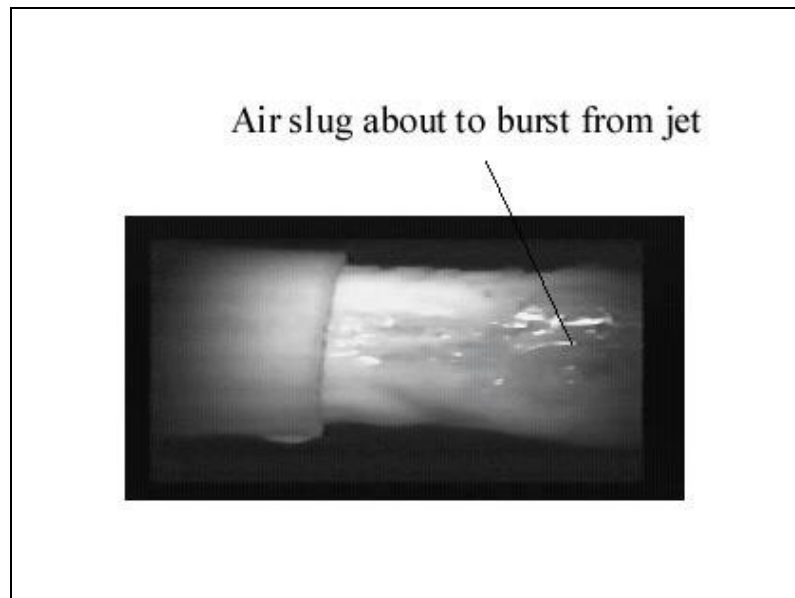


Figure 5:7 Air slugs become visible

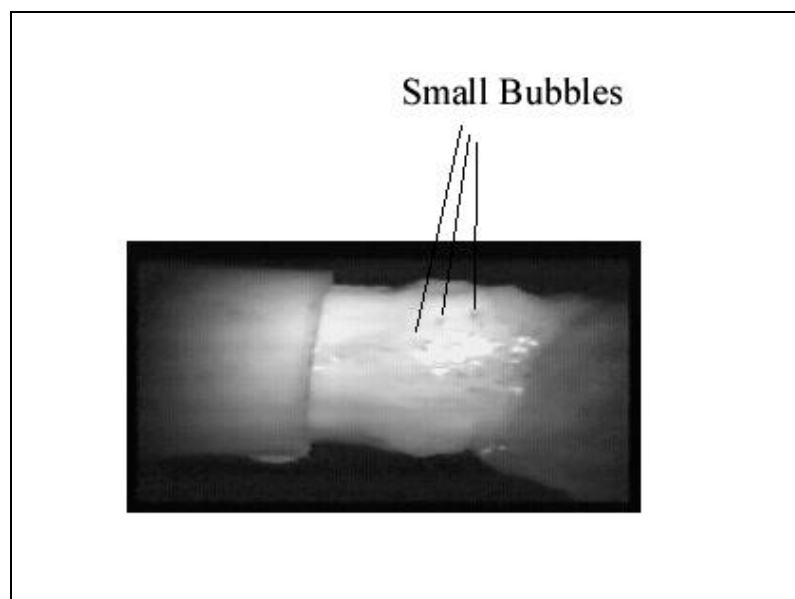


Figure 5:8 Small bubbles become visible

To the naked eye, the jet appears continuous throughout the first 1.1 m of its 1.65 m flight, although the diameter of the jet increases as the jet progresses. At approximately 1.1 m the jet has spread so wide that gaps become visible between droplets. The high-speed video shows that the jet actually consists of large air pockets

between large globules of foam and foam solution from approximately 0.15 m from the end of the branchpipe onwards (see Figure 5:9 and CD Flight.avi).



Figure 5:9 Large air gaps visible within jet (Taken approximately 80 cm from end of branchpipe)

When water was pumped through the system, the jet break-up was characterised by a chaotic array of various sized droplets. However, with the surfactant solution the break-up involved the formation of filaments linking the droplets. This is similar to, although not as dramatic as, the break-up of jets with polymer additives, as described in section 5.2.2 Polymer Additives. As Rockwood's Macrofoam is a commercial product, not all of the constituent chemicals are listed but none of those that are listed is a polymer. However, it is probably reasonable to speculate, given the stringy effect of the jet, that the surfactant does contain a polymer or a polymeric chemical. The droplets formed from the break-up of the surfactant jet often consist of clumps of the 2 mm diameter bubbles. Some droplets may fall back into the main body of the jet

and entrain more air in the plunging jet method described in detail in Chapter Six (Foam Formation Process Stage Three (Collision)).

Although work has been published on the shape and form of bubbles (Isenberg 1978), (Rayleigh 1917), (Monnereau-Pittet and Vignes-Alder 1999) and (Weaire 1996) very little has been written on the blowing of bubbles. The paper by Hinze (Hinze 1955) mainly focuses on the splitting of globules, but does include a series of photographs that show the nature of the break-up of different drops launched in a horizontal flow. One type of drop break-up has a convex part directed downstream which looks very similar to a child's bubble being blown through a wire loop. Hinze suggests that this is due to the pressure distribution along the drop and not to the acceleration effects.

Thin films are sometimes formed between the filaments linking the droplets. Entrained air, moving slower than the film, may blow the film like a child's bubble, which can then separate from the jet. This can be seen in Figure 5:10 and CD Flight.avi. If the film is stretched too thin or too fast, it will burst. If the film remains as a hemisphere, it may become closed on contact with another film of liquid, for example on a solid or liquid surface. Some globules are connected by the slugs that have now expanded into large bubbles. However, the formation of bubbles in this manner does not appear to affect the final expansion of the foam very much, as many bubbles burst either during flight or on collision, or detach from the main jet and float away.



Figure 5:10 Bubbles in flight (large bubbles approx. 25 mm diameter)

Foam from the jet was collected at different flight distances and the expansion calculated. However, the experiments were conducted on different days, at different times of year. The longer flights produced a marginally higher expansion than the shorter flights. To ensure that this was a flight-only property, the experiments were then repeated on the same day and using the same tank of surfactant solution (see Figure 5:11).

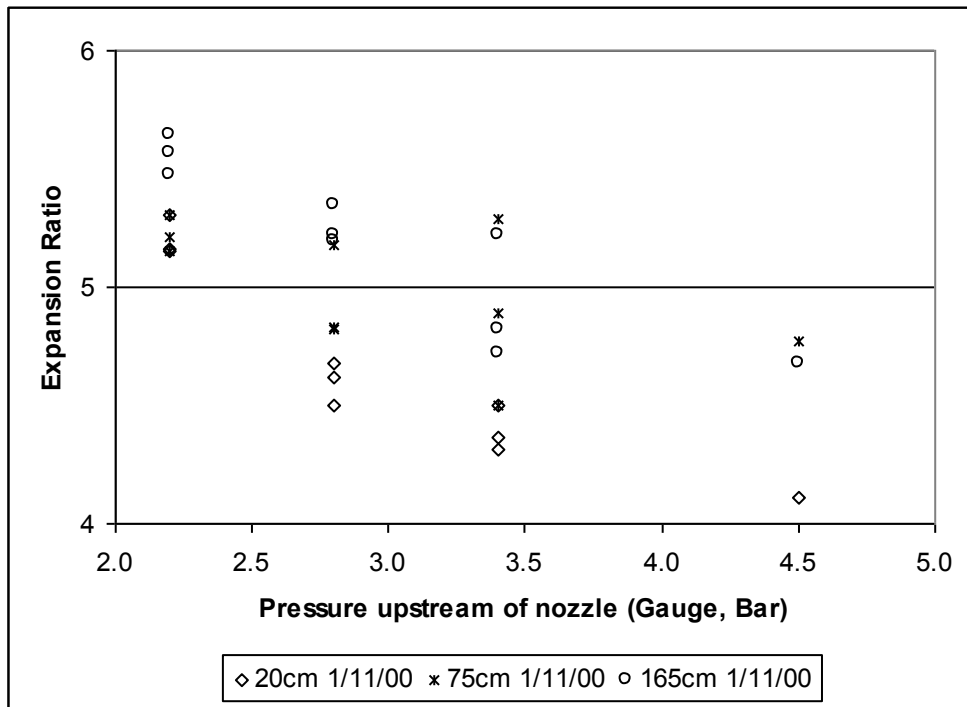


Figure 5:11 Expansion with different flight distances

Although the 20 cm flight does produce the lowest expansion ratio, the difference between ratios at different flight distances is small compared to the experimental error involved in taking the measurements. The amount of experimental error for each piece of equipment is given in Appendix D. However, as all of the foam produced with a 20 cm flight distance is less than that produced with a longer flight distance, experimental error alone probably cannot account for the difference. It is suggested that the force with which the jet hits the collecting vessel at the 20 cm flight distance destroys some of the larger bubbles and some of the entrained air escapes. This could also explain why the expansion ratio gradually decreases with increasing pressure upstream of the nozzle.

The air entrained by the flight of the jet was not calculated, however, the results imply that it has no relevance to the expansion ratio of the foam produced.

5.4 Conclusions

The mixture of air slugs, liquid slugs and bubbles leaves the branchpipe as a free jet, but at the end of the branchpipe, some of the air slugs are seen to escape into atmosphere. The jet appearance changes over distance. During the first 1.1 m of flight, the jet appears to be a coherent “rope” to the naked eye. However, the jet actually consists of large air pockets between large globules of foam and foam solution from approximately 0.15 m onwards. After 1.1 m the jet has become quite dispersed.

During break up of the jet, droplets are sloughed off. Many of these remain connected to the main jet by strands of solution. These strands are pulled into thin films and blown like a child’s bubble. These bubbles often burst or separate from the jet, and play little or no part in the final expansion ratio. Large bubbles are also formed during the flight by the air slugs, already within the jet, expanding. However, this mechanism also contributes little to the overall expansion of the foam. Another minor contributor to the overall expansion is the bubbles produced by the sloughed off droplets falling back into the main body of the jet. This method is described in detail in Chapter Six (Foam Formation Process Stage Three (Collision)).

A shorter flight distance produces a smaller expansion ratio than a long flight, but this difference is small. The difference can probably be attributed to the force with which the jet hits the collecting vessel. This force may burst some of the bubbles. This could also explain why there is a decrease in expansion ratio for all flight distances with an increase in upstream pressure. This hypothesis has not been rigorously tested.

The amount of air entrained by the jet is assumed considerable, but the experimental results imply that this has little relevance to the overall expansion ratio of the foam produced. The early break-up of the jet from the scale model shows that the branchpipe set-up would be unsuitable for projecting the foam a suitable distance for fighting fires. However, the mechanisms of foam formation will be similar in a commercial branchpipe, as the same surfactant solution and principle are used.

The air entrained by the flight of the jet appears not to be incorporated into the final foam and therefore has no relevance to the expansion ratio. Therefore, although bubbles are generated during the flight, the flight distance has little relevance to the overall expansion ratio.

6 Foam Formation Process Stage Three (Collision)

6.1 Introduction

Gas capture by a liquid jet plunging into a pool of stationary liquid is frequently encountered in industrial, domestic and environmental situations. Industrial examples include pouring of molten glass and metal, where bubbles are often undesirable and therefore steps are taken to restrict or prevent them. Air bubbles are also undesirable whilst filling containers with liquids such as paints or food products. However, in many chemical industries, such as fermentation and waste treatment processes, air inclusion is required to increase the gas absorption and ensure good mixing. In many domestic areas, gas capture is highly desirable. It is difficult to imagine a bubble bath with no bubbles or doing the washing-up with no foam. Re-aeration of rivers and streams is often helped by air capture from waterfalls, rapids, weirs and rainfall.

Although there have been comprehensive studies on air capture by the plunging jet method it has not, to the author's knowledge, been applied to the formation of foam. In addition, the majority of previous work on plunging jets has been done with pure water and no references have been found to experiments using surfactant solution.

The Ross-Miles test is commonly used commercially to determine the foaming properties of liquids, but again, to the author's knowledge, it has not been used to determine the actual properties of foam formation.

This chapter describes these methods and how they were combined, with the use of a high-speed video camera, to determine which factors have the most effect on foam

formation. The development of a new method of measuring the amount of air entrained by a plunging jet, which is simpler than those in current use, is also described.

6.2 Literature Review

In 1938 Mertes patented a technique for mixing reacting liquids and gases, as recorded by Burgess (Burgess et al. 1972). His plunging liquid jet reactor was defined as "the flow geometry formed by a coherent liquid jet plunging through an ambient reactive atmosphere into a bath of the same liquid". In 1953 the Ross-Miles pour test, which is based on a plunging jet, was adopted by the American Society for Testing and Materials (ASTM), as quoted by Rieger (Rieger 1995) and Bikerman (Bikerman 1973). It is still used to assess the ability of various liquids to form foam. The test is conducted by allowing a stream of the test solution to impinge on another portion of the test solution to create turbulence.

Since 1970 there have been many more studies on the subject of plunging jets (Lara 1979), (Sheridan 1966), (Burgess et al. 1972), (McKeogh and Ervine 1981), (Van de Sande and Smith 1976), (Van de Sande and Smith 1973), (Sene 1988), (Oguz 1998), (Lin and Donnelly 1966). In 1993, Bin (Bin 1993) produced a comprehensive review of the available literature. He made a critical analysis of various aspects of gas capture by plunging liquid jets and much of this section is based on this work.

The plunging jet method is also evident in fast moving water flows with a free surface. Volkart (Volkart 1980) shows how air bubbles are mainly generated in moving water by water particles being thrown out and then falling back into the main flow. The

produced bubbles increase in size as diameter and velocity of the pertinent drops increase.

There are two stages to the plunging jet method. The first is when air, entrained by the jet, is carried into the water, and the second is where the sheath of air surrounding the turbulent jet is captured.

Low velocity jets use only the first stage. The gas capture mechanism is governed by the interaction between the disturbances on the jet surface with the surface of the receiving pool (Figure 6:1). The liquid surface has a small depression that is caused by the impact pressure of the associated boundary layer gas (Figure 6:1 a-c). The horizontal movement of the free surface is not fast enough to follow the roughness of the jet as it moves past, resulting in a toroidal hole filled with air (Figure 6:1 d). Shear stresses then break up the captured air into bubbles. The disturbances on the jet produce an irregular gas entrainment. With a more turbulent jet, the surface disturbances become bigger, producing a greater entrainment and therefore greater capture. Gas capture by low viscosity jets depends on the magnitude of disturbances on the jet surface. The magnitude depends on the velocity, diameter and length of the jet and on the physical properties of the liquid. It is also influenced by the environment, as well as nozzle design.

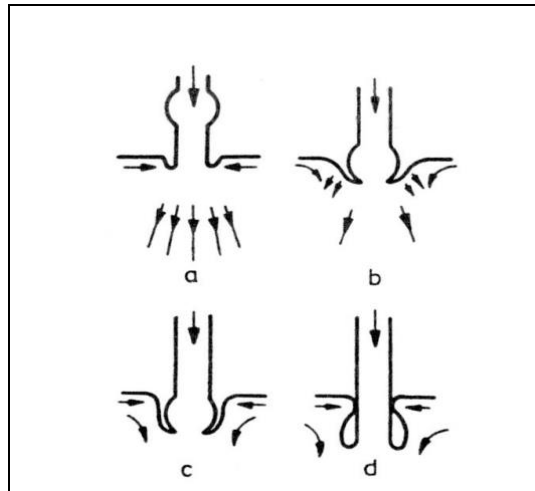


Figure 6:1 Air capture mechanism (Bin 1993)

(a)-(d) show subsequent phases as a disturbance in the jet moves downwards.

High velocity jets use both of the stages. The entrained air is carried along with the jet, encompassed within the envelope defining the limits of the rough surface. An associated boundary layer is also carried along. When the jet impacts on the pool surface, both of these air movements are carried under the free liquid. The subsequent breakdown of the captured annulus gas film requires significant time before disintegration. High velocity jets have a regular gas capture rate and small bubbles are produced.

At high jet velocities a third mechanism has been suggested by Thomas, as reported by Bin (Bin 1993). Most of the air captured enters via the layer of foam forming on the surface of the receiving fluid. Air enters the foam, possibly because of wave action and splashing, and is then pulled into the main body of the flow along with the re-circulating foam. At low plunge angles, the foamy re-circulating flows have much higher velocities than those driven by a steeply falling jet do, so that large quantities

of air are captured along with the foam. This may explain why inclined jets capture more air than vertical ones.

Lara (Lara 1979) was the first to establish two regions of the onset of air capture by a vertical plunging liquid jet. Figure 6:2 illustrates the threshold of the two capture regions:

- 1) where the jet breaks into droplets before reaching the pool surface
- 2) where the jet is continuous

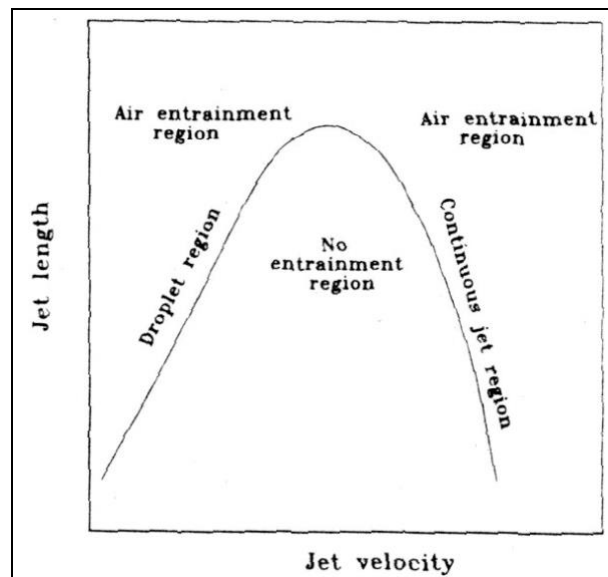


Figure 6:2 Threshold of air capture region (Bin 1993)

Lara concludes:

- 1) At low velocities, when the jet breaks up before touching the surface, air is captured.
- 2) If the velocity is increased such that the break-up distance becomes equal to the nozzle to water surface distance, capture ceases.

3) There is a critical nozzle to water surface distance, above which air is always captured.

4) After the no-capture condition is attained, if the velocity is increased further, capture will commence again, but no break-up of the jet is observed.

The amount of gas captured is largely controlled by the jet velocity. The other primary variables (jet diameter, jet length and the physical properties of the fluids) also play a considerable part. However, secondary features, such as nozzle design, angle of jet inclination, presence of vibrations, etc. also exert a profound influence on the jet behaviour and hence capture rate. In order to simplify quantitatively the effect of different parameters on the entrainment ratio (Q_A/Q_w), Bin (Bin 1993) proposed a relationship between this ratio, the jet Froude number and the ratio L_j/d_o , for vertical jets:

$$\frac{Q_A}{Q_w} = 0.04 Fr_j^{0.28} \left(\frac{L_j}{d_o} \right)^{0.4} \quad \text{Equation 6:1}$$

Where

Q_a = Air capture rate (m^3/s)

Q_w = Liquid flow rate (m^3/s)

Fr_j = Froude Number = $v_j^2 / g d_o$

v_j = Jet velocity at entry of receiving pool (m/s)

g = Acceleration due to gravity = 9.81 m/s^2

L_j = Jet length (m)

d_o = Nozzle diameter (m)

There are essentially two groups of methods of entrained gas flow rate measurement:

- 1) Catching gas after it has been entrained into the pool liquid.
- 2) Measuring the removal of gas from a gaseous space above the pool surface around the plunging point.

The first group includes using inclined jets and bubble traps. The second group has the gaseous space above the pool in the vicinity of the plunging point separated from the ambient, and a supplementary gas is let into this space through an appropriate flow rate device. Both groups have shortcomings. In the case of inclined jets, extrapolation is usually required to get data in the vertical position. Traps or gas removal arrangements may interfere with the fluid flow within the pool and are not very satisfactory in capturing gas bubbles formed with very rough jets. The second group can be particularly cumbersome.

As different authors use different measurement techniques to calculate the amount of air captured, and different nozzle geometry affects the amount captured, comparisons between different authors' results has been difficult. However, Bin has shown that the above equation gives a satisfactory agreement with experiments of other authors, provided that $L_j/d_o \leq 100$ and $l/d_o \geq 10$ (where l = length of cylindrical section of nozzle) and $Fr_j^{0.28} \left(\frac{L_j}{d_o} \right)^{0.4} \geq 10$. The equation is also applicable to all regions of entrainment.

In an attempt to clarify the effects of nozzle geometry and physical properties of the liquid phase on the capture rate a capture rate curve has been established (Figure 6:3). The curve has three distinct regions.

- 1) Initial and or low jet velocity region (up to about 5 m/s)
- 2) Transition region
- 3) High jet velocity region

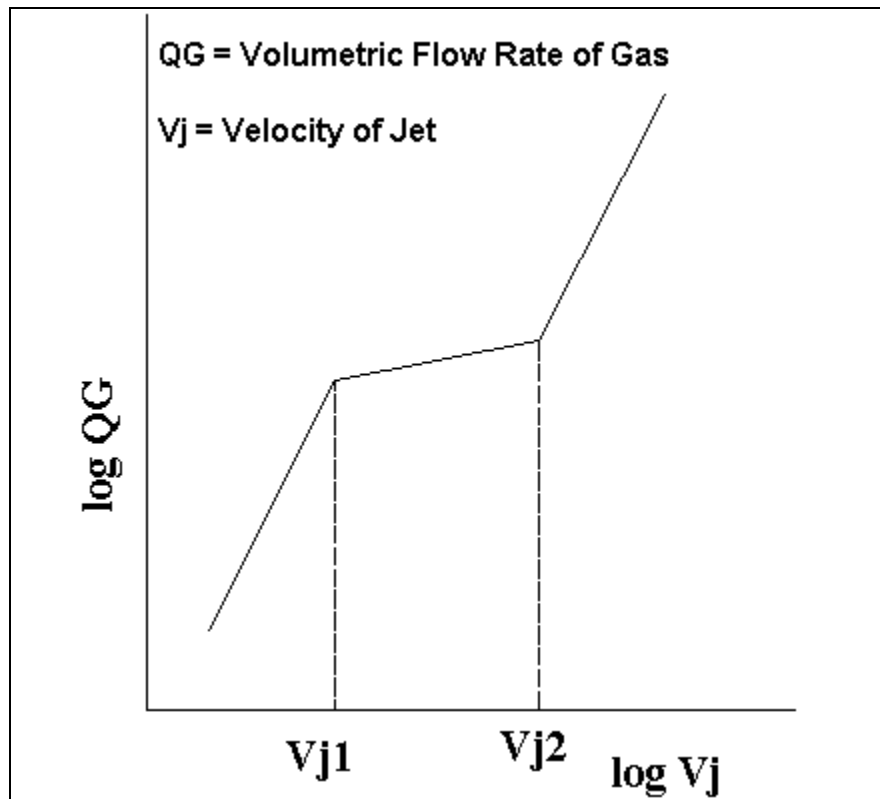


Figure 6:3 Capture rate curve (Bin 1993)

The liquid jet velocity must exceed a certain critical value to capture air. Bin (Bin 1993) highlights that there is, at present, no successful theoretical approach to predict the minimum capture velocity for vertical plunging jets. However, Sheridan (Sheridan 1966) states that for a water jet plunging into a deep pool the critical velocity of air capture varies with the jet diameter. Individual droplets impinging on a liquid surface will also capture air if their velocity is high enough (above 1 m/s, depending on their size), or if successive droplets impinge along the same trajectory (Volkart 1980).

Because of gas capture by vertical plunging liquid jets, bubbles become dispersed below the liquid surface. The dispersed bubbles form two distinctly different regions (see Figure 6:4):

- 1) A bi-phasic conical region comprising bubbles with diameters of less than 1 mm.
- 2) A region of larger rising bubbles which surrounds the bi-phasic region.

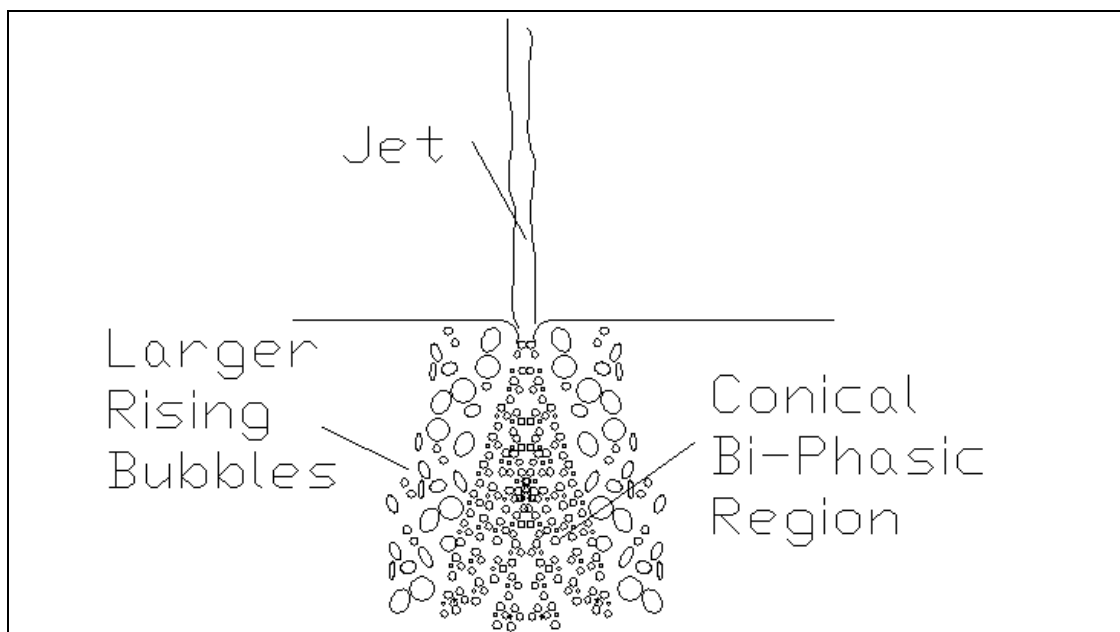


Figure 6:4 Bi-phasic conical region and region of large rising bubbles

Bubbles in the bi-phasic region penetrate the liquid to some maximum depth due to the momentum of the submerged jet. At the maximum depth of penetration, buoyancy forces counteract this momentum and the bubbles may grow by coalescence and escape sideways until they are free to rise to the liquid surface. The larger bubbles are usually of an oblique-spherical shape. The final depth of penetration appears to be dependent on the nozzle geometry and on the ratio between the length of the jet and diameter of the nozzle.

In an inclined jet the bi-phasic region has a different shape since bubbles following the jet velocity (momentum) field penetrate the pool to some distance and then start to rise to the pool surface moving along a resultant trajectory. The shape of the bi-phasic region then resembles a bowl.

6.3 Experimental Findings and Results

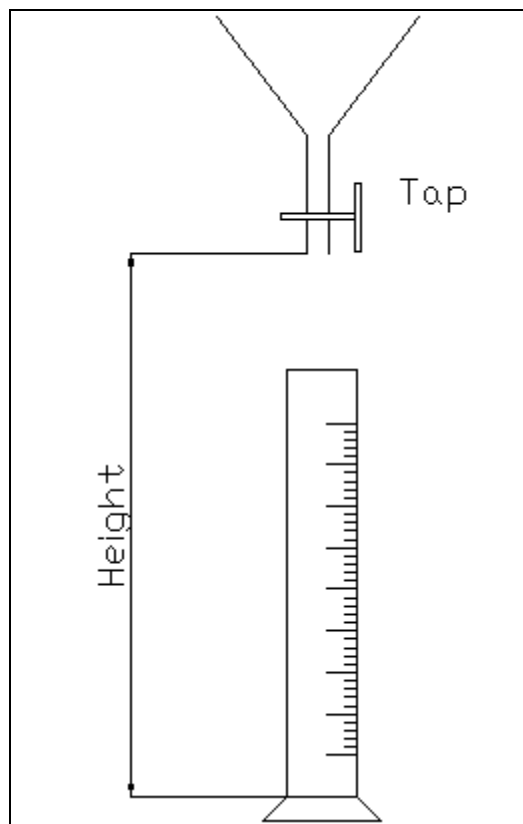


Figure 6:5 Ross-Miles Test Rig

The Ross-Miles pour test was used to examine the formation process of foams generated from a plunging jet. The tests were conducted using 200 ml of surfactant solution (Rockwood Macrofoam at nominal 3%) and the equipment in Figure 6:5. The high-speed video camera was used to investigate the foam formation and the manner of penetration of the jet. The experiments were designed using the factorial

method and three variables, each at two levels, were deemed appropriate. These were the height of the funnel from the bottom of the measuring cylinder (H), the receiving liquid (L) and the initial volume of the receiving liquid (V). The final height of the foam and the liquid were measured after approximately one minute. The experiments were repeated and the average was used in the analysis. The amount of experimental error for each piece of equipment is given in Appendix D. The variables were:

L1 = Surfactant solution

L2 = Tap water

H1 = 600 mm

H2 = 450 mm

V1 = 100 ml

V2 = 0 ml

The 200 ml of liquid took approximately 17 seconds to empty through the tap. This gave a mean flow rate of $1.18 \times 10^{-5} \text{ m}^3/\text{s}$. The smallest diameter in the tap was 4 mm, which gave an area of $1.26 \times 10^{-5} \text{ m}^2$ and therefore an average exit velocity of approximately 0.89 m/s. As the level of the receiving liquid rises as the jet enters, the velocity of the jet at entry changes with time. The velocity at mid-height was

therefore calculated using $v_{final} = \sqrt{2gh + v_{initial}^2}$ (for ideal conditions), where:

v_{final} = velocity of jet at entry to receiving pool

h = height jet has fallen

$v_{initial}$ = velocity of jet at the tap.

A velocity of between 2.75 m/s and 3.40 m/s was found for each of the jet lengths. The video was used to check these values, and the velocity was found to be approximately 3 m/s for each jet length. The distances in the video were very small (approximately 5 cm) and therefore the margin for error in calculating the velocity

from the video is relatively high. This will probably explain the discrepancy between the velocity calculated from the equation and that calculated from the video. The equation values have been used in the following work.

Yates' analysis was applied to the results to see if any variables had a significant effect on the formation of foam and to discover if there were interactions between the variables. The results are given in Appendix E. The Yates' analysis was completed for two measurements - the volume of foam produced (the "head" of foam on top of the liquid) and the expansion ratio of this head of foam. The expansion ratio was

calculated from the equation:
$$\frac{\text{volume of foam in head}}{\text{total volume of liquid} - \text{volume of liquid to interface}}$$

The Yates' analysis showed that the height of the funnel above the bottom of the measuring cylinder had the greatest effect on the volume of foam produced. The average volume of foam produced was 231 ml. The lower position of the funnel (450 mm from the bottom of the measuring cylinder) produced an average of 84 ml less foam than that produced by the funnel in the higher position (600 mm above the bottom of the measuring cylinder).

The type of liquid the jet plunged into had no apparent effect on the total volume of foam produced, although it did affect the foam expansion ratio. The volume of foam produced when there was initially no liquid in the receiving pool was only 5 ml higher than when there was liquid in the pool. This is within the experimental error of the measurements and has therefore been deemed insignificant. The interactions all produced differences of less than 14 ml in the total volume of foam produced and these were also deemed insignificant.

The video clips CD f,w,j,h.avi and CD f,w,j,l.avi show test runs with surfactant solution plunging into a receiving pool of water, with high and low funnel heights respectively. The depth to which all the jets penetrated was over 4 cm. The exact depth was not measured due to fluctuations. However, as the depth of the receiving pool had little effect on the total volume of foam produced, it is assumed that the depth of penetration also has little effect on the volume of foam produced.

McKeogh and Ervine (McKeogh and Ervine 1981) used high-speed photography to determine the break-up length of jets. They state that air capture increases with height of fall until a point is reached where the amount captured levels off and decreases. They state that this point corresponds to the break-up length of the jet, after which the jet begins to break into discrete particles, lose momentum to the surrounding air and capture less air. The jet in the author's experiments was continuous to the eye, but the video, taken at 4500 frames per second (fps) shows that the jet is actually broken into a string of droplets. In the high funnel position, these droplets had mainly separated into individual globules, whereas in the lower position they were still joined together by surfactant solution. This appears to contradict McKeogh and Ervine's findings that less air is captured when the jet is broken up. However, McKeogh and Ervine's graphs indicate that the levelling off occurs over a height change of 1 – 2 metres rather than the 150 mm of the author's experiments, and this may explain the discrepancy. Over the short distance involved in the author's experiments, the amount of momentum lost to the surrounding air is probably not as significant as in the experiments by McKeogh and Ervine.

The break-up is the only visible difference between the jets from the high and low funnel positions. The separation of the jet into droplets is likely to increase the jet diameter, which will cause the indentations on the surface of the receiving pool to become highly irregular in form. This may contribute to the increase in the amount of air trapped, by increasing the surface area over which the jet plunges and dispersing the captured air over a wider area within the pool.

For the foam expansion ratio, the type of liquid in the receiving pool played an important part. If the jet entered surfactant solution, a higher expansion foam was produced than if it entered water (an increase of 5.03 on an average of 16.51). The interaction between the type and volume of receiving liquid was also important (an increase of 5.01 above the average was produced if the receiving pool was 100 ml of surfactant solution). All the other interactions produced a slight effect, but the differences were all less than 3. The higher expansion foam produced when the receiving pool was surfactant is probably due to the lower surface tension of the surfactant. With a lower surface tension, larger bubbles remain stable and may coalesce without bursting.

The Ross-Miles experiments were also conducted with the jet impinging onto a smooth flat and / or sloping solid surface. When the jet impinged directly onto either of the smooth solid surfaces, no foam was formed. This was surprising as it was expected that some foam would be produced by the splashing of the liquid. This experiment was repeated using a straight nozzle on test rig three, with a flow rate of 14.8 l/min and an upstream pressure of 0.49 bar. As the jet impinged on the solid sloping surface, again no foam was seen to form. Video clip CD

Straight Jet Collision.avi shows a jet of surfactant solution impinging onto a sloping flat surface, with no bubbles being formed.

The Ross-Miles experiment was then conducted with the jet impinging on a rough surface. A layer of foam was produced, which can be seen as a slightly darker area on the white rough surface in Figure 6:6. The surface properties of the solid therefore play an important part in foam formation at collision.



Figure 6:6 Jet impinging on rough surface

It appears from the full cone nozzle experiments (using Test Rig Three) that more foam is produced when an aerated jet hits a sloping surface. To test this theory a foam of known expansion is required. This should then be dropped onto a solid surface and the expansion of the resulting foam calculated. The properties of the foam required

are very specific. If the bubbles are too large, the nozzle will become blocked. If the expansion is too high, the foam would fall as a lump, and not as a jet. If the drainage time is too short, the expansion ratio may vary over the time taken to complete the experiments. Unfortunately, a monodisperse, very low expansion foam with a high 25% drainage time is required for this, and at present, there is no simple method of producing a foam with these characteristics. This hypothesis has therefore not been tested. It is also assumed that an aerated jet impinging onto a rough surface will produce more foam than one hitting a smooth surface.

Single droplets, rather than jets of liquid were also passed through the Ross-Miles equipment. In most cases the single drop did not have sufficient energy to penetrate the surface tension of the receiving pool and instead just caused an indentation. The indentation was not sustained for long and as it closed a finger of liquid was ejected from the surface, which caused a rippled effect on the surface. The clip CD singledrop.avi shows a single droplet of surfactant solution dropping into water. The high drops produced a deeper but less wide indentation than the low ones. In a few cases, a small bubble of air was captured, as can be seen towards the end of video clip (CD Air Capture.avi) and remained under the surface for some time.

There have been many studies on air capture by plunging jets, as described in the literature review, and various methods of measuring the amount of air captured have been reported. The method used here, of measuring the volume of air trapped in the foam produced whilst using a surfactant solution, does not appear to have been previously published.

To determine if the “surfactant method” is comparable to other methods, the use of

Bin’s equation $\frac{Q_A}{Q_w} = 0.04 Fr_j^{0.28} \left(\frac{L_j}{d_o} \right)^{0.4}$ (Bin 1993) was considered. However, this

equation only gives a satisfactory agreement with experiments of other authors, provided that $L_j/d_o \leq 100$, $l/d_o \geq 10$ (where l = length of cylindrical section of nozzle)

and $Fr_j^{0.28} \left(\frac{L_j}{d_o} \right)^{0.4} \geq 10$. As the author’s results do not fit these criteria (L_j/d_o is in the

region 85 to 140, $l/d_o = 7.5$ and $Fr_j^{0.28} \left(\frac{L_j}{d_o} \right)^{0.4}$ is approximately 4), the equation was

not expected to be in very good agreement with the experimental results.

Nevertheless, as there is no other method known to the author for comparing the air entrainment rate from experiments by different authors, the equation was used to plot

Figure 6:7.

The correlation is actually quite good and implies that the “surfactant method” of measuring entrainment is therefore probably comparable to other methods of measuring the air entrainment rate. This method will require further experimentation, but if it proves successful, many types of experiment would benefit from this simpler method of air entrainment measurement.

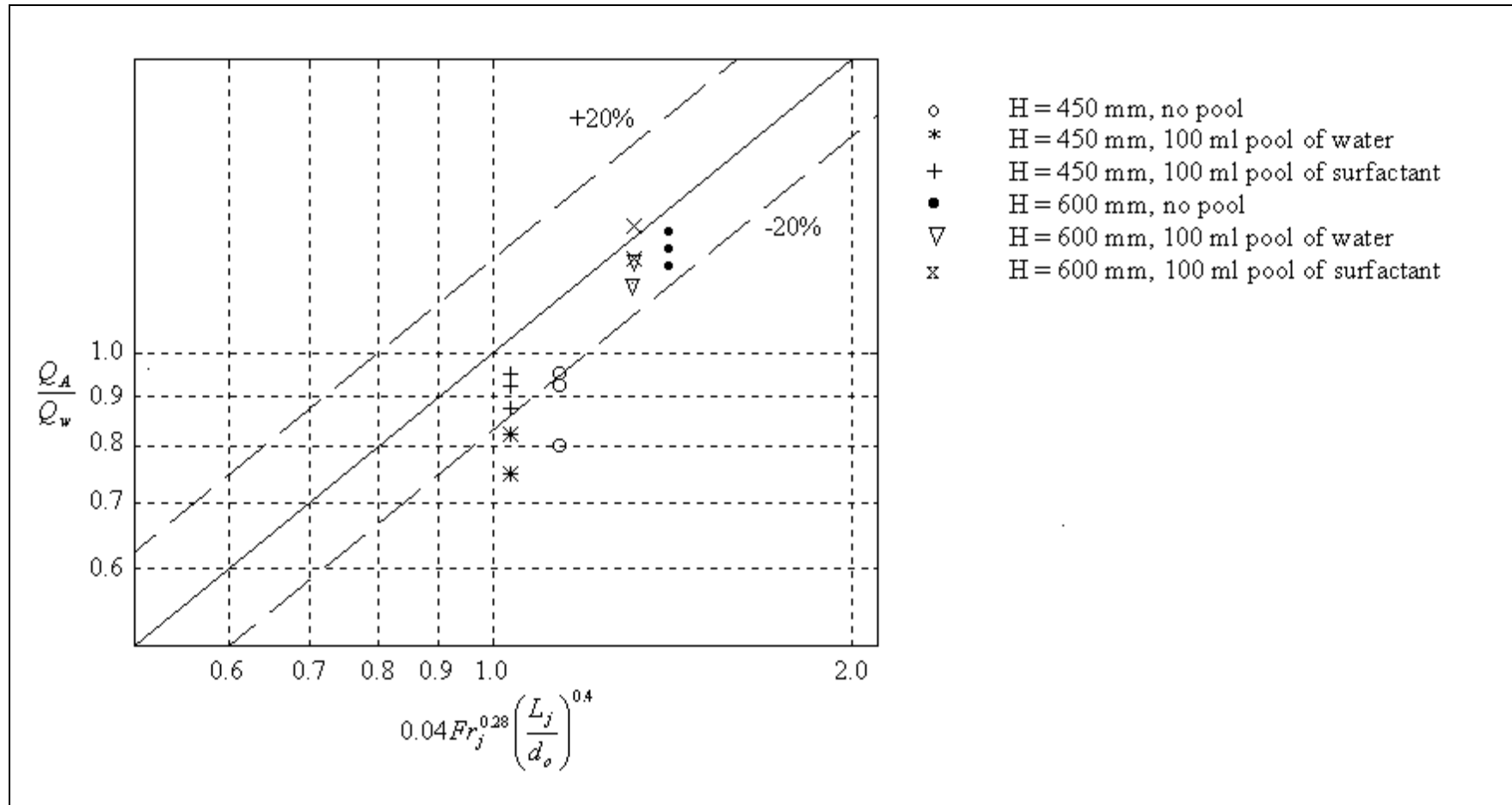


Figure 6:7 Correlation of author's experimental data with Bin's equation

6.4 Conclusions

Although there have been comprehensive studies on air capture by the plunging jet method it has not been applied to the formation of foam. Also, the majority of the work on plunging jets has been done with pure water. The Ross-Miles test is still in common use to determine the foaming properties of liquids, but again, to the author's knowledge, it has not been used to determine the actual properties of foam formation.

Therefore, combining these two methods, and with the use of a high-speed video camera, the author has determined which factors have the most effect on foam formation from a plunging jet. The author has also developed a new method of measuring the amount of air entrained by a plunging jet, which is simpler than those in current use.

In the Ross-Miles tests conducted, the higher funnel position produced a larger volume of foam than from the lower position. However, the expansion ratio of the foam produced remained almost constant with the different funnel heights. It appears, therefore, that in these experiments, the volume of foam produced is a function of height or jet energy but the expansion ratio of the foam is not. The type and depth of liquid the jet plunged into had no apparent effect on the amount of foam produced, although both did affect the foam expansion ratio.

To the naked eye, the jets from both the low and high funnel positions appeared continuous, but when seen on the high-speed video, both jets had begun to break-up. The higher one had split into individual droplets, whilst the lower one was droplets

connected by strands of solution. This was the only visual difference between the two jets.

The jet impinging on a smooth solid surface produced no foam, either through the Ross-Miles equipment or through a straight nozzle on Test Rig Three. However, when the jet impinged on a rough solid surface, foam was produced. Unfortunately, it has been not possible to distinguish between the expansion created by mixing within a branchpipe and that created by collision. Therefore, it has not been possible to test the hypotheses that an aerated jet will produce foam on collision with both a smooth and a rough solid, and on collision with a liquid.

There are various methods of measuring the amount of air captured, although it appears that measuring the air trapped in the foam produced whilst using a surfactant solution has not previously been published. By using published data and calculations, the “surfactant method” of measuring the amount of air captured is shown to be comparable with the results of other methods. The “surfactant method” is much simpler to perform than the other methods and many types of experiment should therefore benefit from this system.

7 Discussions and Conclusions

7.1 Introduction

There is a lack of published work on the design of fire fighting branchpipes. Research into the foam generation process within a branchpipe system apparently has never been attempted. The aims of the work reported in this thesis were therefore:

- To determine, using scale models, the foam generation mechanisms involved in producing foam from a low expansion fire fighting branchpipe.
- To distinguish which mechanism has the greatest effect on the expansion ratio.
- To discuss the relevance of these findings to the design of branchpipes.

In this section the results found are discussed and conclusions are drawn with respect to these aims. Further work is highlighted that would help the efficiency of the design process of fire fighting branchpipe systems. Further work in other areas resulting from this thesis is also discussed.

7.2 Discussion

By focusing on a one-tenth scale model of a simplified, low expansion fire fighting branchpipe, evidence of three distinct methods of bubble formation within the fire fighting system were identified:

- | | |
|---------------------------|---|
| Stage One – Mixing | Mixing of the liquid and gas and the formation of bubbles occurs within the branchpipe. |
| Stage Two – Flight | During the flight, bubbles grow, new bubbles are formed and the jet entrains air. |

Stage Three – Collision Foam forms when the jet collides with a solid or liquid surface.

The jet of foam that leaves the branchpipe consists of slugs of air, liquid and small bubbles of approximately 2 mm diameter. The final collected foam is also non-homogeneous. No liquid / foam interface is present when the foam is collected, which shows that any liquid slugs still existing after leaving the branchpipe are incorporated into the foam either during the flight, or, more likely, during collision. A liquid / foam interface is formed after collection. This implies that a proportion of the foam is very wet with a low drainage rate. The actual drainage rate was not measured.

The bubbles at the bottom of the collection container have a diameter of less than 1 mm. The bubble diameters increased gradually the nearer to the surface they are. The liquid flow rate affects the size of the bubbles. The lower the liquid flow rate, the larger the bubbles appeared, ranging from approximately 25 mm diameter at 8 l/min to approximately 1 mm diameter at the higher flow rate of 22 l/min.

7.2.1 Stage 1 - Mixing

The first stage of foam generation from low expansion fire fighting equipment happens within the branchpipe. As the surfactant solution is pumped through the nozzle into the branchpipe a turbulent jet of fluid is formed. Pressure is reduced around the nozzle by the momentum exchange taking place in the branchpipe; air is drawn into the branchpipe through the air holes by the reduction in pressure at the nozzle. It was initially assumed that the interaction between the air, the surfactant solution and the branchpipe walls caused the vigorous turbulent mixing of the fluids that could be seen through the clear walls of the branchpipe. The shear force

generated on the branchpipe by the jet is proportional to the (liquid flow rate)², but not to the branchpipe length. This may be explained by a liquid-rich layer that is next to the wall, this gives the effect of slip. The roughness of the branchpipe walls therefore may not be significant in the mixing of the fluids. The mixing has been attributed to just the turbulence in the air and liquid flows. Other than Plateau's theory of a cylinder of fluid breaking in two when the length exceeds its perimeter, no theories have been proposed on the process of bubble formation by mixing.

Not all of the air entrained into the branchpipe is incorporated into the final foam in either branchpipe length tested. If the branchpipe is short, some air slugs are seen to escape to the atmosphere at the end of the tube. Escaping slugs are not visible at the end of the long branchpipe. The remainder of the air not incorporated into the final foam may be lost during the flight or at collision. The (liquid flow rate)² and the (entrained air flow rate)² are directly proportional to the pressure upstream of the nozzle. The results of the mixing and collision stages of foam formation cannot be separated. It is possible that more air is lost after leaving the branchpipe than derived from the calculations, but that this is replaced during the collision stage. This is unlikely as the final amount of air within the collected foam is directly related to the amount of air entrained. From this relationship, the final expansion ratio can be predicted from just the pressure, and therefore from the liquid flow rate. The correlation of the predictions and the experimental results is very good. The value of the proportion of air entrained and lost cannot be determined without experimental evidence, as each branchpipe design entrains and loses air at a different rate.

Changing the number or size of the air holes appears to have only a minor effect on the expansion ratio of the foam produced. Witte's mixing shock can be seen only when the air holes in the longer branchpipe are severely restricted. It is not visible under normal operating conditions and the fluid that leaves the branchpipe is a mixture of a jet flow and a froth flow. It appears that Witte's mixing shock does not occur in full scale branchpipes either and the exiting fluid is also a mixture of jet and froth flows. It has been shown in the experimental work that a froth flow has a very restricted flight distance compared to a jet flow. Therefore, there must be an optimum proportion of froth and jet flow to enable the jet to be projected and to keep the expansion ratio high. This proportion has not been investigated.

A branchpipe with no air holes produces one of two distinct flow patterns, depending on whether air is trapped around the nozzle. If air is trapped, a steady jet with throw similar to that from a branchpipe with air holes is seen. If no air is trapped, there is a limited jet throw and air is drawn up the branchpipe from the open end.

Obstructions in the tube do not appear to increase the expansion significantly but severe restrictions limit the distance the jet is projected. The long branchpipe tube produces a slightly higher expansion ratio foam than the short one, but again the flight distance is greatly reduced.

Equipment manufacturers should therefore be aware that, for a full scale fire fighting low expansion branchpipe, there is an optimum branchpipe length that will produce a mixture of jet flow and froth flow in the correct proportions. If the branchpipe is too short, there will be insufficient mixing of the two-phases, if it is too long the throw

will be limited. There is also a minimum air hole area requirement. After this minimum is exceeded, no increase in expansion ratio is seen, however, the velocity of the resultant jet increases.

7.2.2 Stage 2 - Flight

The mixture of air slugs, liquid slugs and bubbles leaves the branchpipe as a free jet. At the end of the branchpipe, some air slugs are seen to escape to atmosphere, as mentioned above. Using a high-speed video camera, large air pockets between globules of foam and surfactant solution were identified.

Bubbles are formed during the flight, either by films being “blown” or by the expansion of the air slugs. These bubbles often burst or separate from the jet during the flight and play little or no part in the final expansion ratio. Another minor contributor to the overall expansion ratio are the bubbles produced by the sloughed off droplets falling back into the main body of the jet.

A shorter flight distance produces a smaller expansion ratio than a long flight, but this difference is small. The difference can probably be attributed to the force with which the jet hits the collecting vessel. This force may burst some of the bubbles. This could also explain why there is a decrease in expansion ratio for all flight distances with an increase in upstream pressure. This hypothesis has not been rigorously tested. The amount of air entrained by the jet is assumed considerable, but the experimental results imply that this has little relevance to the overall expansion ratio of the foam produced. The early break-up of the jet from the scale model shows that the branchpipe set-up would be unsuitable for projecting the foam a typical distance for

fighting fires. However, the mechanisms of foam formation will be similar in a commercial branchpipe, as the same surfactant solution and principle are used.

Although bubbles are generated during the flight, the flight distance has little relevance to the overall expansion ratio of the foam produced. This is of interest to equipment manufacturers. It is not often possible to predetermine the distance from the fire to the fire fighting equipment. Fire fighters would find it difficult to arrange the equipment at a specific distance from a fire in order to produce a foam of an optimum quality. Equipment manufacturers are therefore able to market a more versatile piece of equipment if the throw distance has little effect on the expansion ratio of the foam it produces. Unfortunately, high expansion foams cannot be projected very far, and this may cause limitations on equipment.

7.2.3 Stage 3 - Collision

The final stage of the foam system is the collision of the jet. To investigate the foam formed from a two-phase colliding or plunging jet, a jet of homogeneous low expansion foam of known expansion and low drainage rate is required. This type of foam is very difficult to produce and therefore two-phase plunging and colliding jets have not been investigated.

The amount of foam produced from a one-phase (liquid) vertical jet plunging into liquid or colliding onto a solid is mainly controlled by the velocity at collision. A greater height, and so greater velocity, produces a larger volume of foam than a short one. The expansion ratio of the foam produced remains almost constant with the different heights. Therefore, it is assumed that the volume of foam produced is a

function of velocity, or height, but the expansion ratio of the foam is not. The type and depth of liquid the jet plunges into have no apparent effect on the amount of foam produced, although both do affect the foam expansion ratio.

A new method of measuring the amount of air entrained in a plunging one-phase liquid jet has been determined and is comparable with other methods in use. However, further work is required to confirm the accuracy and limits of the method.

A liquid jet impinging onto a smooth solid surface produces no foam. When a jet impinges on to a rough solid surface, foam is produced. The quantity and expansion ratio of this foam has not been determined. The hypothesis that a two-phase jet will produce foam on collision with either a smooth or a rough solid or in collision with liquid, has not been tested. Early indications from the experiments undertaken imply that this hypothesis is correct.

The collision of the scale model fire fighting jet does not appear to affect the final expansion ratio. Although it has not been possible to be prove this experimentally, it is unlikely that the air gained at collision is proportional to the amount of air entrained into the branchpipe. The volume of any foam generated by collision is insignificant compared to that produced in the branchpipe. Therefore, the mode of collision does not contribute greatly to the overall expansion ratio of the foam produced from a fire fighting branchpipe. This is again useful to the producers of fire fighting equipment, as sales would be severely limited if a predetermined collision mode was necessary to produce a foam of the required expansion ratio.

7.3 Conclusion

It has been shown and proven that there are three foam generation mechanisms involved in producing foam from a low expansion fire fighting branchpipe. These have been termed “Mixing”, “Flight” and “Collision” and are described in detail in this thesis.

The “Mixing” stage, which occurs within the branchpipe, appears to be the only mechanism that has a large effect on the expansion ratio of the foam produced. Further work is required to be able to determine the optimum branchpipe design. However, it is now thought that there is an optimum length and air hole area. The evidence also indicates that the wall roughness has little effect on the foam properties.

The distance travelled by the jet makes little difference to the expansion ratio. However, high expansion foams cannot be projected far enough to fight fires from a distance. In this instance, the branchpipe is required to create a jet flow of droplets with air entrained between them, and / or a very wet froth flow, which can be projected further.

The collision stage has no apparent effect on the expansion ratio on the scale model. It was not possible to investigate the collision stage separately from the mixing stage using two-phase jets and therefore collision experiments were only conducted on one-phase jets. Further work on two-phase jets may show that the collision stage has a significant effect on the expansion ratio.

7.4 Further work

This thesis provides many answers to the questions posed on fire fighting branchpipe design. However, further work is required to determine a mathematical model that could be used to design a system to specified requirements. This includes finding out how the scale model relates to actual fire fighting branchpipes in use in the field. The full cone nozzle of the test rigs is unsuitable for a full-scale system, as the flight is too short. However, straight jets do not produce foam in the scale model. The boundary between the scale where a straight jet has none to some effect on the foam formation process needs to be investigated.

The drainage rate of the foam produced in the scale models is required to ensure the foam produced is suitable for fire fighting. The optimum length of branchpipe and the minimum air hole area need to be determined. Also, the theory that there is a maximum air entrainment rate, above which, no more air is entrained, no matter the size of air holes, should be investigated. The reason why no Witte's mixing shock is seen, yet there is a mixture of jet and froth flow, also needs investigating.

The hypotheses that a two-phase jet will produce foam on collision with a smooth and a rough solid and on collision with a liquid should be tested. The amount and expansion ratio of any foam produced in this manner should be determined.

The accuracy and limits of the new method of measuring the amount of air entrained in a plunging one-phase liquid jet should be tested.

References

- Adamson. (1982). *Physical Chemistry of Surfaces*, John Wiley and Sons.
- Ahmed, A. (1993). "Characterisation of Spray Distribution from Hollow Cone Swirl Nozzles," MSc, Leeds University.
- Amiri, M. C., and Woodburn, E. T. (1990). "A method for the characterisation of colloidal gas apherons." *Trans Inst Chem Eng* , 68(A), pp 154- 160.
- Anderson, D. (1980). "Lecture Notes." , Lancaster University.
- Angus. (1985). "Company Literature." .
- Angus-Fire. (2000). "FP70 DATA SHEET." , www.angusfire.co.uk.
- ASTM_D3825-90. (1990). "American Society for Testing and Materials (ASTM) D3825-90 Standard test method for dynamic surface tension by the fast-bubble technique." , American Society for Testing and Materials.
- Aubert, J. H., Kraynik, A. M., and Rand , P. B. (1986). "Aqueous Foams." *Scientific American*, pp 58-66.
- Ayers, W. H. (1989). "Fundamental Studies of the Extinguishment of Pool Fires in a Crosswind," PhD Theses, Sheffield University.
- Baser, S., and Khakhar, D. (1994). "Modelling of the Dynamics of Water and R-11 Blown Polyurethane Foam Formation." *Polymer Engineering and Science* (34), pp 642-649.
- Benatt, F. C. S., and Eisenklam, P. (1969). "Gaseous Entrainment into Axisymmetric Liquid Sprays." *Journal Of The Institute Of Fuel* (August), pp 309-315.
- Benson, S. P., Bevan, P. R., and Corrie, J. G. (1974). "A Laboratory Fire Test For Foam Liquids." *Fire Research Note No. 1007*, Fire Research Station.
- Benson, S. P., and Corrie, J. G. (1976). "A 50 Litre Per Minute Standard Foam Branchpipe." *Fire Research Note No. 1045/76*, Fire Research Station.
- Benson, S. P., Griffiths, D. J., and Corrie, J. G. (1973a). "The Compatibility of Fluorochemical and Fluoroprotein Foams." *Fire Research Note No.993*, Fire Research Station.
- Benson, S. P., Griffiths, D. J., and Corrie, J. G. (1973b). "A Five Litre per Minute Standard Foam Branchpipe." *Fire Research Note No. 425*, Fire Research Station.
- Benson, S. P., Griffiths, D. J., Tucker, D. M., and Corrie, J. G. (1973c). "Storage Properties of Four Foam Liquids (Final Report)." , Fire Research Station.
- Benson, S. P., Morris, K., and Corrie, J. G. (1973d). "An Improved Method for Measuring the Drainage Rate of Fire Fighting Foams." *Fire Research Note No. 972*, Fire Research Station.
- BHRA. (1968). "Engineering Outline: Jet Pumps Engineering." , BHRA.
- Bikerman, J. J. (1953). *Foams: Theory and Industrial Applications*, Reinhold, New York.
- Bikerman, J. J. (1973). *Foams*, Springer-Verlag, New York.
- Bin, A. K. (1993). "Gas Entrainment by Plunging Liquid Jets." *Chemical Engineering Science* , 48, pp 3585-3630.
- Bobert, M., Persson, H., and Persson, B. (1997). "Foam Concentrates: Viscosity and Flow Characteristics." *Fire Technology* , 33(No 4), pp 336 - 355.
- Box, G. E. P., Hunter, W. G., and J.S., H. (1978). *Statistics for Experimenters - An Introduction to Design, Data Analysis and Model Building*, John Wiley and Sons.

- Briggs, T. (1995). "Foams." *Foams - Theory, Measurements and Applications*, R. K. Prud'homme and S. A. Khan, eds., Marcel Dekker Inc., New York, New York, pp 465-509.
- Burgess, J. M., Molloy, N. A., and McCarthy, M. J. (1972). "A Note on the Plunging Liquid Jet Reactor." *Chemical Engineering Science*, 27, pp 442-445.
- Butlin, R. N. (1967). "High Expansion Foam A Survey Of Its Properties And Uses." *Fire Research Note No 669*, Fire Research Station.
- Calvert, J. R. (1987). "A Review of Literature on the Electrical Properties of Foam." *Personal Communication*.
- Calvert, J. R. (1990). "Pressure-Drop For Foam Flow Through Pipes." *International Journal Of Heat And Fluid Flow*, 11(3), pp 236-241.
- Calvert, J. R., and Nezhati, K. (1986). "A rheological model for a liquid-gas foam." *International Journal of Heat and Fluid Flow*, 7(3), pp 164-168.
- Calvert, J. R., and Nezhati, K. (1987). "Bubble Size Effects In Foams." *International Journal of Heat and Fluid Flow*, 8(2), pp 102-106.
- Cash, T. (1995a). "Fighting Fires with Foam Part One." *Fire Safety* (April), pp 25 - 27.
- Cash, T. (1995b). "Fighting Fires with Foam Part Two." *Fire Safety* (June), pp 25 - 27.
- CEEDO. (1978). "Comparative Nozzle Study for Applying Aqueous Film Forming Foam on Large Scale Fires." *CEEDO-TR-78-22*, Civil and Environmental Engineering Development Office, Department Of The Navy Naval Research Laboratory, Washington DC.
- Champion, F. C. (1943). "Properties of Liquids at Rest Chapter XI." University Physics, Blackie and Son Limited, London and Glasgow.
- Chang, R. C., Schoen, H. M., and Grove, C. S. (1956). "Bubble Size and Bubble Size Determination." *Industrial and Engineering Chemistry*, 48(11), pp 2035-2039.
- Chen, T. F., and Davis, J. R. (1964). "Disintegration of a Turbulent Water Jet." *Journal of the Hydraulics Division, American Society of Civil Engineers* (January), pp 175-206.
- Chitty, T. B., Griffiths, D., and Corrie, J. G. (1972). "Compatibility of Fluorochemical and Protein Fire Fighting Foams." *Fire Research Note No. 924/72*, Fire Research Station.
- Christensen, T. C., Janule, V. P., and Teichmann, A. F. (1995). "Automatic Determination of Dynamic CMCs." , SensaDyne Instrument Division, Chem Dyne Research Corp..
- Colletti, D., and Davis, L. (1998). "Specifications for CAFS - Get the right system for the job." , WEB - www.vfire.com/Presentation24/cafs.htm.
- Corrie, J. G. (1975). "Problems With The Use Of Fire Fighting Foams." *CP 25/75*, Fire Research Station.
- Corrie, J. G. (1976a). "A 200 Litre Per Minutes Standard Foam Branchpipe." *Fire Research Note No. 1056/76*, Fire Research Station.
- Corrie, J. G. (1976b). "Experimental Methods for the Study of Fire Fighting Foams." *Foams - Proceedings of a symposium organised by the Society of Chemical Industry, Colloid and Surface Chemistry 1975*, Akers, ed., Academic Press, London, pp 195-215.
- Corrie, J. G. (1976c). "Measuring The Shear Stress Of Fire Fighting Foams." *Fire Research Note No. 1055*, Building Research Establishment.
- Cunningham, R. G. (1956). "Jet Pump Theory And Performance With Fluids Of High Viscosity." *Transactions Of The A. S. M. E.*, pp 1807-1820.

- Cunningham, R. G. (1975). "Liquid Jet Pump Modelling: Effects of Axial Dimensions on Theory-Experiment Agreement." 2nd Symposium on Jet Pumps & Ejectors and Gas Lift Techniques, pp F1-1 -- F1-15.
- Cunningham, R. G. (1995). "Liquid Jet Pumps For Two Phase Flows." *Journal Of Fluids Engineering* , pp 309-316.
- Cunningham, R. G., and Dopkin, R. J. (1974). "Jet Breakup and Mixing Throat Length for the Liquid Jet Gas Pump." *ASME Journal of Fluids Engineering* , 96(3), pp 216-226.
- Dahlberg. (1994). "Foam Spread Experiments on a Water Surface." *SP report 1994:16*, Swedish National Testing And Research Institute Fire Technology.
- Davies. (1963). *The design and analysis of industrial experiments*, Oliver and Boyd, London.
- DiMaio, L. R., Lange, R. F., and Cone, F. J. (1984). "Aspirating vs. Nonaspirating Nozzles for Making Fire Fighting Foams - Evaluation of a Non Aspirating Nozzle." *Fire Technology* , 20(1), pp 5-10.
- Exerowa, D., and Kruglyakov, P., M. (1998). *Foam and Foam Films*, Stoyanova, Khristov, Khristo, translator, Elsevier, Amsterdam, Lausanne, New York, Oxford, Shannon, Singapore, Tokyo.
- Exploratorium. (1997). "Web Page: http://www.exploratorium.edu/ronh/bubbles/shape_of_bubbles.html.", www.
- Fittes, D. W., and Nash, P. (1965). "The Design and Development of an Experimental Gas Turbine Operated Foam Generator." *Fire Research Note 583/1965*, Joint Fire Research Organisation.
- Foster, J. A. (1984). "Brigade Trials of a High Expansion Foam Generator." *Research Report 23*, Reprint Of Home Office SRDB Publication 84/43.
- Foster, J. A. (1992). "The Use of Foam Against Large Scale Petroleum Fires Involving Lead Free Petrol - Summary." *Research Report 49*, FRDG.
- Freeman, J. R. (1889). "Experiments relating Hydraulics of Fire Streams." *Trans. ASCE* , XXL(426).
- French, R. J. (1952). "The Resistance of Fire-Fighting Foams to Destruction by Radiant Heat." *Journal of Applied Chemistry* , 2(February), pp 60 - 64.
- French, R. J., and Hird, D. (1961). "Air Foam In The Control And Extinction Of Petrol Fires By Surface Application." *Fire Research Note No. 451*, Fire Research Station.
- Fry, J. F., and French, R. J. (1951a). "A Laboratory Method of Comparing The Efficiencies of Fire Fighting Air-Foams." *Journal of Applied Chemistry* , I(October), pp 429-433.
- Fry, J. F., and French, R. J. (1951b). "A Mechanical Foam-Generator for use in Laboratories." *Journal of Applied Chemistry* , I(October), pp 425-429.
- Gardiner, B. S., Dlugogorski, B. Z., and Jameson, G. J. (1998). "Yield Stress Measurements of Aqueous Foams in the Dry Limit." *Journal of Rheology* , 42(6), pp 1437-1450.
- Germick, Rehill , and Narsimhan. (1994). "Experimental Investigation of Static Drainage of Protein Stabilized Foams - Comparison with Model." *Journal of Food Engineering* , 23, pp 555-578.
- Grant, R. P., and Middleman, S. (1966). "Newtonian Jet Stability." *AICHE Journal* , 12(4), pp 669 - 678.
- Hatton. (1993). "Balanced Pressure Proportioner." *Handwritten* .
- Hatton, and Osborne. (1979). "The Trajectories of Large Fire Fighting Jets." *The International Journal of Heat And Fluid Flow* , 1(1).

- Heller, J. P., and Kuntamukkula, M. S. (1987). "Critical Review of the Foam Rheology Literature." *Ind. Eng. Chem. Res.* , 26(2), pp 318-325.
- Hendrickson, C. M. (1990). "Use of highly stabilized High-Expansion Foams in Fighting Forest Fires." Fire and polymers, G. L. Nelson, ed..
- Heskestad, Kung, and Todtenkopf. (1976). "Air Entrainment Into Water Sprays And Spray Curtains." *The American Society Of Mechanical Engineers* .
- Hill, B. J. (1972). "Measurement Of Local Entrainment Rate In The Initial Region Of Axisymmetric Turbulent Air Jets." *Journal Of Fluid Mechanics* , 51(4), pp 773-779.
- Hinze, J. O. (1955). "Fundamentals of the Hydrodynamic Mechanism of Splitting in Dispersion Processes." *AIChE Journal* , 1, pp 289-295.
- Hird, D., Fittes, D. W., and French, R. J. (1961). "The Development Of A Fire Test For Foam Liquids." *Fire Research Note No. 478*, Fire Research Station.
- Holder, G. N. (1977). "The Categorisation Of Fire Fighting Foam," University Final Year Project, Southampton University.
- Hoover, S. M. (1989). "Foam Generator Adjustable to Produce Foam Having Various Expansion Ratios." United States Patent, Mine Safety Appliances Company, USA.
- Hosseini, S., M. "Dynamic Surface Property Measurement of Aqueous Surfactant Solutions." *NE Regional Meeting XXI, American Chemical Society*, University of Massachusetts, Amherst.
- Hoyt, J. W., and Taylor, J. J. (1977a). "Effect Of Nozzle Shape And Polymer Additives On Water Jet Appearance." *ASME* .
- Hoyt, J. W., and Taylor, J. J. (1977b). "Waves On Water Jets." *Journal of fluid mechanics* , 83(Part 1), pp 119--127.
- Hoyt, J. W., Taylor, J. J., and Runge, C. D. (1974). "The Structure Of Jets Of Water And Polymer Solution In Air." *Journal Of Fluid Mechanics* , 63(Part 4), pp 635--640.
- Isaksson, and Persson. (1997). "Fire Extinguishing Foam - Test Method For Heat Exposure Characterisation." *SP report 1997:09*, Swedish National Testing And Research Institute Fire Technology.
- Isenberg, C. (1978). *The Science of Soap Films and Soap Bubbles*, Tieto, Clevedon.
- ISO-7203-1. (1995). "Fire Extinguishing Media-Foam Concentrates-Part 1: Specification For Low Expansion Foam Concentrates For Top Application To Water Immiscible Liquids." , British Standard.
- ISO-7203-2. (1995). "Fire Extinguishing Media-Foam Concentrates-Part 2: Specification For Medium And High Expansion Foam Concentrates For Top Application To Water Immiscible Liquids." , British Standard.
- Jacobi, W. M., Woodcock, K. E., and Grove, C. S. (1956). "Theoretical Investigation of Foam Drainage." *Industrial and Engineering Chemistry* , 48(11), pp 2046-2051.
- Jamison, W. B. (1967). "High Expansion Foam In The Fire Department." *Fire Journal* , 61(6).
- Jamison, W. B. (1969). "Stability - The Key To Effective High Expansion Foam." *73rd annual meeting of the national fire protection association, New York, New York.* (May).
- Jeulink, J. (1983). "Mitigation Of The Evaporation Of Liquids By Fire Fighting Foams." *Institute Of Chemical Engineers Symposium*, Number 80, pp e12-e22.
- Johnson, B., P. (1988). "Additives For Hose Reel Systems: Preliminary Trials Of Foam On Small Scale Isopropanol Fires." , pp 62.

- Johnson, B., P. (1992). "Additives For Hose Reel Systems: Trials Of Foam On Tyre Fires." *FRDG* , pp 85.
- Johnson, B., P. (1994). "A Comparison Of Various Low Expansion Foams When Used Against The Proposed ISO And CEN Standard Medium Scale (4.5 m2) Hydrocarbon Fuel Test Fire." *1858931835*.
- Johnson, B. P. (1993). "A Comparison Of Various Foams When Used Against Large Scale Petroleum Fires." *FRDG* , pp 192.
- Johnson, J. H. (1877), Britain.
- Jumpeter, A. M. (Approx. 1960). "Jet Pumps." , Schutte Koerting Co?.
- Klempner, and Frisch. (1991). *Polymeric Foams*.
- Kraynik, A. M. (1988). "Foam Flows." *Annual Review of Fluid Mechanics* , 20, pp 325-357.
- Kraynik, A. M., and Hansen, M. G. (1987). "Foam Rheology: A Model Of Viscous Phenomena." *Journal of rheology* , 31(0) ?.
- Lancaster_ Univ_ Chem_ Dpt. (1998). "Laboratory Notes: Determination of the Critical Micelle Concentration of Aqueous Solutions of Sodium Dodecyl Sulphate by Surface Tension Measurements (CHEM 231).", Lancaster University Chemistry Department.
- Langford, B., and Stark, G. W. V. (1964a). "Control of Fires in Large Spaces with Inert Gas and Foam Produced by a Turbo-Jet Engine - Part 7 -The Selection of Foaming Agents for the Production of High Expansion Foam." *Fire Research Note No. 519*, Fire Research Station.
- Langford, B., and Stark, G. W. V. (1964b). "Control of Fires in Large Spaces with Inert Gas and Foam Produced by a Turbo-Jet Engine - Part 10 -A Comparative Study of High Expansion Foams Produced with Air and with the JFRO Inert Gas and Foam Generator." , Fire Research Station.
- Langford, B., Stark, G. W. V., and Rasbash, D. J. (1962). "Control of Fires in Large Spaces with Inert Gas and Foam Produced by a Turbo-Jet Engine - Part 5 -The Production of High Expansion Foam." *Fire Research Note No. 511*, Fire Research Station.
- Lara, P. (1979). "Onset of Air Entrainment for a water Jet impinging Vertically on a Water Surface." *Chemical Engineering Science* , 34, pp 1164-1165.
- Laurent. (1904). *Imp. Russ. Tech Inst. Chem Sec* .
- Lewis, D. A., Nicol, R. S., and Thompson, J. W. (1984). "Measurement of Bubble Sizes and Velocities in Gas-Liquid Dispersions." *Chemical Engineering Design Review* , 62, pp 334-336.
- Lin, T. J., and Donnelly, H. G. (1966). "Gas Bubble Entrainment by Plunging Laminar Jets." *A.I.Ch.E. Journal* , 12(3), pp 563 - 571.
- Lucassen, J. (1981). "Dynamic Properties of Free Liquid Films and Foams." *Anionic surfactants: Physical Chemistry of Surfactant Action* , 11, pp 217-265.
- Martin, G. T. O. (Approx. 1970). "Fire Fighting Foam - A Chemist's View." *The Institution of Fire Engineers Quarterly* , pp 165 -175.
- McCarthy, M. J., and Molloy, N. A. (1974). "Review Of Stability Of Liquid Jets And The Influence Of Nozzle Design." *The Chemical Engineering Journal* , 7, pp 1--20.
- McKeogh, E. J., and Ervine, D. A. (1981). "Air Entrainment Rate and Diffusion Pattern of Plunging Liquid Jets." *Chemical Engineering Science* , 36, pp 1162-1172.
- McQuaid, J. (1975). "Air Entrainment into Bounded Axisymmetric Sprays." *The IMechE Thermodynamics and Fluid Mechanics Group* , 189.

- McQuaid, J. (1976). "The Design of Water Spray Ventilators." *Journal of Occupational Accidents* .
- Merrington, C., and Richardson, E. G. (1947). "The Break-up of Liquid Jets." *The Proceedings of the Physical Society* , 59 Part1(331), pp 1--13.
- Miesse, C. C. (1955). "Correlation Of Experimental Data On The Disintegration Of Liquid Jets." *Industrial And Engineering Chemistry* , 47, pp 1690--1701.
- Monnereau-Pittet, C., and Vignes-Alder, M. (1999). "Topology of Three-Dimensional Soap Foams." *Foams and Films*, MIT Verlag Bremen.
- Mueller, N. H. G. (1964). "Water Jet Pump." *Journal Of The Hydraulics Division Proceedings Of The American Society Of Civil Engineers* (May).
- Murakami, M., and Katayama, K. (1966). "Discharge Coefficients of Fire Nozzles." *Transactions of the ASME* (December), pp 706--716.
- Murphy, D., G. (1996). "Formulation Of A Mathematical Model For Kinematic Froth Visualisation," PhD thesis, UMIST.
- Nash, P. (1975). "Fire Protection of flammable liquid storages by water spray and foam." *CP 42/75*, Building Research Establishment.
- Nash, P., and Fittes, D. W. (1968). "The Extinction Of Industrial Fires By Foams." *Fire Research Note No. 724*, Fire Research Station.
- Neethling, S., and Cilliers, J. J. (1999). "Visualisation of Coalescence and Drainage in Flowing Foams." *Foams*, D. Weaire, ed., MIT Press.
- Neve. (1993). "Computational Fluids Dynamics Analysis of Diffuser Performance in Gas Powered Jet Pumps." *International Journal of Heat and Fluid Flow* , 4(4), pp 401-407.
- NFPA. (1988). "NFPA 11 Standard for low expansion foam and combined agent systems." .
- NFPA. (1992). "National Fire Codes." .
- Noronha, F. A. F., Franca, F. A., and Alhanati, S. P. E. (1997). "Improved two-phase model for Hydraulic jet Pumps." *Proceedings - Society of Petrochemical Engineers Operations Symposium* , pp 333-340.
- Oguz, H., N. (1998). "The role of surface disturbances in the entrainment of bubbles by a liquid jet." *J.Fluid Mechanics* , 372, pp 189-212.
- Perri, J. M. (1953). "Fire Fighting Foams." *Foams: Theory and Industrial Application*, Bikerman, ed., Reinhold, New York, pp 189 - 242.
- Perry, R. H., and Green, D. W. (1984). "Perry's Chemical Engineer's Handbook." , McGraw-Hill Book Company.
- Persson. (1992). "Fire Extinguishing Foams - Resistance Against Heat Radiation." *SP report 1992:54*, Swedish National Testing And Research Institute Fire Technology.
- Persson. (1997). "FAIRFIRE - A small scale fire test method for fire fighting foams." *"Presented at NFPRF Fire suppression and Detection Symposium, Orlando"* .
- Persson, and Dahlberg. (1994). "A Simple Model of Foam Spreading on Liquid Surfaces." *SP report 1994:27*, Swedish National Testing And Research Institute Fire Technology.
- Phinney, R. E. (1973). "The Breakup Of A Turbulent Liquid Jet In A Gaseous Atmosphere." *Journal Of Fluid Mechanics* , 60 part 4, pp 689--701.
- Phinney, R. E. (1975). "The Breakup Of A Turbulent Liquid Jet In A Low-Pressure Atmosphere." *AIChE Journal* , 21(5), pp 996-999.
- Prud'homme, R. K., and Khan, S. A. (1995). "Foams." *Surfactant Science Series*, M. J. Schick and F. M. Fowkes, eds., Marcel Dekker Inc., New York, New York, pp 596.

- Ramesh, and Malwitz. (1994). "Computer Simulation Of Polyurethane Foam Reactions Using Material And Energy Balance Equations." *Annual Technical Conference Proceedings, ANTEC* , Part 2, pp 1941-45.
- Rasbash, D. J., and Stark, G. W. V. (1962). "Some Aerodynamic Properties of Sprays." *The Chemical Engineer* (December), pp A83--A88.
- Ratzer, A. F. (1956). "History and Development of Foam as a Fire Extinguishing Medium." *Industrial and Engineering Chemistry* , 48(11), pp 2013-2016.
- Rayleigh. (1917). "On the Pressure Developed in a Liquid During the Collapse of a Spherical Cavity." *Philosophical Magazine* , XXXIV, pp 94-98.
- Rieger, M. (1995). "Foams in Personal Care Products." *Foams*, R. K. Prud'homme and S. A. Khan, eds., Marcel Dekker Inc., New York, New York, pp 381 - 412.
- Rivier, N. (1996). "Seifenblasenrhetorik, or the Sound of the Last Trumpet?" *The Kelvin problem : foam structures of minimal surface area*, D. Weaire, ed., Taylor & Francis, London.
- Rivkind, L. E., and Myerson, I. (1956). "Foams for Industrial Fire Protection." *Industrial and Engineering Chemistry* , 48(11), pp 2017-2020.
- Rochna, R. (1998). "The Evolution of CAFS - 57 Years of Fire Suppression." , WEB - www.vfire.com/Presentation24/cafs1.htm.
- Rogers, L. E., Widden, M. W., and Osborne, M. J. "Foam Formation in Low Expansion Fire Fighting Equipment." *EuroFoam 2000*, Delft, Holland, pp 40-47.
- Rosen, M. J. (1985). "Surfactants: Designing Structure for Performance." *Chemtech* (May).
- Rouse, H., Howe, J. W., and Metzler, D. E. (1951). "Experimental Investigation of Fire Monitors and Nozzles." *American Society of Civil Engineers* , Paper 2529, pp 1147 - 1188.
- Sadr-Kazemi, N., and Cilliers, J. J. (1997). "An Image Processing Algorithm For Measurement Of Flotation Froth Bubble Size And Shape Distributions." *Minerals Engineering* , 10(10), pp 1075-1083.
- Sarma, D. S. H. S. R., and Khilar, K. C. (1988). "Effects of Initial Gas Volume on Stability of Aqueous Air Foams." *Ind. Eng. Chem. Res.* , 27(5), pp 892-894.
- Savage, N. (1958). "The Relation Between Critical Shear Stress And "25 Per Cent Drainage Time" Of Air Foam." *Fire Research Note No. 344*, Fire Research Station.
- Scheffey, J. L. (1997). "Foam Extinguishing Agents and Systems." *Fire Protection Handbook*, NFPA, pp 6_349 - 6367.
- Schweitzer, P. H. (1937). "Mechanisms of Disintegration of Liquid Jets." *Journal of Applied Physics* , 8(August), pp 13--521.
- Sene, K. J. (1988). "Air Entrainment by Plunging Jets." *Chemical Engineering Science* , 43, pp 2615-2623.
- SensaDyne. (1995). "SensaDyne Promotional Material - Surface Tensionometers." .
- Sheridan, A. T. (1966). "Surface Entrainment of Air by a Water Jet." *Nature* , 208, pp 799-800.
- Theobald, C. (1975). "A Photographic Technique for the Study Water Jets." *Fire Research Note No. 1041/73*, Fire Research Station.
- Theobald, C. (1981). "The Effect of Nozzle Design on the Stability and Performance of Turbulent Water Jets." *Fire Safety Journal* , 4, pp 1--13.
- Thomas, M. (1994). "Trials Of A Compressed Air Foam System." *Fire Research News* , 17(Summer), pp 12-14.

- Thorne, P. F. (1970). "Drainage Laws For Fire Fighting Foams." *Fire Research Note No. 12*, Fire Research Station.
- Ting, R. Y., and Hunston, D. L. (1977). "Polymeric Additives as Flow Regulators." *Industrial Engineering Chemical Production Research Development* , 16(2), pp 129-135.
- Tucker, D. M., Griffiths, D. J., and Corrie, J. G. (1972). "The effect of the velocity of foam jets on the control and extinction of laboratory fires." *Fire Research Note No. 918*, Fire Research Station.
- Tuve, R. L., and Peterson, H. B. (1956). "Characterization of Foams for Fire Extinguishment." *Industrial and Engineering Chemistry* , 48(11), pp 2024-2031.
- US_Dpt.Commerce. (Approx. 1950). "A Fundamental Study of Foams and Emulsions." *US Department of Commerce, obtained from UK's Fire Research Station, ref: M130, NRD.1* .
- Van de Sande, E., and Smith, J., M. (1973). "Surface Entrainment of air by high velocity water jets." *Chemical Engineering Science* , 28, pp 1161-1168.
- Van de Sande, E., and Smith, J. M. (1976). "Jet Break-up and Air Entrainment by Low Velocity Turbulent Water Jets." *Chemical Engineering Science* , 31, pp 219-224.
- Volkart, P. (1980). "The Mechanism of Air Bubble Entrainment in Self -Aerated Flow." *Int. J. Multiphase Flow* , 6, pp 411-423.
- Wakefield, A. W. (1989). "An Introduction To The Jet Pump." , Wakefield, ed., Wakefield Consulting Engineer, Stamford, Lincolnshire.
- Weaire, D. L. (1996). *The Kelvin problem : foam structures of minimal surface area*, Taylor & Francis, London.
- Witte, J. H. (1962). "Mixing Shocks and Their Influence on the Design of Liquid - Gas Ejectors," PhD, Delft University, Delft.
- Witte, J. H. (1969). "Mixing shocks in Two-Phase Flows." *Journal of Fluid Mechanics* , 36(part 4), pp 639-655.

Glossary

Aspiration	The entrainment of air into the stream of foam solution.
ASTM	American Society for Testing and Materials.
Burnback	Re-ignition of a liquid fuel occurs.
Concentration	The percentage of surfactant concentrate mixed with the water.
Contamination resistance	The ability of the foam to resist contamination by the fuel.
Discharge rate (high expansion)	The discharge rate of a high expansion foam generator measured in cubic metres/min (m ³ /min) of foam at a stated expansion ratio.
Drainage time	The time taken for a percentage of the liquid content of a foam sample of a stated depth to drain to the bottom.
Expansion ratio	Ratio of the volume of foam to the volume of surfactant solution from which it was made.
Finished foam	The foam as applied to the fire. It may be aspirated (surfactant concentrate + water + air) or non-aspirated (surfactant concentrate + water only).
Flow requirement	The nominal supply rate of surfactant solution required by a foam branchpipe, measured in litres/min.
Foam concentrate	See surfactant concentrate.
Foam generator (high expansion)	A mechanical device in which surfactant solution is sprayed onto a net screen through which air is being forced by a fan.
Foam generator (low expansion)	Similar to a FMB, but inserted in a line of hose so that the finished foam passes along the hose to a discharge nozzle.
Foam monitor	A larger version of a FMB which cannot be hand-held.
Foam solution	See surfactant solution.
Foam-making branch (FMB)	The equipment by which the surfactant solution is normally aspirated.
Fuel pick-up	Contamination of the foam during application by the petrochemical it is protecting.
High expansion	Applied to foam with expansion greater than 200, and to associated equipment, systems and concentrates.
Induction	The entrainment of surfactant concentrate into the water stream.
Inline inductor	A device inserted in a hose line in order to induce the foam concentrate before the water reaches the FMB.
ISO	International Standards Organisation.
Knockdown	Method of extinguishing a fire rapidly.
Low expansion	Applied to foam with expansion in the range 1 to 20, and to associated equipment, systems and concentrates.
Medium expansion	Applied to foam with expansion in the range 21 to 200, and to associated equipment, systems and concentrates.
Mono-disperse	Foam with all constituent bubbles of approximately equal size.
NFPA	National Fire Protection Association (USA).
Polar fuels	Generally water-miscible solvents, e.g. alcohols, ketones. They require special alcohol-resistant foam concentrates.

Rheology	The science dealing with the flow and deformation of matter.
Shear stress	The stiffness of a foam sample. This is dependent on the size of the bubbles.
Surfactant concentrate	The surfactant as supplied by the manufacturer in liquid form.
Surfactant solution	A solution of surfactant concentrate in water at the appropriate concentration.
UL listing	United Laboratories listing, similar to ISO Standard.

Appendices

Appendix A. Foam Formation in Low Expansion Fire Fighting Equipment	162
Appendix B. Test Rig One Results and Conclusions	176
Appendix C. Comparison of ISO and Amiri Results	190
Appendix D. Experimental Error	193
Appendix E. Yates' Analysis of Plunging Jet	196
Appendix F. Experimental Data - Test Rig Three.....	197
Appendix G. Experimental Data Using Ross-Miles Test Rig	204

Appendix A. Foam Formation in Low Expansion Fire Fighting Equipment

Lucy E Rogers

Lancaster University Engineering Department / CounterFire Limited

Martin B Widden

Lancaster University Engineering Department

Michael J Osborne

CounterFire Limited

Abstract

The paper describes an investigation into the mechanics of low expansion foam generation in fire fighting branchpipes. The experimental branchpipes were of a much smaller scale than those in common use and incorporated a full cone nozzle rather than straight, but the same air entrainment method as commercially available equipment was used.

A high-speed video camera was used to study the formation of the foam and provided evidence of three methods of bubble formation within this type of system:

- Stage 1 - Mixing within the branchpipe
- Stage 2 - Air entrainment and bubble growth during the flight of the jet
- Stage 3 - Aeration produced from the collision of the high speed jet onto a solid surface.

Each stage is described in detail and hypotheses advanced to explain the processes involved.

1. Introduction

Foams were first used as a fire fighting agent in 1877 [1]. They are now in general use throughout the world to control and extinguish fires of flammable liquids and for inhibiting re-ignition. Many fire fighters disagree over the optimal fire fighting foam for specific situations and so there is a strong incentive to stay with the tried and trusted. There has been relatively low investment in (published) scientific effort related to fire fighting equipment. The design of branchpipes appears to have progressed by empirical means.

Large scale tests are difficult to control and expensive to run. In the 1970's the UK's Fire Research Station developed branchpipes for standard tests to determine properties of foam concentrates [2], [3] and to see how the properties of the foam affected its ability to extinguish fires. The actual process of foam generation has not, to the authors' knowledge, been investigated for fire fighting equipment.

One method of categorising equipment is by the expansion ratio of the foam it produces. This is defined as the ratio of the volume of surfactant solution to the volume of finished foam. A ratio in the range of 1 to 20 is low expansion, between 21 and 200 is medium expansion and high expansion is over 200. This paper focuses on low expansion foams and related equipment.

A typical low expansion branchpipe system is shown in Figure 1. The surfactant solution is pumped through a nozzle into the branchpipe. Air is induced into the liquid stream and the foam is formed by violent turbulence. The authors have termed

this Stage One (Mixing). The foam is projected from the branchpipe as a “rope” or free jet. During this stage, more air is entrained and films of solution are blown into bubbles. This has been termed Stage Two (Flight). When the jet hits a surface, the air caught during the previous stage is trapped to form bubbles. If the surface is liquid, the plunging jet also produces foam as it would in a bubble bath. This has been called Stage Three (Collision).

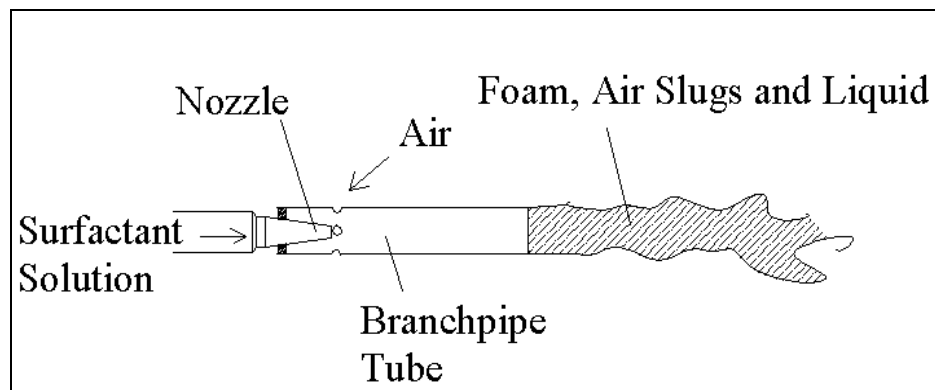


Figure 1 Low Expansion Foam Making Branchpipe

Low-expansion branchpipe sizes are stated in terms of the liquid throughput. A 200 l/min branchpipe can produce a throw of around 15 m. In larger sizes, the low expansion branchpipe is called a monitor. Large monitors, having a capacity of up to 20,000 l/min, can have a throw of over 100 m.

2. Test Rig Set-up

A simplified scale model, variable between 10 and 25 l/min, was produced. Pre-mixed surfactant solution was pumped through a 60 degree full cone nozzle into a 22 mm inside diameter tube. The air holes were equally spaced around the tube. Different length branchpipes were constructed - five of 100 mm and one of 500 mm. They were all made from clear acrylic, to enable the mixing inside the branchpipe to

be viewed. The 100 mm branchpipes had different numbers and sizes of air hole, and also some had obstructions within the tube to see the effect of turbulence.

The ISO standard for measuring the expansion ratio [4] is designed so that the foam impinges on a sloping board and drains into the measuring vessel. This method was not particularly successful when using the scale model, as any under-expanded surfactant solution drained more quickly down the slope and into the vessel than the expanded foam, thus giving a false overall expansion reading. The method was therefore changed and all of the foam (both under-expanded and fully expanded) was collected in a purpose built measuring vessel. This was then weighed and the expansion ratio calculated using the equation given in the ISO standard, with the assumption that the density of the surfactant solution is 1000 kg/m³:

$$E = \frac{V}{m_2 - m_1}$$

Where: V is the volume in litres of the collecting vessel
 m₁ is the mass, in kilograms, of the empty vessel
 m₂ is the mass, in kilograms, of the full vessel.

The type of surfactant used greatly affects the type of foam produced, so only one type (Rockwood Macrofoam) was used in all the experiments. Measured variables included the pressure and flow rate of the surfactant solution upstream of the nozzle, the shear force caused by the walls of the branchpipe, the speed and flow rate of the air entrained into the branchpipe and the air temperature.

A Kodak HS 4540 high speed video camera was used to capture images of the jet from the nozzle to the final collision. These images were taken between 4500 and 18000 frames per second.

3. Stage One - Mixing

The entrained air and surfactant solution are partially mixed within the branchpipe. This produces a few large air slugs and many more smaller bubbles. Some air slugs remain within the main body of the jet and these are dealt with in Stage Two (Flight). Others are not enclosed by the surfactant solution and so disperse to atmosphere at the end of the branchpipe.

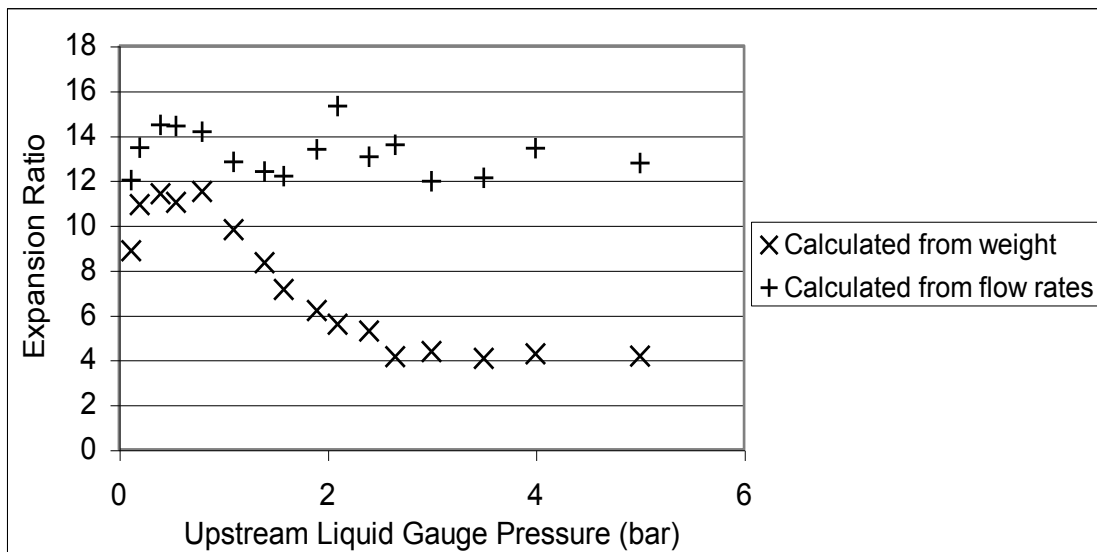


Figure 2 Graph of Pressure versus Expansion

(100 mm branchpipe, 200 mm Flight)

In tests on the model, the expansion ratio was measured as described above, collecting the foam in a measuring vessel. The flow rates of the liquid and of the air entrained

into the branchpipe were also measured. A comparison of the expansion ratios measured by the two methods is shown in Figure 2. This shows that the expansion ratio calculated from the weight of the foam is a factor of 2 – 3 lower than that calculated by the flow rates. This confirms that not all of the entrained air is incorporated into the final foam.

The first theoretical treatment of mixing behaviour was published by Plateau in 1869, as reported by Bikerman [5]. He showed that a static cylindrical column of fluid was unstable if its length exceeded its perimeter. If a bubble, which has become elongated, happens to drift into a more quiescent zone, it will separate into two or more nearly spherical bubbles. This is due to the capillary pressure being unbalanced. It was observed that the 500 mm branchpipe generated a higher expansion foam than the 100 mm branchpipe. However, within the 100 mm branchpipe, adding cross bars or coarse gauze over the end of the tube did not significantly affect the expansion. Changing the number or size of the air holes also appeared to have no effect.

The shear force from the walls of the branchpipe slows the surfactant solution at the boundary and therefore causes more turbulence and also quiescent zones within the branchpipe. These again decrease the bubble size. The shear force appears proportional to the upstream liquid pressure, as seen in Figure 3. As the upstream pressure (and hence flow rate) of the solution increases, the time the solution spends within the tube decreases and therefore the opportunity for the bubbles to enter regions of different flow rate is smaller, and the slugs are not broken down to the same extent.

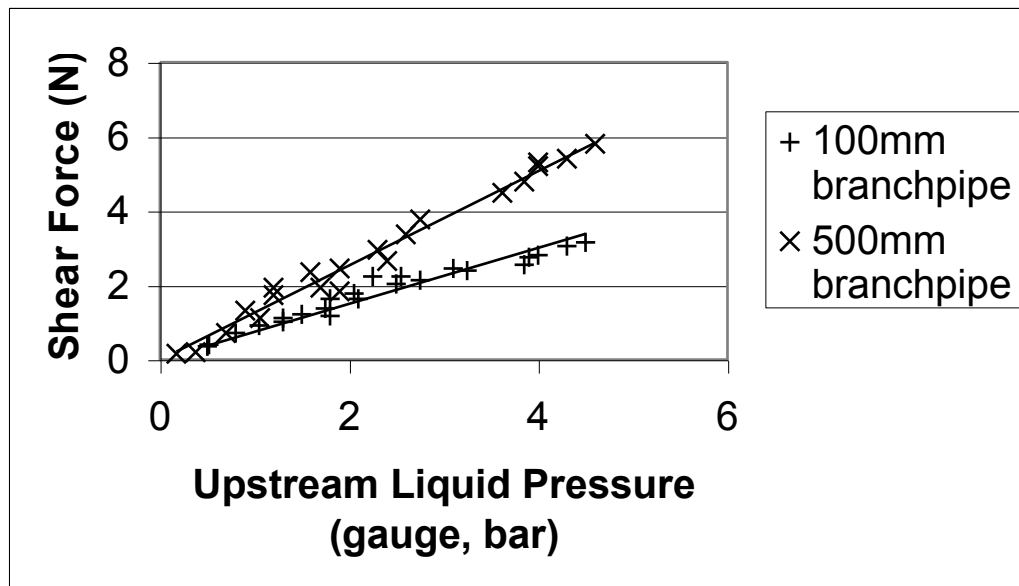


Figure 3 Pressure versus Shear Force

In 1969 Witte [6] described a “mixing shock” where a transition from jet flow to froth flow occurs in gas and liquid flows (see Figure 4). He characterised the jet flow as a core of fast-moving liquid droplets surrounded by a gas. The froth flow consists of liquid in which the gas is dispersed in the form of bubbles. He postulated that the shock could only exist when the jet flow impinges on a free surface which prevents the jet flow from penetrating further. He also assumed that the gas entrainment mechanism is similar to air enclosure during the impact of a water droplet on a free surface. This process is also known as the plunging jet mechanism, and is described in detail in Stage Three (Collision). Mixing shock does not appear to occur within the shorter (100 mm) branchpipe system, however, it was reproduced in the longer (500 mm) branchpipe system by restricting the air holes considerably (with a corresponding increase in back pressure). The assumption that the jet flow is stopped by impingement of a free surface appears correct in view of video evidence.

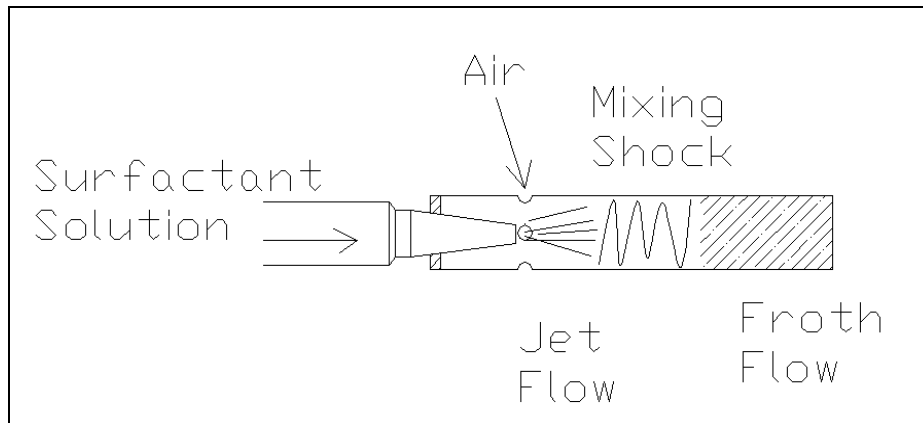


Figure 4 Mixing Shock

The branchpipe can also be described as a jet pump without a diffuser section. The amount of air entrained is governed by the pressure difference generated between the jet of surfactant solution and atmosphere. The volume of gas induced is, at best, only a few times that of the driving fluid [7]. Studies of the mixing process within the throat of a jet pump have mainly focussed on increasing the pump efficiency, and do not determine the mixing process. The details of the mixing process are avoided by using impulse-momentum equations, which include an assumption that the primary and pumped fluids are incompressible and of equal density.

4. Stage Two Flight

As the jet exits the branchpipe and flies it entrains some of the still air and carries this along with it. Entrainment by water sprays and jets has been studied by various authors [8], [9], [10]. However, the amount of air entrained in a turbulent jet is difficult to quantify.

Eventually the jet starts to break up. Laminar jet break-up has been well defined [11], but the break-up pattern of liquid jets in regimes beyond the surface tension controlled

case is not nearly so well understood. Because of the complex break-up process, no simple criteria for ultimate drop size and break-up length exist. It is determined by the nozzle and branchpipe geometry, the time of flight, the surface tension of the liquid and the turbulence and velocity of the jet [12], [13]. During the break-up droplets are sloughed off, but many remain connected to the main jet by strands of solution. As the jet rotates, these strands may be pulled into thin films. If entrained air is moving slower than the film, the film is blown like a child's bubble and separates. This only happens when break-up is near completion. If the film remains as a hemisphere, it may become closed on contact with another film of liquid, for example on a solid or liquid surface. If the film is stretched too thin or too fast, it will pop. The sloughed off droplets may also fall back into the main body of the jet and entrain more air in the plunging jet method described later.

As the jet leaves the branchpipe the flow appears relatively smooth. Within two diameters though, the jet becomes lumpy and the air slugs become visible (see Figure 5). At about this stage, the small bubbles, approximately 2 mm in diameter, become apparent throughout the mixture. During flight many of the slugs grow in size as the enclosed gas, which was compressed as it was entrained into the branchpipe, expands. Others are pulled apart and then squashed together again by the turbulence and swirl introduced by the nozzle. This may cause some of them to split into two bubbles, as described in Stage One (Mixing).

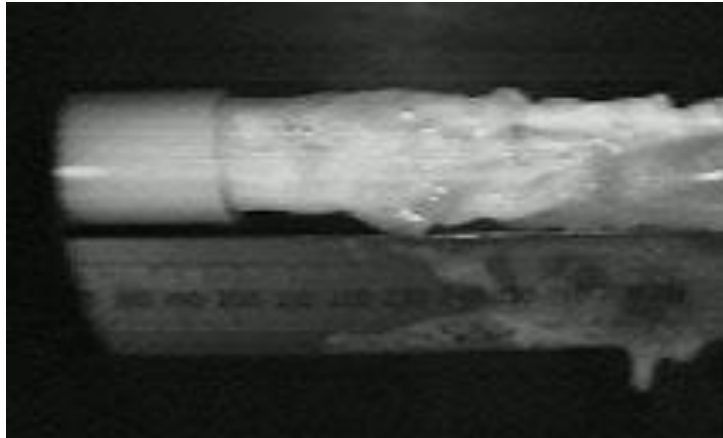


Figure 5 Transition from relatively smooth to lumpy flow.

Still from video - End of 500 mm branchpipe is at 200 mm on the rule

5. Stage 3 Collision

When the jet hits a surface, more bubbles are formed. This is either by capture of air entrapped within the hemispheres of film produced during flight, or through the "plunging jet" method, where air is entrained by a jet entering a liquid surface. In 1938 Mertes [14] patented a technique for mixing liquids and gases by this method, but he was mainly interested in mixing a liquid with a reactive gas.

There are two stages to the plunging jet method. The first is the air being entrained by the jet hitting the water, and the second where the sheath of air surrounding a turbulent jet is also entrained. Low velocity jets only use the first stage. They have disturbances on their surfaces and the entrainment mechanism is governed by the interaction of these disturbances with the surface of the receiving pool (Figure 6). The horizontal movement of the free surface is not fast enough to follow the roughness of the jet as it moves past, resulting in the capture of gas bubbles. The successive disturbances on the jet produces an irregular gas entrainment.

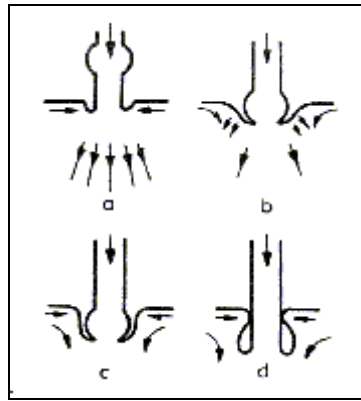


Figure 6 Air entrainment mechanism [15]

(a)-(d) show subsequent phases as a disturbance in the jet moves downwards.

High velocity jets use both of the stages. The entrained air is carried along with the jet, encompassed within the envelope defining the limits of the rough surface. An associated boundary layer is also carried along. When the jet impacts on the pool surface both of these air movements are carried under the free liquid. The subsequent breakdown of the entrained annulus gas film requires significant time before disintegration. High velocity jets have a regular entrainment rate and small bubbles are produced.

At high jet velocities a third mechanism has been suggested by Thomas, as reported by Bin [15]. Most of the air entrained enters via the layer of foam forming on the surface of the receiving fluid. Air enters the foam, possibly as a result of wave action and splashing, and is then entrained into the main body of the flow along with the recirculating foam. At low plunge angles, the foamy recirculating flows have much higher velocities than those driven by a steeply falling jet, so that large quantities of air are entrained along with the foam.

The liquid jet velocity must exceed a certain critical value to entrain air. Individual droplets impinging on a liquid surface will also entrain air if their velocity is high enough (above 1m/s, depending on their size), or if successive droplets impinge along the same trajectory [16]. The amount of gas entrained is largely controlled by the jet velocity. The other primary variables (jet diameter, jet length and the physical properties of the fluids) also play a considerable part. However, secondary features, such as nozzle design, angle of jet inclination, presence of vibrations etc. also exert a profound influence on the jet behaviour. These are much more difficult to quantify and, as such, predictions of bubble formation and air entrainment are difficult to produce.

6. Conclusions and discussions

Focus on the foam generation mechanisms within low expansion fire fighting branchpipes has shown that there are three distinct areas of foam formation. Each of these contributes to the properties of the foam.

The first stage, mixing within the branchpipe, produces small (2 mm diameter) bubbles and also larger slugs of air. Some of these slugs escape to atmosphere and are not incorporated into the final foam. The 500 mm branchpipe generates a higher expansion foam than the 100 mm branchpipe. Within the 100 mm branchpipe, adding cross bars or coarse gauze over the end of the tube did not affect the expansion. Changing the number or size of the air holes also appears to have no effect.

During the second stage, the flight of the jet, a slight increase in expansion is noticed when the flight distance increases. This is mainly due to more air being entrained into the turbulent jet and forming foam in the collision stage. In addition, large bubbles blown during the flight will increase the expansion ratio. As the jet travels it slows down. The force with which it collides at Stage Three will effect the amount of foam generated in this stage.

The final stage, collision, produces foam mainly by the plunging jet method. This is where the jet plunges into a pool of liquid and the air, entrained in Stage Two, is carried under the surface. This method produces the majority of the foam within the whole system. The capture of air entrapped within hemispheres of film produced during flight also adds to the expansion ratio.

The next stage of this work is to try to model each of the stages, and to answer many of the questions it has generated. These include:

How much of the air entrained by the branchpipe escapes to atmosphere? Can mixing shock occur in free air? Do disturbances in longer branchpipes produce a higher expansion, and if so, is this caused by an increase in back pressure, and therefore mixing shock, or by an increase in turbulence, or both? Does mixing shock occur in the 100 mm branchpipe at low upstream liquid pressures - and does this explain the high expansions below 2 bar? How much foam is produced by the plunging jet method? How does the scale model relate to actual fire fighting branchpipes in use in the field?

7. Acknowledgements

This programme was funded by CounterFire Limited. The high speed video equipment was kindly loaned by the EPSRC engineering instrument pool at Rutherford Appleton Laboratory.

8. References

1. Johnson, J.H., . 1877: Britain.
2. Benson, S.P., D.J. Griffiths, and J.G. Corrie, *A 5 Litre per Minute Standard Foam Branchpipe*, . 1973, Fire Research Station.
3. Corrie, J.G., *A 200 Litre Per Minutes Standard Foam Branchpipe*, . 1976, Fire Research Station.
4. ISO-7203-1, *Fire Extinguishing Media-Foam Concentrates-Part 1: Specification For Low Expansion Foam Concentrates For Top Application To Water Immiscible Liquids*, . 1995, British Standard.
5. Bikerman, *Foams*. 1973.
6. Witte, J.H., *Mixing shocks in Two-Phase Flows*. Journal of Fluid Mechanics, 1969. **36**(part 4): p. 639-655.
7. Wakefield, A.W., *An Introduction To The Jet Pump*. 4th ed. 1989.
8. Hinze, J.O., *Fundamentals of the Hydrodynamic Mechanism of Splitting in Dispersion Processes*. AIChE Journal, .
9. McQuaid, *Air Entrainment into Bounded Axisymmetric Sprays*. The IMechE Thermodynamics and Fluid Mechanics Group, 1975. **189**.
10. Benatt, F.C.S. and P. Eisenklam, *Gaseous Entrainment into Axisymmetric Liquid Sprays*. Journal Of The Institute Of Fuel, 1969(August): p. 309-315.
11. Weber, C., *Zum Zerfall eines Fluessigkeitsstrahles*. Z.angew. Math. Mech, 1931. **11**(136).
12. Merrington, C., Richardson,E.G., *The Break-up of Liquid Jets*. The Proceedings of the Physical Society, 1947. **59 Part1**(331): p. 1--13.
13. Phinney, R.E., *The Breakup Of A Turbulent Liquid Jet In A Gaseous Atmosphere*. Journal Of Fluid Mechanics, 1973. **60 part 4**: p. 689--701.
14. Burgess, J.M., N.A. Molloy, and M.J. McCarthy, *A Note on the Plunging Liquid Jet Reactor*. Chemical Engineering Science, 1972. **27**: p. 442-445.
15. Bin, A.K., *Gas Entrainment by Plunging Liquid Jets*. Chemical Engineering Science, 1993. **48**: p. 3585-3630.
16. Volkart, P., *The Mechanism of Air Bubble Entrainment in Self -Aerated Flow*. Int. J. Multiphase Flow, 1980. **6**: p. 411-423.

Appendix B. Test Rig One Results and Conclusions

Introduction

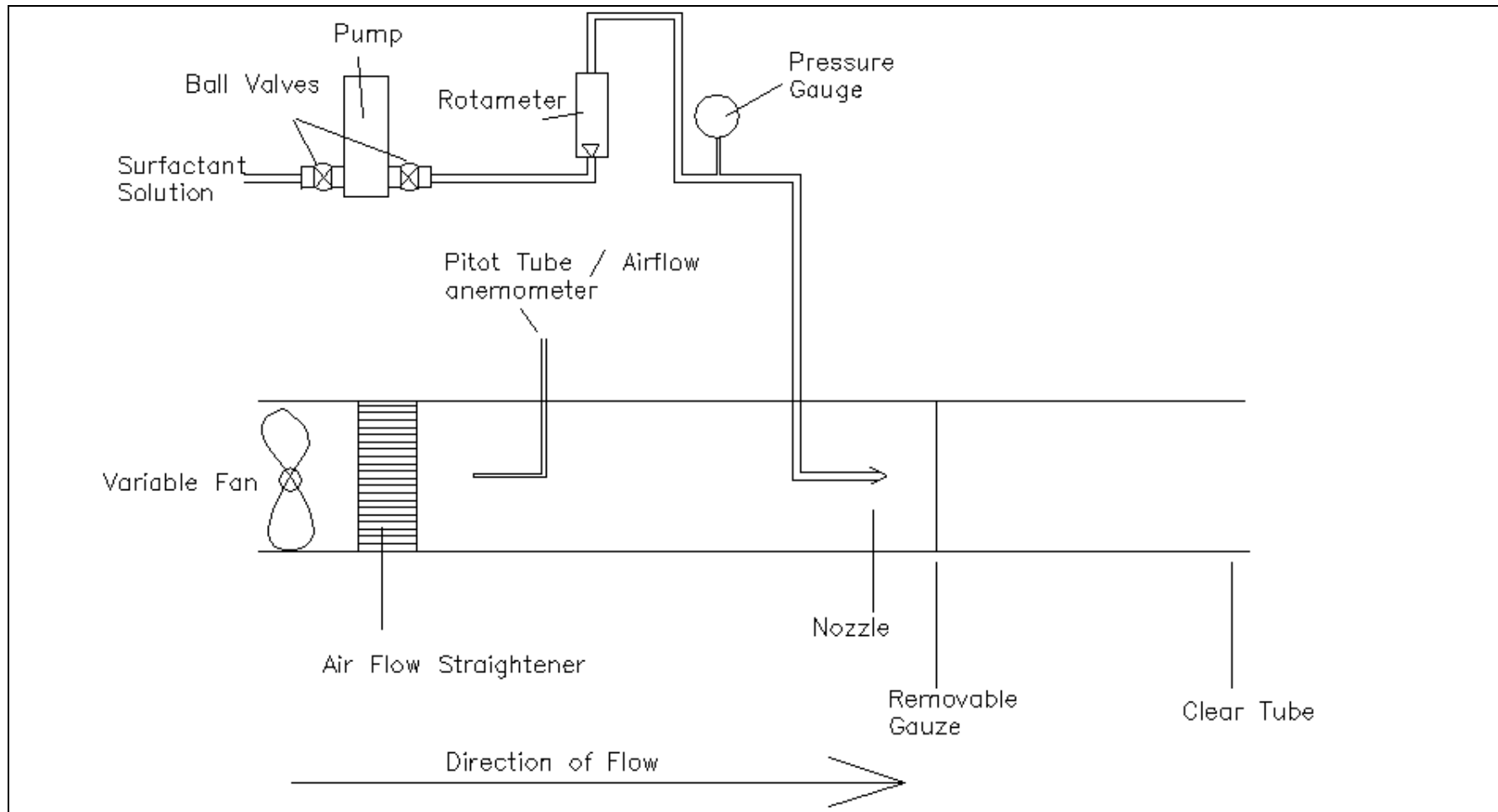
The initial aim of the project was to determine which physical characteristics of the generating equipment would have the most influence on the properties of expansion ratio and drainage rate. CounterFire suggested various parameters that they thought would be major contributors to these properties. The two-level factorial design method was used to determine which experiments would be most efficient. The two levels for each of the six variables chosen were:

Description	ID	Low Setting	High Setting
Fan setting	(F)	Off	Full
Pump Setting	(P)	Low	High
Gauze	(G)	None	Gauze
Nozzle Angle	(A)	120°	60°
Cone Type	(E)	Full	Hollow
Concentration	(C)	1%	8%

The type of surfactant used can greatly affect the type of foam produced, as described in Chapter 2. Therefore only one type of surfactant (Angus' FP70, a low to medium expansion protein foam concentrate) was used in all the experiments, unless stated otherwise.

Results

Experiments were run at every possible combination of the variables using Test Rig One (Figure Test Rig One – Schematic with 200 mm diameter tube). This led to a 2^6 factorial design and 64 experiments. Many of these were repeated to enable a statistical variance to be calculated. The Yates' analysis was conducted on Test Rig One (see Figure Yates' Analysis) with the 8% surfactant solution and the 200 mm diameter tube. The basic Yates' method did not produce any significant effects or interactions, and it was thought that the effects may be multiplicative, rather than additive. Therefore the log of the expansion ratio was taken and Yates' Analysis applied to these results. This can be seen in Figure "Yates' Analysis using logarithm of results". The log of the average of these experiments was 0.57 ± 0.106 . The effects are very small compared to the standard error, and the only slightly significant result was the angle of the nozzle - a nozzle angle of 120° produces a higher expansion ratio foam than an angle of 60° . The interaction between the gauze and the angle and the interaction between the pump level, the cone type and the nozzle angle produced effects very similar in magnitude to the standard error.



Test Rig One – Schematic with 200 mm diameter tube

F	P	G	A	E	C	Average ISO & Amiri Exp.	1	2	3	4	5	6	Divisor	estimate	id
-	-	-	-	-	-	1.84	3.55	7.18	14.25	26.80	49.96	174.32	64	2.72	average
+	-	-	-	-	-	1.71	3.63	7.07	12.55	23.16	124.36	-5.83	32	-0.18	F
-	+	-	-	-	-	1.89	3.54	6.24	11.76	63.73	-1.16	-8.59	32	-0.27	P
+	+	-	-	-	-	1.75	3.53	6.32	11.40	60.62	-4.68	3.92	32	0.12	FP
-	-	+	-	-	-	1.84	3.18	5.99	36.46	-1.14	2.40	7.84	32	0.24	G
+	-	+	-	-	-	1.69	3.06	5.76	27.27	-0.01	-10.99	4.64	32	0.14	FG
-	+	+	-	-	-	1.95	3.15	5.97	39.78	0.28	0.28	-13.59	32	-0.42	PG
+	+	+	-	-	-	1.58	3.16	5.43	20.85	-4.96	3.64	-8.56	32	-0.27	FPG
-	-	-	+	-	-	1.65	2.57	16.59	-0.80	-0.03	-0.80	-30.16	32	-0.94	A
+	-	-	+	-	-	1.52	3.42	19.87	-0.34	2.43	8.64	-1.04	32	-0.03	FA
-	+	-	+	-	-	1.56	2.92	14.21	0.04	-1.71	-0.29	14.40	32	0.45	PA
+	+	-	+	-	-	1.50	2.85	13.06	-0.05	-9.28	4.93	2.52	32	0.08	FPA
-	-	+	+	-	-	1.66	2.53	15.64	1.39	0.02	-1.06	-15.00	32	-0.47	GA
+	-	+	+	-	-	1.50	3.44	24.14	-1.11	0.26	-12.54	-5.77	32	-0.18	FGA
-	+	+	+	-	-	1.58	2.35	11.42	-3.02	-1.84	-0.72	10.37	32	0.32	PGA
+	+	+	+	-	-	1.58	3.09	9.43	-1.93	5.48	-7.84	10.17	32	0.32	FPGA
-	-	-	-	+	-	1.38	7.10	-0.28	0.07	-0.03	-2.05	-6.76	32	-0.21	E
+	-	-	-	+	-	1.19	9.50	-0.53	-0.11	-0.77	-28.11	-4.10	32	-0.13	FE
-	+	-	-	+	-	1.59	11.03	-0.19	0.78	2.13	0.37	-5.10	32	-0.16	PE
+	+	-	-	+	-	1.83	8.84	-0.15	1.65	6.51	-1.41	7.56	32	0.24	FPE
-	-	+	-	+	-	1.46	7.16	0.05	0.21	-0.22	0.70	3.65	32	0.11	GE

+	-	+	-	+	-	1.45	7.05	-0.01	-1.92	-0.07	13.70	8.99	32	0.28	FGE
-	+	+	-	+	-	1.42	7.43	-0.02	-12.55	-1.96	-0.16	-1.12	32	-0.03	PGE
+	+	+	-	+	-	1.43	5.63	-0.03	3.27	6.89	2.68	-4.42	32	-0.14	FPGE
-	-	-	+	+	-	1.27	9.36	0.87	-0.23	0.04	-0.10	-8.40	32	-0.26	AE
+	-	-	+	+	-	1.26	6.28	0.52	0.25	-1.09	-14.90	3.03	32	0.09	FAE
-	+	-	+	+	-	1.73	16.80	0.25	0.45	-6.27	0.33	19.01	32	0.59	PAE
+	+	-	+	+	-	1.71	7.33	-1.36	-0.19	-6.26	-6.09	-8.63	32	-0.27	FPAE
-	-	+	+	+	-	1.14	4.92	-4.44	-3.47	-0.14	0.95	-6.56	32	-0.21	GAE
+	-	+	+	+	-	1.21	6.50	1.42	1.63	-0.58	9.42	-3.84	32	-0.12	FGAE
-	+	+	+	+	-	1.60	3.87	-1.48	3.95	-1.93	0.54	4.12	32	0.13	PGAE
+	+	+	+	+	-	1.49	5.57	-0.46	1.53	-5.91	9.63	0.88	32	0.03	FPGA
-	-	-	-	-	+	3.29	-0.14	0.08	-0.12	-1.70	-3.65	74.40	32	2.32	C
+	-	-	-	-	+	3.81	-0.14	-0.01	0.08	-0.36	-3.11	-3.52	32	-0.11	FC
-	+	-	-	-	+	4.57	-0.15	-0.12	-0.23	-9.18	1.13	-13.39	32	-0.42	PC
+	+	-	-	-	+	4.92	-0.38	0.01	-0.53	-18.93	-5.23	3.36	32	0.11	FPC
-	-	+	-	-	+	4.56	-0.13	0.85	3.27	0.47	2.46	9.44	32	0.29	GC
+	-	+	-	-	+	6.47	-0.05	-0.07	-1.15	-0.09	-7.56	5.22	32	0.16	FGC
-	+	+	-	-	+	5.12	-0.16	0.92	8.50	-2.50	0.25	-11.48	32	-0.36	PGC
+	+	+	-	-	+	3.72	0.00	0.74	-1.98	1.09	7.31	-7.12	32	-0.22	FPGC
-	-	-	+	-	+	3.57	-0.19	2.40	-0.25	-0.18	-0.73	-26.06	32	-0.81	AC
+	-	-	+	-	+	3.59	0.24	-2.19	0.03	0.88	4.39	-1.78	32	-0.06	FAC
-	+	-	+	-	+	3.41	-0.01	-0.12	-0.06	-2.13	0.15	13.00	32	0.41	PAC
+	+	-	+	-	+	3.64	0.00	-1.80	-0.01	15.82	8.84	2.83	32	0.09	FPAC
-	-	+	+	-	+	4.41	-0.01	-3.08	-0.36	0.48	-1.13	-14.80	32	-0.46	GAC
+	-	+	+	-	+	3.02	-0.01	-9.47	-1.60	-0.63	0.01	-6.42	32	-0.20	FGAC
-	+	+	+	-	+	2.80	0.07	1.57	5.87	5.10	-0.44	8.47	32	0.26	PGAC

+	+	+	+	-	+	2.83	-0.11	1.70	1.02	-2.42	-3.98	9.08	32	0.28	FPGAC
-	-	-	-	+	+	6.98	0.52	-0.01	-0.09	0.20	1.34	0.54	32	0.02	EC
+	-	-	-	+	+	2.38	0.35	-0.23	0.13	-0.30	-9.74	-6.36	32	-0.20	FEC
-	+	-	-	+	+	3.06	1.91	0.08	-0.91	-4.42	-0.56	-10.03	32	-0.31	PEC
+	+	-	-	+	+	3.22	-1.39	0.16	-0.18	-10.48	3.59	7.07	32	0.22	FPEC
-	-	+	-	+	+	7.84	0.02	0.43	-4.59	0.28	1.06	5.12	32	0.16	GEC
+	-	+	-	+	+	8.96	0.23	0.02	-1.68	0.04	17.95	8.70	32	0.27	FGEC
-	+	+	-	+	+	3.52	-1.39	-0.01	-6.39	-1.24	-1.11	1.14	32	0.04	PGEC
+	+	+	-	+	+	3.82	0.03	-0.18	0.12	-4.85	-7.52	-3.54	32	-0.11	FPGEC
-	-	-	+	+	+	3.06	-4.61	-0.16	-0.22	0.21	-0.50	-11.08	32	-0.35	AEC
+	-	-	+	+	+	1.86	0.16	-3.30	0.08	0.74	-6.06	4.15	32	0.13	FAEC
-	+	-	+	+	+	3.39	1.12	0.21	-0.41	2.91	-0.24	16.89	32	0.53	PAEC
+	+	-	+	+	+	3.11	0.30	1.42	-0.17	6.51	-3.60	-6.41	32	-0.20	FPAEC
-	-	+	+	+	+	2.20	-1.20	4.77	-3.14	0.30	0.52	-5.55	32	-0.17	GAEC
+	-	+	+	+	+	1.67	-0.28	-0.82	1.21	0.24	3.60	-3.37	32	-0.11	FGAEC
-	+	+	+	+	+	2.75	-0.53	0.92	-5.60	4.35	-0.06	3.08	32	0.10	PGAEC
+	+	+	+	+	+	2.82	0.07	0.61	-0.31	5.28	0.93	0.99	32	0.03	FPGAEC
SUM OF SQUARES CHECK						647	1295	2590	5179	10358	20717	41433			

Yates' Analysis

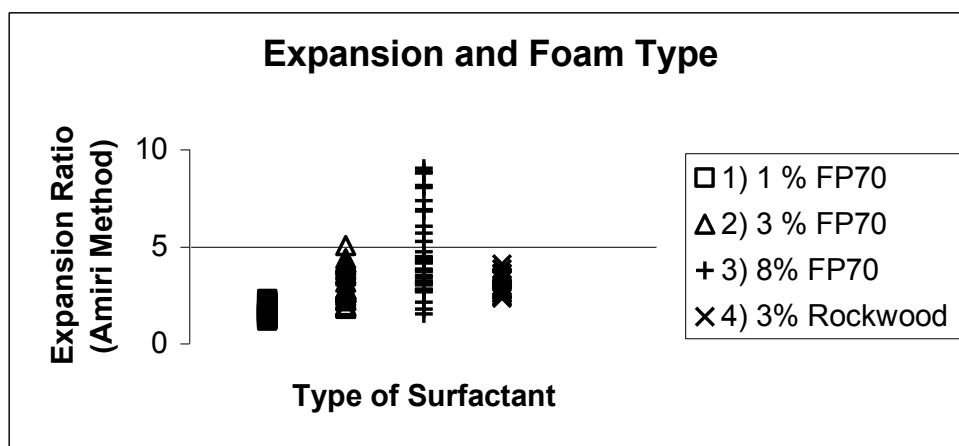
Fan	Pump	Gauze	Angle	Cone	Concentration
F	P	G	A	E	C
Off (-)	Low (-)	None (-)	120 (-)	F (-)	1% (-)
High (+)	High (+)	Knit1 (+)	60 (+)	H (+)	8% (+)

			H=+	120=+	Amiri								
			F=-	60=-	Log Exp								
Fan	Pump	Gauze	Cone	Angle		1	2	3	4	5	Divisor	Estimate	ID
F	P	G	C	A									
-	-	-	-	-	0.50	1.08	2.15	4.10	7.24	18.20	32	0.569	Average
+	-	-	-	-	0.58	1.07	1.95	3.14	10.96	0.55	16	0.034	F
-	+	-	-	-	0.54	1.06	1.74	5.49	0.52	0.21	16	0.013	P
+	+	-	-	-	0.53	0.89	1.40	5.47	0.03	0.25	16	0.016	FP
-	-	+	-	-	0.62	0.74	2.53	0.12	-0.46	-0.62	16	-0.039	G
+	-	+	-	-	0.44	1.00	2.96	0.40	0.67	0.04	16	0.002	FG
-	+	+	-	-	0.45	0.51	2.37	-0.23	0.47	-1.03	16	-0.064	PG
+	+	+	-	-	0.44	0.89	3.10	0.26	-0.22	0.54	16	0.034	FPG
-	-	-	+	-	0.49	1.05	-0.06	0.18	0.53	0.98	16	0.061	C
+	-	-	+	-	0.25	1.48	0.18	-0.64	-1.15	-0.76	16	-0.048	FC
-	+	-	+	-	0.51	1.55	0.26	-0.28	-0.13	-0.41	16	-0.026	PC
+	+	-	+	-	0.49	1.41	0.14	0.95	0.17	-1.44	16	-0.090	FPC
-	-	+	+	-	0.33	1.32	-0.22	0.10	-0.05	0.16	16	0.010	GC
+	-	+	+	-	0.18	1.05	-0.01	0.37	-0.98	-0.95	16	-0.059	FGC
-	+	+	+	-	0.44	1.89	0.32	-0.69	-0.18	-0.42	16	-0.026	PGC
+	+	+	+	-	0.44	1.21	-0.06	0.47	0.72	-0.29	16	-0.018	FPGC
-	-	-	-	+	0.43	-0.07	0.01	0.19	0.96	-3.72	16	-0.233	A
+	-	-	-	+	0.62	0.01	0.17	0.34	0.01	0.49	16	0.031	FA
-	+	-	-	+	0.72	0.18	-0.26	-0.42	-0.28	-1.12	16	-0.070	PA
+	+	-	-	+	0.76	0.00	-0.37	-0.73	-0.48	0.68	16	0.043	FPA
-	-	+	-	+	0.64	0.24	-0.42	-0.25	0.82	1.68	16	0.105	GA
+	-	+	-	+	0.91	0.02	0.14	0.11	-1.23	-0.31	16	-0.019	FGA
-	+	+	-	+	0.84	0.14	0.26	-0.21	-0.27	0.94	16	0.059	PGA
+	+	+	-	+	0.57	0.00	0.68	0.38	-1.17	-0.89	16	-0.056	FPGA
-	-	-	+	+	0.84	-0.19	-0.08	-0.16	-0.15	0.95	16	0.059	CA

+	-	-	+	+	0.48	-0.03	0.18	0.11	0.30	0.21	16	0.013	FCA
-	+	-	+	+	0.51	-0.27	0.23	-0.57	-0.36	2.04	16	0.128	PCA
+	+	-	+	+	0.55	0.26	0.14	-0.42	-0.59	0.89	16	0.056	FPCA
-	-	+	+	+	0.95	0.36	-0.15	-0.26	-0.27	-0.45	16	-0.028	GCA
+	-	+	+	+	0.94	-0.04	-0.54	0.08	-0.15	0.23	16	0.014	FGCA
-	+	+	+	+	0.57	0.00	0.40	0.38	-0.34	-0.12	16	-0.007	PGCA
+	+	+	+	+	0.64	-0.07	0.07	0.33	0.05	-0.39	16	-0.024	FPGCA
					11.41	22.82	45.64	91.28	182.56	365.12			

Yates' Analysis using logarithm of results

Other experiments with different variations were then conducted. Angus specifies that FP70 should be used at 3%, so the experiments were repeated with a surfactant concentration of 3 %. The low expansion surfactant produced foam with a much lower expansion ratio than expected. To determine the effect of tube diameter on the expansion ratio of the foam produced, an adapter was used to enable the tube diameter to be reduced from 200 mm to 100 mm. To try to determine the effect of the fan, some test runs were repeated using the four different settings of the fan. Some of the test runs were repeated using Rockwood High Expansion surfactant solution, at 3%, to see what difference the surfactant would make in these circumstances. (Rockwood is a high expansion foam surfactant. It is recommended to be diluted at 2% for fire fighting purposes and should produce foam with an expansion higher than 200). Figure Surfactant Type versus Expansion Ratio shows the range of expansion ratios generated by the different settings, with each type and dilution of foam concentrate.



Surfactant Type versus Expansion Ratio

					Pump	Low	Low	Low	Low	Full	Full	Full	Full
					Fan	Off	>	>>	>>>	Off	>	>>	>>>
Tube	Surfact.	Conc.	Gauze	Cone	Angle								
mm					Deg								
200	FP70	1%	Gauze	H	60	1.2			(1.2)	1.6			1.5
200	FP70	1%	Gauze	H	120	1.3			1.3	1.5			1.5
200	FP70	1%	Gauze	F	60	1.5			1.5	1.6			(1.5)
200	FP70	1%	Gauze	F	120	2.1			(1.7)	2.3			1.7
200	FP70	1%	None	H	60	1.3			1.3	1.7			1.7
200	FP70	1%	None	H	120	1.4			1.3	1.7			2.1
200	FP70	1%	None	F	60	(1.6)			1.5	(1.6)			1.4
200	FP70	1%	None	F	120	2.1			1.8	2.2			1.9
200	FP70	8%	Gauze	H	60	2.1			1.5	2.8			2.8
200	FP70	8%	Gauze	H	120	(10.9)			(6.6)	3.7			4.3
200	FP70	8%	Gauze	F	60	4.2			2.8	2.8			2.8
200	FP70	8%	Gauze	F	120	(4.4)			(8.6)	(5.2)			3.7
200	FP70	8%	None	H	60	3.1			1.8	3.2			3.1
200	FP70	8%	None	H	120	(10.5)			3.0	3.2			3.5
200	FP70	8%	None	F	60	3.2			3.8	3.5			3.4
200	FP70	8%	None	F	120	2.7			4.2	5.3			5.7
100	FP70	8%	None	H	60								
100	FP70	8%	None	H	120	8.0			2.7				
100	FP70	8%	None	F	60								
100	FP70	8%	None	F	120								
50	FP70	8%	None	H	60								
50	FP70	8%	None	H	120	7.4	6.0	4.2	4.2				
50	FP70	8%	None	F	60								
50	FP70	8%	None	F	120								
200	FP70	3%	Gauze	H	60					1.8			
200	FP70	3%	Gauze	H	120	2.2			3.8	2.5			2.6
200	FP70	3%	Gauze	F	60								
200	FP70	3%	Gauze	F	120								
100	FP70	3%	None	H	60	2.6	2.3	1.9	2.0	5.0	4.2	3.6	3.2
100	FP70	3%	None	H	120	2.8	2.3	1.9	1.9	2.8	2.8	2.8	2.6
100	FP70	3%	None	F	60	2.7	2.6	2.7	2.8	4.2	4.2	4.1	4.4
100	FP70	3%	None	F	120	2.7	2.6	2.7	2.8	3.9	4.0	3.5	3.6
100	R'wood	3%	None	H	60	2.9	2.8	2.4	2.6	4.1	3.6	3.6	3.9
100	R'wood	3%	None	H	120	3.0	2.8	2.3	2.5	3.3	3.4	2.7	2.6
100	R'wood	3%	None	F	60								
100	R'wood	3%	None	F	120	2.6	2.7	2.9	2.8	3.4	3.3	3.4	3.4

Expansion Ratio of Foam Produced

Brackets indicates an average of two or more runs, bold indicates expansion over 6.

The expansion was measured using the Amiri method.

The figure Expansion Ratio of Foam Produced gives the numerical expansion ratio from each of the set-ups. It can be seen that none of the 1% FP70 surfactant solution runs produced an expansion ratio of greater than 2.3, whereas the 8% FP70 surfactant solution generated expansion ratios ranging from 1.5 to 11. The 3% Rockwood and the 3% FP70 surfactant solutions produced expansion ratios of less than 5. This was much lower than expected as this dilution is both the manufacturers' specified concentration. The FP70 should produce foam with an expansion ratio nearer the industry standard of 10-20 and the Rockwood should produce high expansion foams, with ratios above 200.

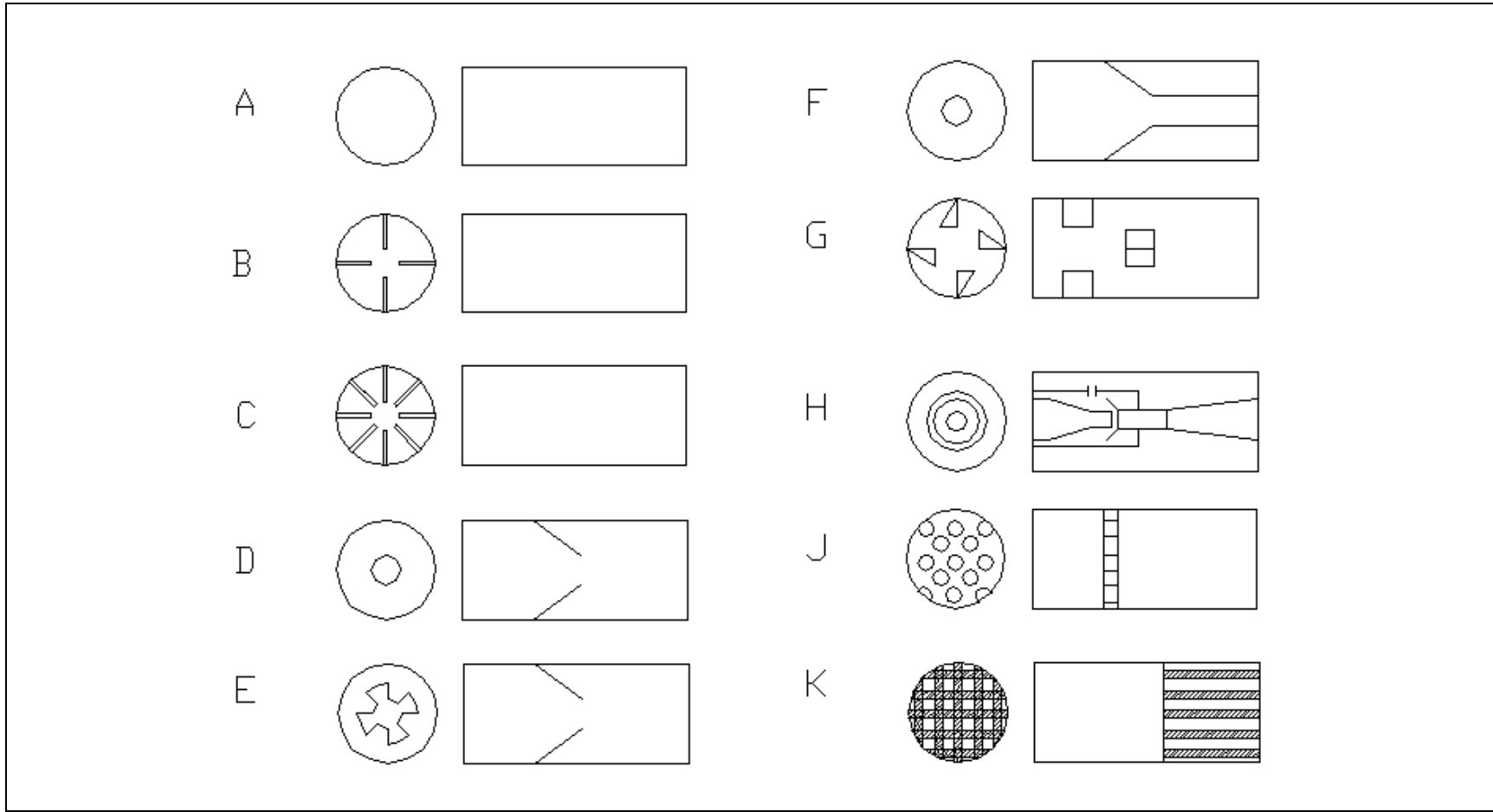
If the fan was switched off, slightly higher expansion foams were produced, in general, than when it was switched on. Therefore, the faster the speed of the fan (and hence air flow) the lower the expansion ratio. This again was surprising as it was expected that the more air that was introduced, the higher the expansion ratio would be. However, this may be a similar problem to that experienced when blowing a child's bubble. If the film is blown too hard, the bubble bursts. The pump setting, and hence surfactant solution flow rate, also produced a slightly higher expansion at a lower flow rate. This again was surprising and again may be similar to the child's bubble bursting as described above.

The figure also shows that there are four settings that produce an expansion of 6 or greater. These are all at 8% FP70, 120 Degree angle, hollow cone jet and the low pump setting. These higher expansion results are repeated with the different sizes of tube.

Data on insertion of obstructions

Obstructions were inserted into Test Rig One, as shown in the Figure “Obstructions” below. The pressure was kept at 4 bar and the liquid flow rate at 25 l/min.

Ref	Obstruction	Expansion
A	Nothing	2.8
B	4 bolts	2.8
C	8 bolts	2.8
D	Funnel	3
E	Castellations	3.5
F	Adapter	4
G	Blades	4
H	Jet pump	2.5
J	Sponge	5.4
K	Air flow straightener	6.6



Obstructions

Conclusion

Using Test Rig One, the variables of fan setting, pump setting, gauze, nozzle angle, cone type and surfactant concentration had little effect on the expansion ratio. Even with a vastly suppressed surface tension, the foam expansion rose only slightly, and not to the accepted industry standard of between 10 and 20. However, four settings did produce foam with an expansion of greater than 6. The reason for this could not be determined accurately from the results obtained. One hypothesis that the author proposes that may explain this phenomenon, at least in part, is that the hollow cone, large angled nozzle projects the surfactant solution almost as a film, which may be blown into bubbles more easily.

Some of the experiments were repeated using the high expansion foam concentrate, Rockwood's Macrofoam. This again had little effect on the expansion ratio of the foam produced. It was therefore assumed that Test Rig One was unable to expand the foam concentrate sufficiently.

Appendix C. Comparison of ISO and Amiri Results

Tube	200 mm	H = hollow	F = full						25%	25%	25%	50%	50%	50%
						Expansion	Expansion	Difference	Drainage	Drainage	Difference	Drainage	Drainage	Difference
Run	Fan	Pump	Gauze	Nozzle	Conc	ISO	Amiri	Expansion	ISO	Amiri	25%	ISO	Amiri	50%
									sec	sec		sec	sec	
1	None	Full	None	H120	1%	1.50	1.68	-0.18	143	124	19	250	197	54
2	Full	Full	None	H120	1%	1.56	2.10	-0.54	120	197	-78	197	271	-74
3	None	Low	None	H120	1%	1.39	1.38	0.01	46	19	26	91	39	52
4	Full	Low	None	H120	1%	1.12	1.27	-0.15	56	63	-7	112	86	26
7	None	Full	Knit1	H120	1%	1.39	1.45	-0.06	86	0		162	83	79
8	Full	Full	Knit1	H120	1%	1.38	1.47	-0.09	71	0		140	58	82
5	None	Low	Knit1	H120	1%	1.60	1.33	0.28	41	0		81	0	
6	Full	Low	Knit1	H120	1%	1.63	1.28	0.35	23	0		47	0	
15	None	Full	None	F120	1%	1.62	2.16	-0.54	138	46	92	225	155	70
16	Full	Full	None	F120	1%	1.57	1.92	-0.35	161	67	94	233	189	44
14	None	Low	None	F120	1%	1.59	2.10	-0.52	98	0		196	128	67
13	Full	Low	None	F120	1%	1.59	1.83	-0.24	186	0		284	128	156
10	None	Full	Knit1	F120	1%	1.61	2.29	-0.68	106	82	24	162	143	19
9	Full	Full	Knit1	F120	1%	1.46	1.69	-0.24	127	79	48	213	145	69
11	None	Low	Knit1	F120	1%	1.59	2.10	-0.52	208	66	142	332	118	214
12	Full	Low	Knit1	F120	1%	1.53	1.86	-0.32	124	0		170	130	40
34	None	Full	None	H60	1%	1.75	1.71	0.05	181	53	128	223	192	32
33	Full	Full	None	H60	1%	1.68	1.74	-0.06	65	57	8	130	243	-113
35	None	Low	None	H60	1%	1.25	1.28	-0.03	33	18	15	66	36	30
36	Full	Low	None	H60	1%	1.25	1.27	-0.02	57	19	38	113	38	75
39	None	Full	Knit1	H60	1%	1.62	1.57	0.06	101	53	48	197	171	27
40	Full	Full	Knit1	H60	1%	1.49	1.49	0.01	95	38	57	190	128	62
38	None	Low	Knit1	H60	1%	1.10	1.18	-0.08	42	18	24	84	36	48
37	Full	Low	Knit1	H60	1%	1.19	1.22	-0.03	58	19	39	115	37	78
48	None	Full	None	F60	1%	1.49	1.62	-0.13	67	35	33	135	98	37

47	Full	Full	None	F60	1%	1.60	1.41	0.19	74	28	47	149	55	93
46	None	Low	None	F60	1%	1.77	1.54	0.24	33	21	12	66	42	23
45	Full	Low	None	F60	1%	1.56	1.48	0.08	28	22	6	57	44	13
41	None	Full	Knit1	F60	1%	1.52	1.64	-0.12	84	35	48	168	87	81
42	Full	Full	Knit1	F60	1%	1.64	1.53	0.12	153	41	111	238	117	122
43	None	Low	Knit1	F60	1%	1.79	1.53	0.26	46	20	26	91	40	51
44	Full	Low	Knit1	F60	1%	1.48	1.51	-0.03	46	22	24	91	43	48
32	None	Full	None	H120	8%	2.91	3.20	-0.29	183	176	8	349	564	-215
31	Full	Full	None	H120	8%	2.91	3.54	-0.63	143	101	43	276	413	-136
29	None	Low	None	H120	8%	7.06	6.91	0.15	72	55	17	144	238	-93
30	Full	Low	None	H120	8%	1.74	3.01	-1.27	61	33	28	123	81	41
25	None	Full	Knit1	H120	8%	3.31	3.73	-0.42	147	160	-13	357	433	-76
26	Full	Full	Knit1	H120	8%	3.29	4.34	-1.05	105	48	58	258	240	18
28	None	Low	Knit1	H120	8%	6.81	8.87	-2.05	212	376	-164	449	750	-301
27	Full	Low	Knit1	H120	8%	9.15	8.78	0.37	34	29	5	68	59	9
18	None	Full	None	F120	8%	3.86	5.28	-1.42	152	315	-163	380	725	-345
17	Full	Full	None	F120	8%	4.16	5.69	-1.53	206	444	-238	523	1004	-481
20	None	Low	None	F120	8%	3.86	2.72	1.14	47	28	19	98	55	43
19	Full	Low	None	F120	8%	3.44	4.17	-0.73	33	37	-4	104	138	-34
23	None	Full	Knit1	F120	8%	3.39	6.84	-3.45	159	81	79	291	195	96
24	Full	Full	Knit1	F120	8%	3.71	3.73	-0.01	177	218	-41	380	575	-195
22	None	Low	Knit1	F120	8%	4.78	4.34	0.44	48	76	-29	113	218	-105
21	Full	Low	Knit1	F120	8%	4.79	8.15	-3.37	56	49	7	155	170	-16
64	None	Full	None	H60	8%	3.55	3.22	0.33	161	188	-26	363	558	-195
63	Full	Full	None	H60	8%	3.11	3.11	0.00	176	194	-18	362	545	-183
61	None	Low	None	H60	8%	3.04	3.08	-0.05	45	24	20	89	49	41
62	Full	Low	None	H60	8%	1.95	1.77	0.18	53	33	20	106	67	39
57	None	Full	Knit1	H60	8%	2.72	2.77	-0.06	92	137	-45	214	354	-140
58	Full	Full	Knit1	H60	8%	2.86	2.78	0.08	160	134	26	286	403	-117
60	None	Low	Knit1	H60	8%	2.27	2.13	0.14	38	32	6	77	64	12
59	Full	Low	Knit1	H60	8%	1.81	1.53	0.28	64	34	30	128	68	61
49	None	Full	None	F60	8%	3.36	3.46	-0.09	109	194	-85	249	603	-354
50	Full	Full	None	F60	8%	3.89	3.38	0.51	137	273	-136	302	680	-379

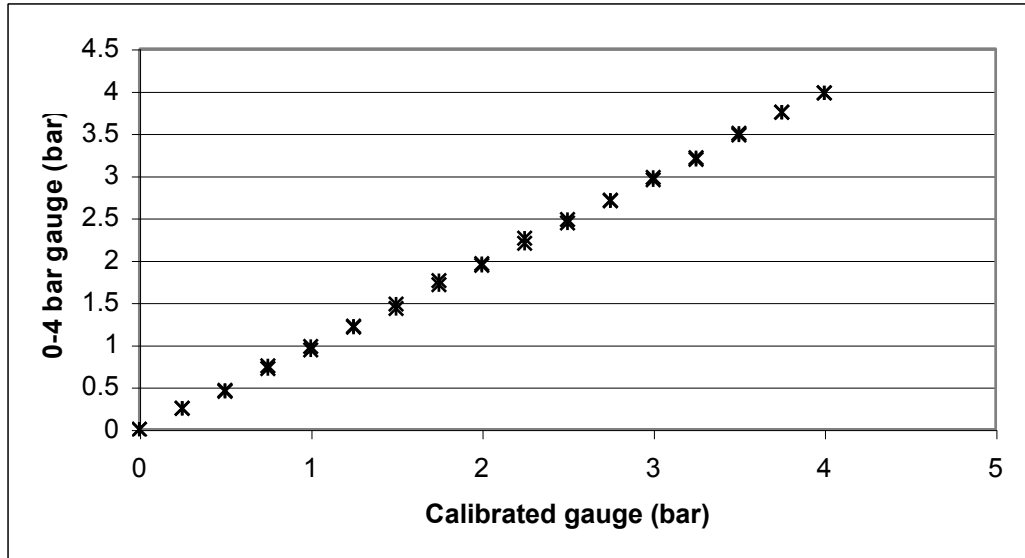
51	None	Low	None	F60	8%	3.96	3.19	0.77	44	36	8	89	163	-75
52	Full	Low	None	F60	8%	3.42	3.76	-0.35	51	37	14	121	87	34
53	None	Full	Knit1	F60	8%	2.79	2.81	-0.02	84	176	-92	168	555	-387
54	Full	Full	Knit1	F60	8%	2.88	2.78	0.09	98	217	-119	205	618	-413
55	None	Low	Knit1	F60	8%	4.64	4.18	0.47	45	49	-4	90	228	-138
56	Full	Low	Knit1	F60	8%	3.29	2.75	0.54	48	43	5	97	206	-110
Average						2.61	2.84	-0.23	96	82	4	188	225	-40

Appendix D. Experimental Error

The only significant zero error noted was in the weighing scales. This error was measured and taken into account in calculating the actual mass of items.

The extent of the random errors was calculated from the minimum practical graduation against the highest reading taken. The random errors were minimised by repeating the experiments and calibrating the equipment, where possible. See Table Random error of equipment).

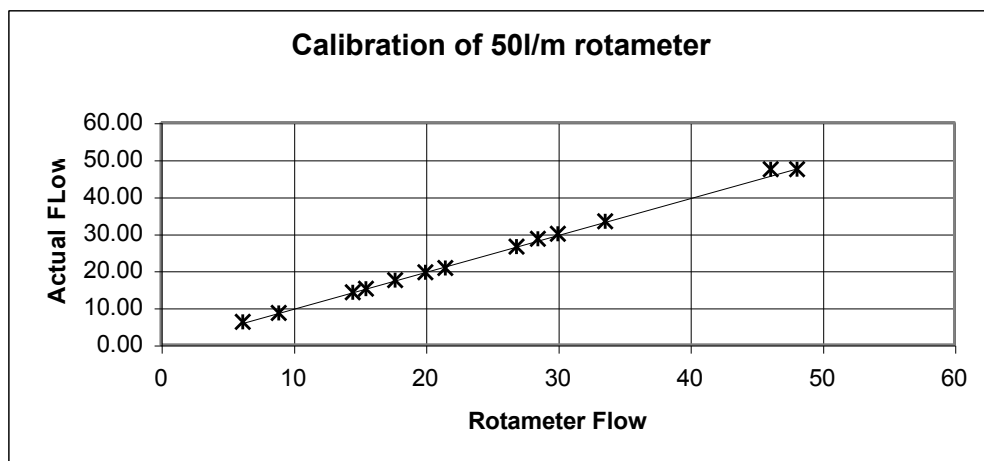
The volumes of the ISO and the 14 litre measuring vessels were calculated by filling them with water and emptying the water into a measuring cylinder. The accuracy of the measuring cylinders, the mercury thermometer and the ruler were determined from the minimum graduations. The weighing scales were calibrated by comparison of different known weights on either side of the scales. The pressure gauges were calibrated using a certified calibrated gauge and a calibration kit (see Figure Pressure Gauge Calibration).



Pressure Gauge Calibration

During use the needle vibrated due to fluctuations from the pump and nozzle, hence the random error is larger than expected.

The rotameter was calibrated by timing how long it took to fill a 30 litre bucket, and comparing this flow rate with the rotameter reading (see Figure Rotameter Calibration)



Rotameter Calibration

The manometer used with the pitot tube had a very large scale in comparison to the measurements taken, and this led to the high random error. The accuracy of the thermal anemometer air velocity and thermometer was given in the manufacturer's literature. The accuracy of the shear force measurements was dependent on the minimum mass of the weights available. The concentration of surfactant was initially measured with an accuracy of approximately 5%, however, as the solution was recycled, and presumably, some water evaporated, the overall accuracy is estimated to approximately 25%. However, it is assumed that the surface tension of the solution did not vary considerably during the tests, as repeats using different tanks of recycled solution produced consistent expansion ratios. The accuracy of the stop clock was determined by the speed with which the start / stop button could be pressed.

Equipment	Random Error
ISO measuring vessel	0.25%
Measuring cylinder	0.45%
14 litre measuring vessel	5.00%
Mercury thermometer	± 0.5 °C
Weighing scales	0.50%
Pressure gauge (0-16 bar)	8.00%
Pressure gauge (0-4 bar)	4.00%
Rotameter 50 l/min	1.50%
Pitot tube and manometer	25.00%
Thermal anemometer air velocity	1.00%
Thermal anemometer thermometer	1.00%
Ruler	0.20%
Shear force	10.00%
Concentration of surfactant	25.00%
Stop clock	0.1 sec

Random error of equipment

Appendix E. Yates' Analysis of Plunging Jet

				head height ml						
	L	H	V	Result	-1.00	-2.00	-3.00	Divisor	Estimate	ID
Mmm	-	-	-	200.00	387.50	932.50	1845.00	8.00	230.63	Average
Pmm	+	-	-	187.50	545.00	912.50	0.00	4.00	0.00	L
Mpm	-	+	-	280.00	367.50	27.50	-335.00	4.00	-83.75	H
Ppm	+	+	-	265.00	545.00	-27.50	0.00	4.00	0.00	LH
Mmp	-	-	+	177.50	12.50	-157.50	20.00	4.00	5.00	V
Pmp	+	-	+	190.00	15.00	-177.50	55.00	4.00	13.75	LV
Mpp	-	+	+	265.00	-12.50	-2.50	20.00	4.00	5.00	HV
Ppp	+	+	+	280.00	-15.00	2.50	-5.00	4.00	-1.25	LHV
				foam exp						
	L	H	V	Result	-1.00	-2.00	-3.00	Divisor	Estimate	ID
Mmm	-	-	-	16.67	32.00	70.38	132.09	8.00	16.51	Average
Pmm	+	-	-	15.33	38.38	61.71	-20.11	4.00	-5.03	L
Mpm	-	+	-	18.50	31.76	-0.04	-4.56	4.00	-1.14	H
Ppm	+	+	-	19.88	29.95	-20.06	-5.26	4.00	-1.31	LH
Mmp	-	-	+	8.88	1.33	-6.38	8.66	4.00	2.17	V
Pmp	+	-	+	22.89	-1.38	1.81	20.02	4.00	5.01	LV
Mpp	-	+	+	11.95	-14.01	2.71	-8.19	4.00	-2.05	HV
Ppp	+	+	+	18.00	-6.05	-7.96	10.67	4.00	2.67	LHV

Appendix F. Experimental Data - Test Rig Three

Data using different designs of branchpipe at different upstream pressures.

All foam expansion ratios measured using measuring vessel method.

Flight distance: 750 mm Type of branchpipe: 8 holes, 3.2 mm diameter, branchpipe 100 mm long

Date		31-Jan-00	14-Jul-00	14-Jul-00	14-Jul-00	14-Jul-00								
Pressure	bar	2.3	1	3	3.5	4	5	2	1	4.5	3.9	3.1	2.4	
Flow	l/min	17.9	11.7	20	22	23	25	16.5	11.5	23.8	22.5	19.8	18.2	
Air Speed	m/s	2.1	1.43	2.3	2.68	3.16	3.25	1.83	1.36	2.7	2.5	2.55	1.95	
Air Temp	deg C	16.1	15.6	14.3	13.9	13.7	13.4	13.7	15	16.7	16.9	16.8	17	
Expansion		5.78	9.76	6.01	5.44	5.55	5.46	6.17	9.82	5.43	5.53	5.83	6.13	
Air Flow	l/min	209.40	142.59	229.34	267.23	315.10	324.07	182.48	135.61	269.23	249.29	254.27	194.44	
Max Exp		12.70	13.19	12.47	13.15	14.70	13.96	12.06	12.79	12.31	12.08	13.84	11.68	
Date		14-Jul-00	14-Jul-00	1-Nov-00										
Pressure	bar	1.35	0.98	4.5	2.8	2.8	2.8	2.2	2.2	2.2	3.4	3.4	3.4	
Flow	l/min	13	11.2	25	19.5	19.5	19.5	17	17	17	21.2	21.2	21.2	
Air Speed	m/s	1.43	1.29	2.86	1.78	2.49	2.01	1.9	1.89	1.96	2.47	2.6	2.48	
Air Temp	deg C	16.8	17.1	12.9	14.5	15.2	13.8	13.4	13.2	13.1	12.9	12.9	12.9	
Expansion		7.71	9.76	4.77	5.18	4.82	4.83	5.31	5.21	5.15	4.50	4.89	5.29	
Air Flow	l/min	142.59	128.63	285.18	177.49	248.29	200.43	189.46	188.46	195.44	246.29	259.26	247.29	
Max Exp		11.97	12.48	12.41	10.10	13.73	11.28	12.14	12.09	12.50	12.62	13.23	12.66	

Flight distance: 750 mm Type of branchpipe: 8 holes, 3.2 mm diameter, branchpipe 500 mm long

Date		26-May-00								
Pressure	bar	0.48	1.12	1.38	1.87	2.7	2.31	1.9	3.85	3.15
Flow	l/min	7.9	12.6	13.9	16.1	19.1	18	16.3	22.5	21
Air Speed	m/s	0.48	1.18	1.39	1.71	2.09	1.93	1.72	2.43	2.16
Air Temp	deg C	14.1	13.4	13.3	13.1	13	12.9	12.8	12.8	12.5
Expansion		5.84	7.88	8.45	7.61	8.78	8.41	8.65	8.90	8.77
Air Flow	l/min	47.86	117.66	138.60	170.51	208.40	192.45	171.51	242.31	215.38
Max Exp		7.06	10.34	10.97	11.59	11.91	11.69	11.52	11.77	11.26
Date		26-May-00	26-May-00	26-May-00	26-May-00					
Pressure	bar	1	4.25	3.95	0.3					
Flow	l/min	11.5	24	22.5	6					
Air Speed	m/s	1.09	2.62	2.36	0.38					
Air Temp	deg C	11.8	12.5	12.6	12					
Expansion		8.33	7.93	9.28	4.82					
Air Flow	l/min	108.69	261.25	235.33	37.89					
Max Exp		10.45	11.89	11.46	7.32					

Flight distance: 750 mm Type of branchpipe: 4 holes, 3.2 mm diameter, branchpipe 100 mm long

Date		25-Jan-00	25-Jan-00	25-Jan-00	25-Jan-00	25-Jan-00	25-Jan-00	26-Jan-00	26-Jan-00	26-Jan-00	26-Jan-00	26-Jan-00	26-Jan-00
Pressure	bar	2.3	2.3	2.3	2.3	2.3	2.3	2.3	2.3	2.3	2.3	2.3	2.3
Flow	l/min	18.1	18.1	18.1	18.1	18.1	18.1	18.1	18.1	18.1	18.1	18.1	18.1
Air Speed	m/s	1.18	1.18	1.2	1.36	1.37	1.44	1.36	1.29	1.31	1.21	1.2	1.28
Air Temp	deg C	17.6	19.8	20.9	20.5	17.1	16.1	20.4	21.1	21.3	21.1	21.1	21.1
Expansion		5.26	5.37	5.42	5.63	5.59	5.73	5.29	5.79	5.31	5.33	5.85	5.48
Air Flow	l/min	117.66	117.66	119.66	135.61	136.61	143.59	135.61	128.63	130.63	120.65	119.66	127.63
Max Exp		7.50	7.50	7.61	8.49	8.55	8.93	8.49	8.11	8.22	7.67	7.61	8.05
Date		26-Jan-00	26-Jan-00	26-Jan-00	26-Jan-00	14-Jul-00	14-Jul-00	14-Jul-00	14-Jul-00	14-Jul-00	14-Jul-00		
Pressure	bar	2.3	2.3	2.3	2.3	1.2	0.6	1.7	2.9	3.6	4.5		
Flow	l/min	18.1	18.1	18.1	18.1	13	9.2	15.6	19.6	22	24		
Air Speed	m/s	1.29	1.6	1.35	1.35	1.02	0.77	1.16	1.37	1.5	1.66		
Air Temp	deg C	20.7	19.9	19.2	17.7	20.3	18.9	18.1	17.8	17.4	17.3		
Expansion		5.52	5.41	5.69	5.56	6.65	7.89	7.10	5.98	5.49	5.68		
Air Flow	l/min	128.63	159.54	134.61	134.61	101.71	76.78	115.67	136.61	149.57	165.53		
Max Exp		8.11	9.81	8.44	8.44	8.82	9.35	8.41	7.97	7.80	7.90		

Flight distance: 200 mm Type of branchpipe: 8 holes, 3.2 mm diameter, branchpipe 100 mm long

Date		31-Jan-00											
Pressure	bar	0.12	0.2	0.4	0.8	0.55	1.1	1.4	1.9	1.58	2.1	2.4	2.65
Flow	l/min	3.8	5.2	7.1	10.3	8.4	12.4	14	16.5	14.8	17.2	18.2	19.1
Air Speed	m/s	0.42	0.65	0.96	1.36	1.13	1.47	1.6	2.05	1.66	2.47	2.2	2.41
Air Temp	deg C	15.9	15.7	15.3	14.8	14.7	14.8	16.8	18.1	18.5	18.6	16.2	15.1
Expansion		8.87	10.91	11.41	11.51	11.02	9.80	8.32	6.19	7.13	5.58	5.28	4.13
Air Flow	l/min	41.88	64.81	95.73	135.61	112.68	146.58	159.54	204.41	165.53	246.29	219.37	240.31
Max Exp		12.02	13.46	14.48	14.17	14.41	12.82	12.40	13.39	12.18	15.32	13.05	13.58
Date		31-Jan-00	31-Jan-00	31-Jan-00	31-Jan-00	01-Nov-00							
Pressure	bar	4	5	3.5	3	4.5	2.8	2.8	2.8	2.2	2.2	2.2	
Flow	l/min	23	25	22	20	25	19.5	19.5	19.5	17	17	17	
Air Speed	m/s	2.87	2.95	2.45	2.2	2.84	1.96	2.11	2.1	1.73	1.73	1.76	
Air Temp	deg C	15.8	14.8	14.4	14.4	13.5	12	18.6	14.9	13.3	13	13.2	
Expansion		4.28	4.17	4.06	4.37	4.11	4.68	4.62	4.50	5.31	5.15	5.16	
Air Flow	l/min	286.18	294.16	244.30	219.37	283.19	195.44	210.40	209.40	172.51	172.51	175.50	
Max Exp		13.44	12.77	12.10	11.97	12.33	11.02	11.79	11.74	11.15	11.15	11.32	
Date		01-Nov-00	01-Nov-00										
Pressure	bar	3.4	3.4										
Flow	l/min	21.2	21.2										
Air Speed	m/s	2.43	2.28										
Air Temp	deg C	12.9	12.9										
Expansion		4.36	4.50										
Air Flow	l/min	242.31	227.35										
Max Exp		12.43	11.72										

Flight distance: 1650 mm Type of branchpipe: 8 holes, 3.2 mm diameter, branchpipe 100 mm long

Date		19-Oct-00	01-Nov-00	01-Nov-00	01-Nov-00	01-Nov-00	01-Nov-00							
Pressure	bar	3.7	2.82	2.3	2	3.55	4.5	4	4.5	2.8	2.8	2.8	2.2	
Flow	l/min	22	19.8	17.5	16	21.5	24	22.5	25	19.5	19.5	19.5	17	
Air Speed	m/s	2.4	2.01	1.83	1.7	2.28	2.58	2.36	2.85	1.83	2.06	1.99	1.74	
Air Temp	deg C	11.8	11.7	11.9	11.9	11.8	11.9	11.7	12.7	17.6	16.6	14	13.3	
Expansion		5.99	5.67	5.61	7.24	4.69	4.69	4.79	4.67	5.35	5.22	5.19	5.56	
Air Flow	l/min	239.31	200.43	182.48	169.51	227.35	257.26	235.33	284.19	182.48	205.41	198.43	173.50	
Max Exp		11.88	11.12	11.43	11.59	11.57	11.72	11.46	12.37	10.36	11.53	11.18	11.21	
Date		01-Nov-00	01-Nov-00	01-Nov-00	01-Nov-00	01-Nov-00								
Pressure	bar	2.2	2.2	3.4	3.4	3.4								
Flow	l/min	17	17	21.2	21.2	21.2								
Air Speed	m/s	1.74	1.71	2.14	2.14	2.14								
Air Temp	deg C	13.2	13.1	12.8	13.1	13								
Expansion		5.47	5.65	5.22	4.82	4.72								
Air Flow	l/min	173.50	170.51	213.39	213.39	213.39								
Max Exp		11.21	11.03	11.07	11.07	11.07								

Flight distance: 1650 mm Type of branchpipe: 8 holes, 3.2 mm diameter, branchpipe 100 mm long (to side of jet)

Date		24-Oct-00									
Pressure	bar	3.95	4.5	3.2	2.5	2.2	3.3	3.9			
Flow	l/min	22.5	24	21	18	17	21	23.5			
Air Speed	m/s	2.42	2.68	2.25	1.96	1.77	2.2	2.5			
Air Temp	deg C	13.6	13.3	13.3	13.4	13.4	13.3	13.2			
Expansion		4.12	4.03	4.30	4.64	5.54	4.83	4.41			
Air Flow	l/min	241.31	267.23	224.36	195.44	176.49	219.37	249.29			
Max Exp		11.72	12.13	11.68	11.86	11.38	11.45	11.61			

Flight distance: 750 mm Type of branchpipe: 4 holes, 2.1 mm diameter, branchpipe 100 mm long

Date		14-Jul-00	14-Jul-00	14-Jul-00	14-Jul-00	14-Jul-00	14-Jul-00				
Pressure	bar	4.5	3.9	3.5	1.6	0.8	2.5				
Flow	l/min	24	23	22	14.9	11.4	18.8				
Air Speed	m/s	0.82	0.78	0.76	0.49	0.36	0.67				
Air Temp	deg C	17	16.8	16.7	16.7	16.8	16.8				
Expansion		4.93	4.93	4.99	4.91	5.34	4.94				
Air Flow	l/min	81.77	77.78	75.78	48.86	35.90	66.81				
Max Exp		4.41	4.38	4.44	4.28	4.15	4.55				

Flight distance: 750 mm Type of branchpipe: 8 holes, 2.1 mm diameter, branchpipe 100 mm long

Date		14-Jul-00	14-Jul-00	14-Jul-00	14-Jul-00	14-Jul-00	14-Jul-00				
Pressure	bar	0.98	1.35	2.5	3.89	2.9	4.5				
Flow	l/min	11.2	13.6	18.6	23	20	24				
Air Speed	m/s	0.67	0.75	1.09	1.4	1.16	1.35				
Air Temp	deg C	17.3	17.4	17.3	17.1	17.1	17.2				
Expansion		4.93	4.93	4.93	4.93	4.93	4.93				
Air Flow	l/min	66.81	74.79	108.69	139.60	115.67	134.61				
Max Exp		6.97	6.50	6.84	7.07	6.78	6.61				

Data on Shear Force Generated

Tube	Pressure	Flow	Flow²	Mass	Force
Length	Bar	l/m		g	N
Mm				Approx	approx
100	0.5	8.1	65.61	35	0.36
100	1.3	13.3	176.89	110	1.12
100	1.75	15.3	234.09	135	1.38
100	1.8	16	256	115	1.17
100	2.05	17	289	175	1.78
100	2.5	18.6	345.96	200	2.04
100	2.75	19.5	380.25	210	2.14
100	3.25	21	441	235	2.40
100	4	23.2	538.24	275	2.80
100	4.5	24	576	310	3.16
100	4.3	24.5	600.25	300	3.06
100	3.1		0	240	2.45
100	3.9	22.5	506.25	270	2.75
100	2.25	17.8	316.84	220	2.24
100	3.85	23.7	561.69	250	2.55
100	1.5	14.6	213.16	120	1.22
100	1.8	15.9	252.81	160	1.63
100	2.1	17.1	292.41	160	1.63
100	1.05	11.9	141.61	90	0.92
100	0.8	10.4	108.16	70	0.71
100	0.52	7.6	57.76	40	0.41
100	1.3	13.5	182.25	100	1.02
100	2.55	18.9	357.21	220	2.24
500	1.9	16.2	262.44	180	1.83
500	0.175	3.9	15.21	15	0.15
500	0.375	7.1	50.41	20	0.20
500	1.06	12.1	146.41	110	1.12
500	1.7	15.4	237.16	190	1.94
500	0.9	10.8	116.64	130	1.33
500	1.2	13	169	190	1.94
500	1.59	14.8	219.04	230	2.34
500	1.9	16.2	262.44	240	2.45
500	2.6	18.9	357.21	330	3.36
500	2.3	18	324	290	2.96
500	1.2	12.9	166.41	170	1.73
500	0.7	9.3	86.49	70	0.71
500	2.4	18.3	334.89	260	2.65
500	2.75	19.8	392.04	370	3.77
500	3.62	22	484	440	4.49
500	3.85	22.8	519.84	470	4.79
500	4	23.2	538.24	510	5.20
500	4.6	24.5	600.25	570	5.81
500	4.3	24.5	600.25	530	5.40
500	4	23.2	538.24	520	5.30

Appendix G. Experimental Data Using Ross-Miles Test Rig

Results											
		Surfactant Solution	Volume in cylinder	Total Lqd	Liquid in pool	Height of nozzle					
LHV	Run	in funnel	V		L	H	Foam +lqd	Liquid	Foam height	Exp foam	Exp total
mpm	1	200	0	200	W	600	455	170	285	9.5	2.275
mmm	2	200	0	200	W	450	385	185	200	13.33333	1.925
mmm	10	200	0	200	W	450	390	190	200	20	1.95
mmp	6	200	100	300	W	450	450	280	170	8.5	1.75
mmp	14	200	100	300	W	450	465	280	185	9.25	1.825
mpm	9	200	0	200	W	600	465	190	275	27.5	2.325
mpp	5	200	100	300	W	600	535	275	260	10.4	2.175
mpp	13	200	100	300	W	600	550	280	270	13.5	2.25
pmm	4	200	0	200	FS	450	390	185	205	13.66667	1.95
pmm	12	200	0	200	FS	450	360	190	170	17	1.8
pmp	8	210	100	310	FS	450	485	305	180	36	1.833333
pmp	16	200	100	300	FS	450	475	285	190	12.66667	1.875
pmp	17	200	100	300	FS	450	490	290	200	20	1.95
ppm	3	200	0	200	FS	600	445	180	265	13.25	2.225
ppm	11	200	0	200	FS	600	455	190	265	26.5	2.275
ppp	7	200	100	300	FS	600	570	270	300	10	2.35
ppp	15	200	100	300	FS	600	550	290	260	26	2.25

AVERAGES											
	Foam height	Exp foam	Exp total			Foam height	Exp foam	Exp total			
mmm	200	16.666667	1.9375			mmp	177.5	8.875	1.7875		
pmm	187.5	15.333333	1.875			pmm	187.5	15.333333	1.875		
mpm	280	18.5	2.3			pmp	190	22.888889	1.886111		
ppm	265	19.875	2.25			mmm	200	16.666667	1.9375		
mmp	177.5	8.875	1.7875			ppm	265	19.875	2.25		
pmp	190	22.888889	1.886111			mpp	265	11.95	2.2125		
mpp	265	11.95	2.2125			mpm	280	18.5	2.3		
ppp	280	18	2.3			ppp	280	18	2.3		

Head height Yates' Analysis											
	L	H	V	Head height							
				Result	-1	-2	-3	Divisor	Estimate	ID	
mmm	-	-	-	200	387.5	932.5	1845	8	230.625	Average	
pmm	+	-	-	187.5	545	912.5	0	4	0	L	0
mpm	-	+	-	280	367.5	27.5	-335	4	-83.75	H	-0.36
ppm	+	+	-	265	545	-27.5	0	4	0	LH	0.00
mmp	-	-	+	177.5	12.5	-157.5	20	4	5	F	0.02
pmp	+	-	+	190	15	-177.5	55	4	13.75	LF	0.06
mpp	-	+	+	265	-12.5	-2.5	20	4	5	HF	0.02
ppp	+	+	+	280	-15	2.5	-5	4	-1.25	LHF	-0.01

Foam expansion Yates' Analysis				Foam exp							
	L	H	V	Result	-1	-2	-3	Divisor	Estimate	ID	
mmm	-	-	-	16.67	32.00	70.38	132.09	8	16.51	Average	
pmm	+	-	-	15.33	38.38	61.71	-20.11	4	-5.03	L	-0.30
mpm	-	+	-	18.50	31.76	-0.04	-4.56	4	-1.14	H	-0.07
ppm	+	+	-	19.88	29.95	-20.06	-5.26	4	-1.31	LH	-0.08
mmp	-	-	+	8.88	1.33	-6.38	8.66	4	2.17	F	0.13
pmp	+	-	+	22.89	-1.38	1.81	20.02	4	5.01	LF	0.30
mpp	-	+	+	11.95	-14.01	2.71	-8.19	4	-2.05	HF	-0.12
ppp	+	+	+	18.00	-6.05	-7.96	10.67	4	2.67	LHF	0.16